Observational Cosmology

(C. Porciani / K. Basu)

Lectures 4 + 5

The Cosmic Microwave Background

Course website:

http://www.astro.uni-bonn.de/~kbasu/ObsCosmo

Outline of the CMB Lectures

Lecture 1

➡ Discovery of the CMB

➡ Thermal spectrum of the CMB

➡ CMB angular power spectrum

➡ Meaning of the temperature anisotropies

➡ WMAP & Planck satellites

Lecture 2

➡ CMB map making and foreground subtraction

➡ CMB secondary anisotropies

➡ CMB Polarization and its measurement

➡ Balloon and interferometric measurement of ΔT

Microwave Background Radiation

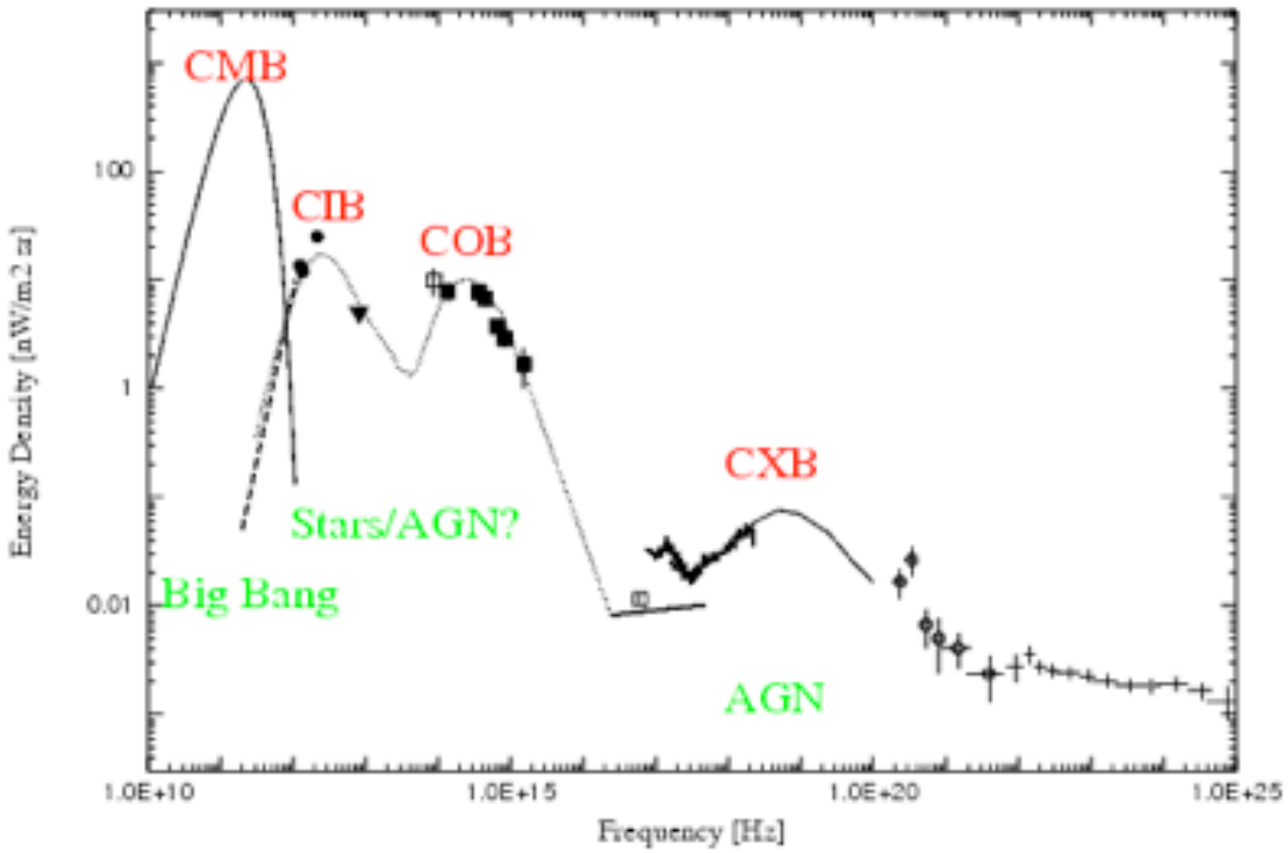

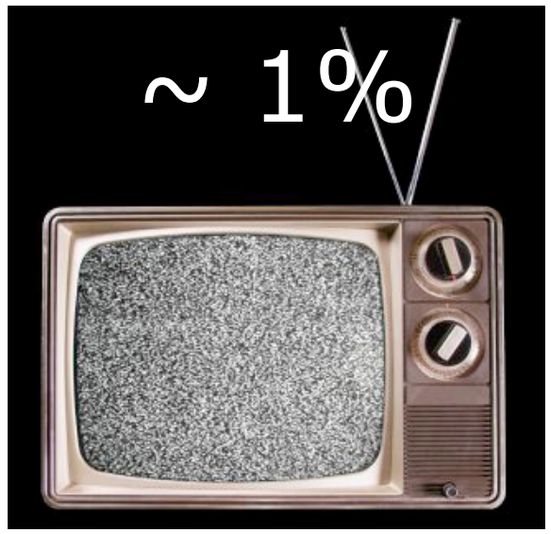

400 photons per cm^3
~1 eV/cm^3

- CMB dominates the radiation content of the universe

- It contains nearly 93% of the radiation energy density and 99% of all the photons

Discovery of the CMB

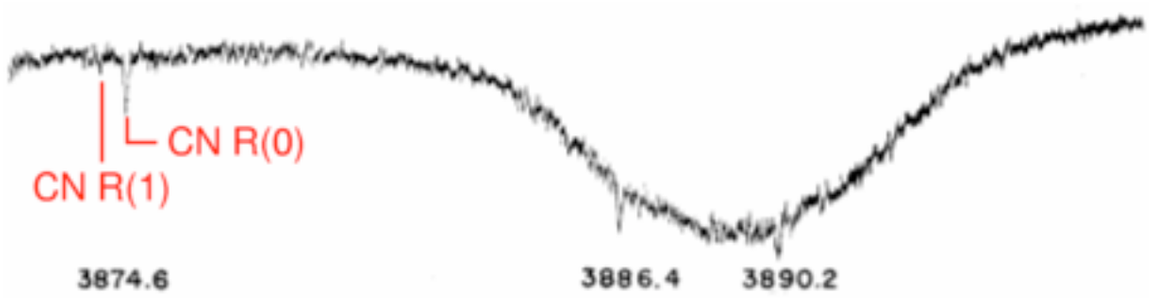

McKellar (1940)

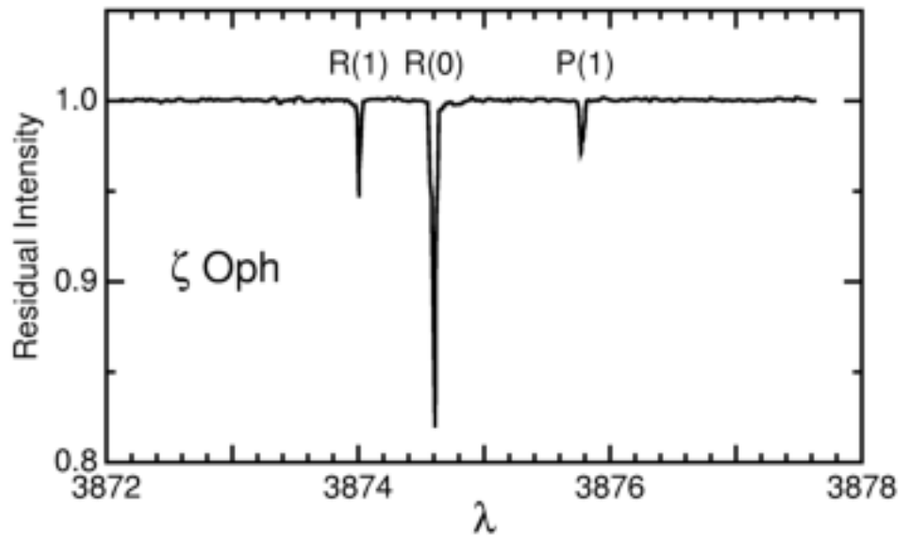

• In 1940, McKellar discovers CN molecules in interstellar space from their absorption spectra (one of the first IS-molecules)

• From the excitation ratios, he infers the "rotational temperature of interstellar space" to be 2° K (1941, PASP 53, 233)

• In his 1950 book, the Nobel prize winning spectroscopist Herzberg remarks: "From the intensity ratio of the lines with K=0 and K=1 a rotational **temperature of 2.3° K follows, which has of course only a very restricted meaning**."

Discovery of the CMB

- After the "α–β–γ paper", Alpher & Herman (1948) predict 5 K radiation background as by-product of their theory of the nucleosynthesis in the early universe (with no suggestion of its detectability).

- Shmaonov (1957) measures an uniform noise temperature of 4±3 K at λ=3.2 cm.

- Doroshkevich & Novikov (1964) emphasize the detectability of this radiation, predict that the spectrum of the relict radiation will be a blackbody, and also mention that the twenty-foot horn reflector at the Bell Laboratories will be the best instrument for detecting it!

No Nobel prize for these guys!

Discovery of the CMB

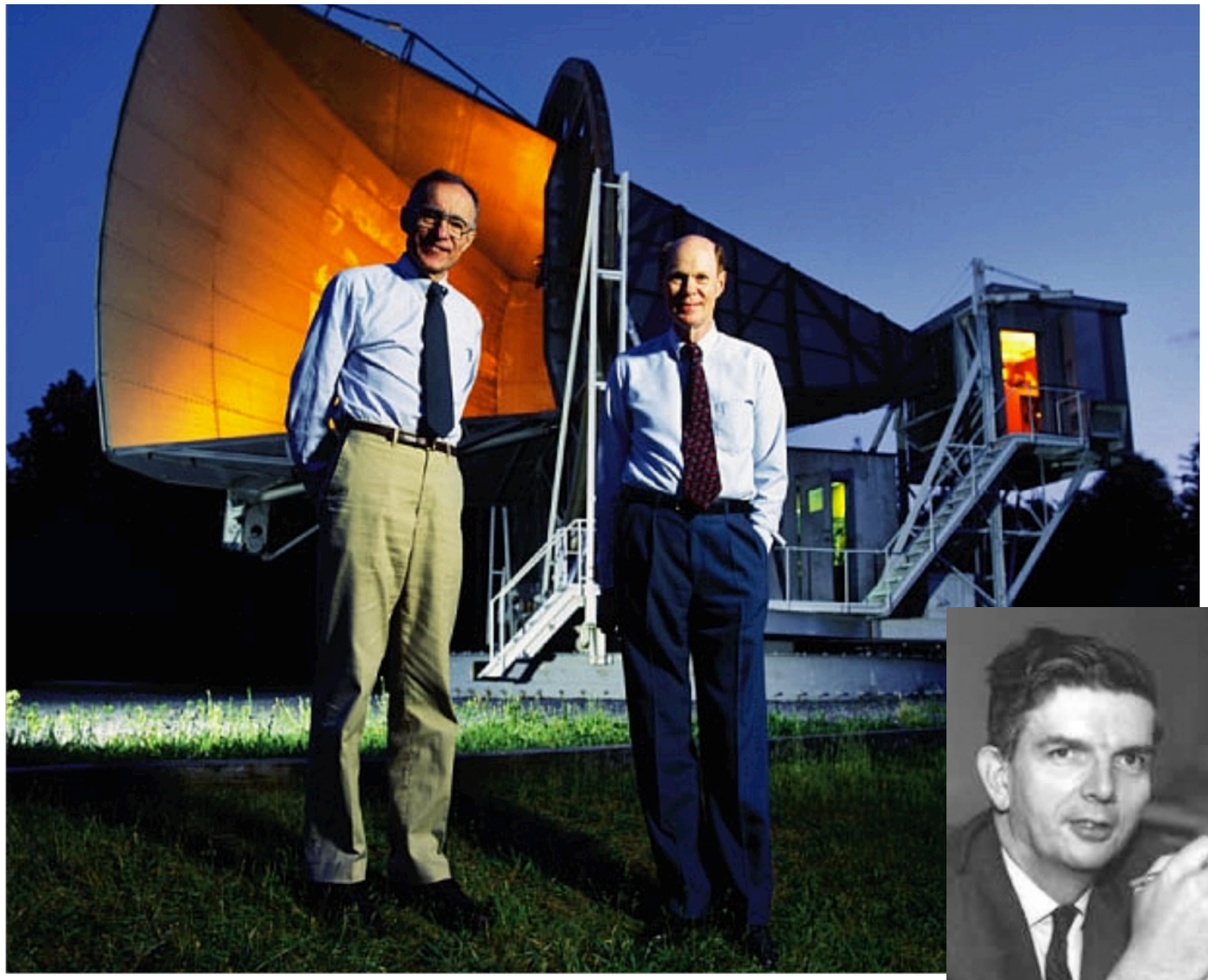

- Originally wanted to measure Galactic emission at λ=7.3 cm

- Found a direction-independent noise (3.5±1.0 K) that they could not get rid of, despite drastic measures

- So they talked with colleagues..

- Explanation of this "excess noise" was given in a companion paper by Robert Dicke and collaborators
(no Nobel prize for Dicke either, not to mention Gamow!)

Measurement of T_{CMB}

Credit: D. Samtleben

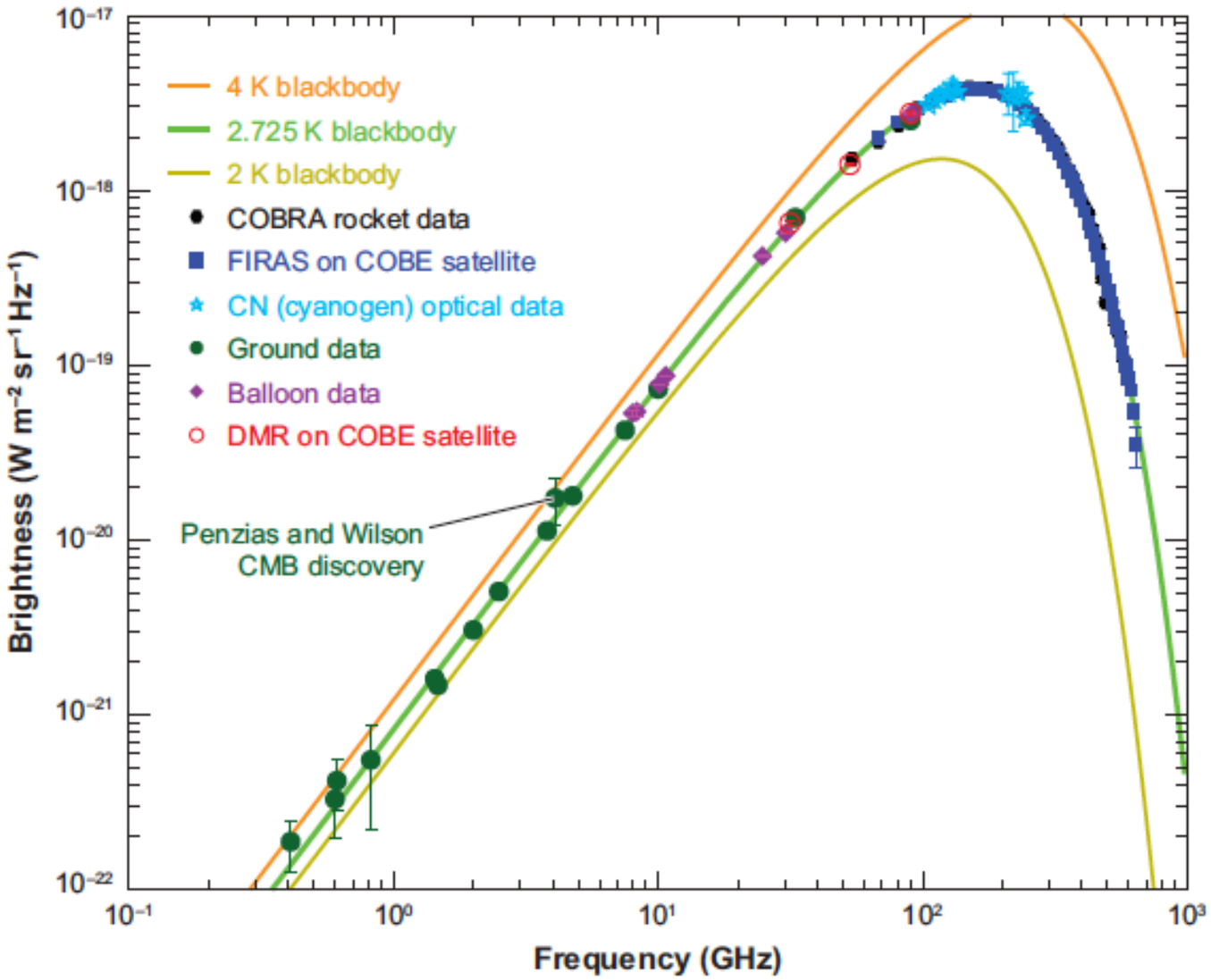

Measured blackbody spectrum of the CMB, with fit to various data

Ground- and balloon-based experiments have been measuring CMB temperature for decades with increasing precision

but it was realized that one has to go to the stable thermal environment of outer space to get a really accurate measurement.

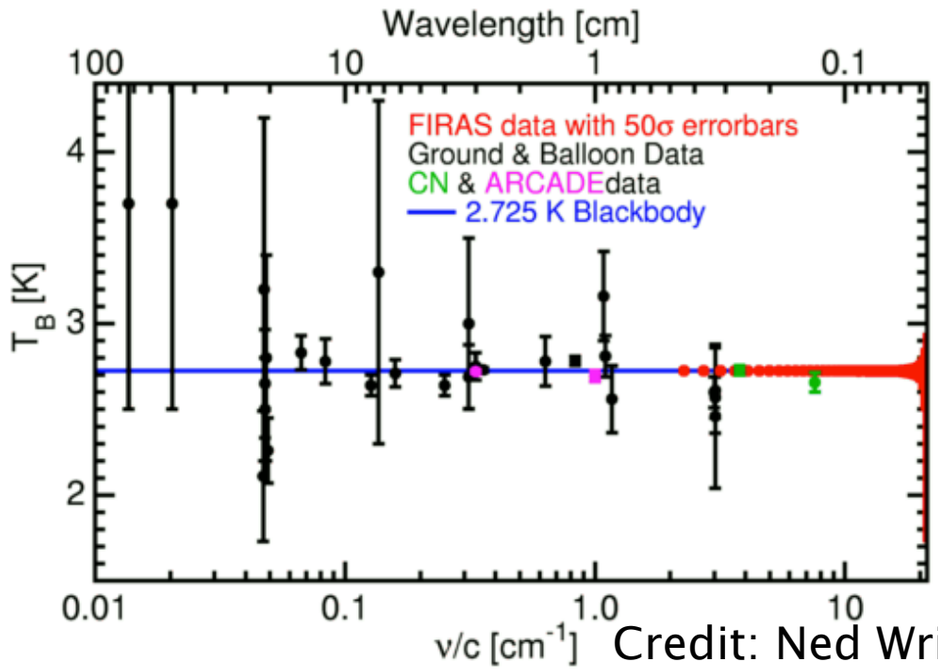

Credit: Ned Wright

COBE

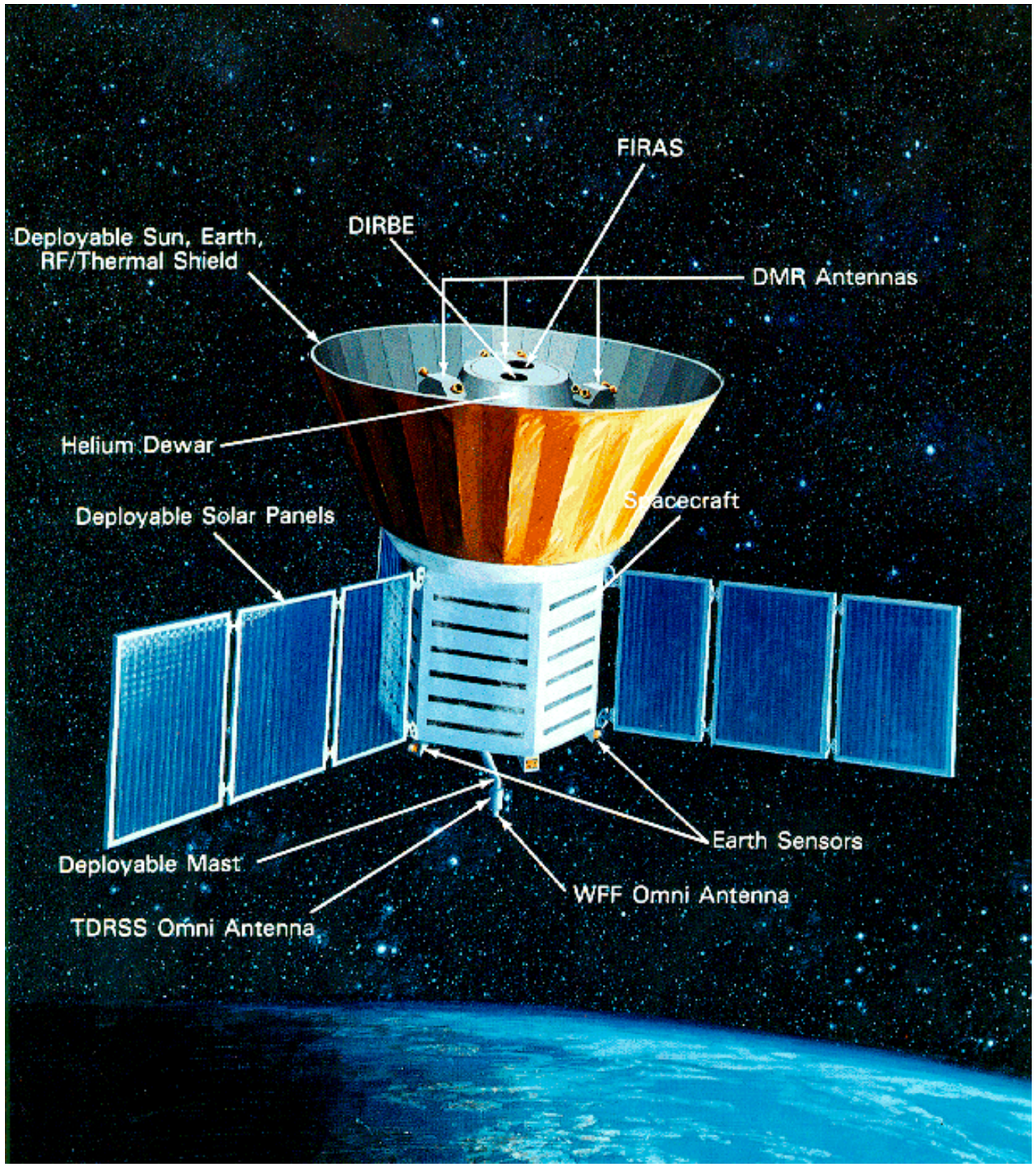

Credit: NASA

Launched on Nov. 1989 on a Delta rocket.

DIRBE: Measured the absolute sky brightness in the 1–240 μm wavelength range, to search for the Infrared Background

FIRAS: Measured the spectrum of the CMB, finding it to be an almost perfect blackbody with $T_0 = 2.725 \pm 0.002$ K

DMR: Found "anisotropies" in the CMB for the first time, at a level of 1 part in 10^5

2006 Nobel prize in physics

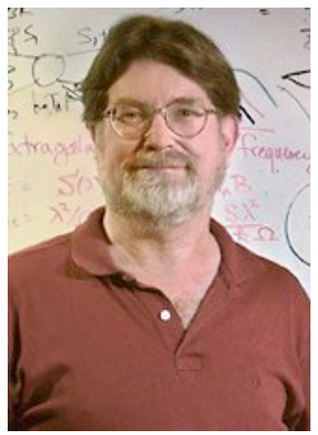

Thermalization of the CMB

Change of photon energy, not number:

Compton scattering: $e + \gamma = e + \gamma$

Processes that creates photons:

Bremsstrahlung: $e + Z = e + Z + \gamma$

Inelastic (double) Compton scattering:

$e + \gamma = e + \gamma + \gamma$

At an early enough epoch, timescale of thermal processes must be shorter than the expansion timescale. They are equal at $z \sim 2 \times 10^6$, or roughly two months after the big bang.

The universe reaches thermal equilibrium by this time through scattering and photon-generating processes. Thermal equilibrium generates a blackbody radiation field. Any energy injection before this time cannot leave any spectral signature on the CMB blackbody.

The universe expands adiabatically, hence a blackbody spectrum, once established, is maintained.

Bose-Einstein spectrum

Kinetic equilibrium can be established by any process with a timescale less than H^{-1}

Under KE, as opposed to thermal equilibrium, the spectrum is Bose-Einstein: $n = [\exp(h\nu/kT + \mu) - 1]^{-1}$

Clearly, μ plays a only small role at high frequencies, but the discrepancy becomes larger as the frequency drops.

The claim that thermal equilibrium is established at the high redshift of ~2×10^6 is equivalent to the claim that μ is driven essentially to zero by that redshift. However, if energy is added to the CMB radiation field after an epoch corresponding to a redshift of ~2×10^6, there may still be time to reintroduce kinetic equilibrium, but not full thermal equilibrium.

Limits on Spectral Distortions

• Energy added after $z \sim 2 \times 10^6$ will show up as spectral distortions. Departure from a Planck spectrum at fixed T is known as "μ distortion" (B-E distribution). μ distortion is easier to detect at wavelengths $\lambda > 10$ cm.

COBE measurement: $|\mu| < 9 \times 10^{-5}$ (95% CL)

• The amount of inverse Compton scattering at later epochs ($z < 10^5$) show up as "y distortion", where $y \sim \sigma_T n_e kT_e$ (e.g. the Sunyaev-Zel'dovich effect). This rules out a uniform intergalactic plasma as the source for X-ray background.

COBE measurement: $y < 1.2 \times 10^{-5}$ (95% CL)

• Energy injection at much later epochs ($z << 10^5$), e.g. free-free distortions, are also tightly constrained.

COBE measurement: $Y_{ff} < 1.9 \times 10^{-5}$ (95% CL)

FIRAS on COBE

Far Infra-Red Absolute Spectrophotometer

A differential polarizing Michelson interferometer

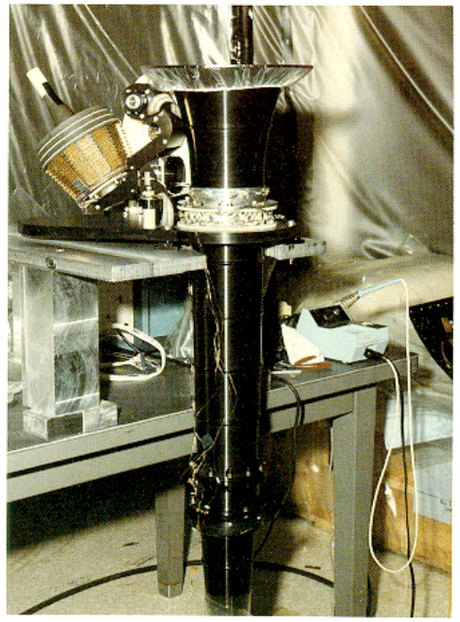

Horn antenna with movable calibrator. Protective plastic covers will be removed.

- One input is either the sky or a blackbody, other is a pretty good blackbody
- Zero output when the two inputs are equal
- Internal reference kept at T_0 ("cold load"), to minimize non-linear response of the detectors
- Residual is the measurement!

Credit: NASA

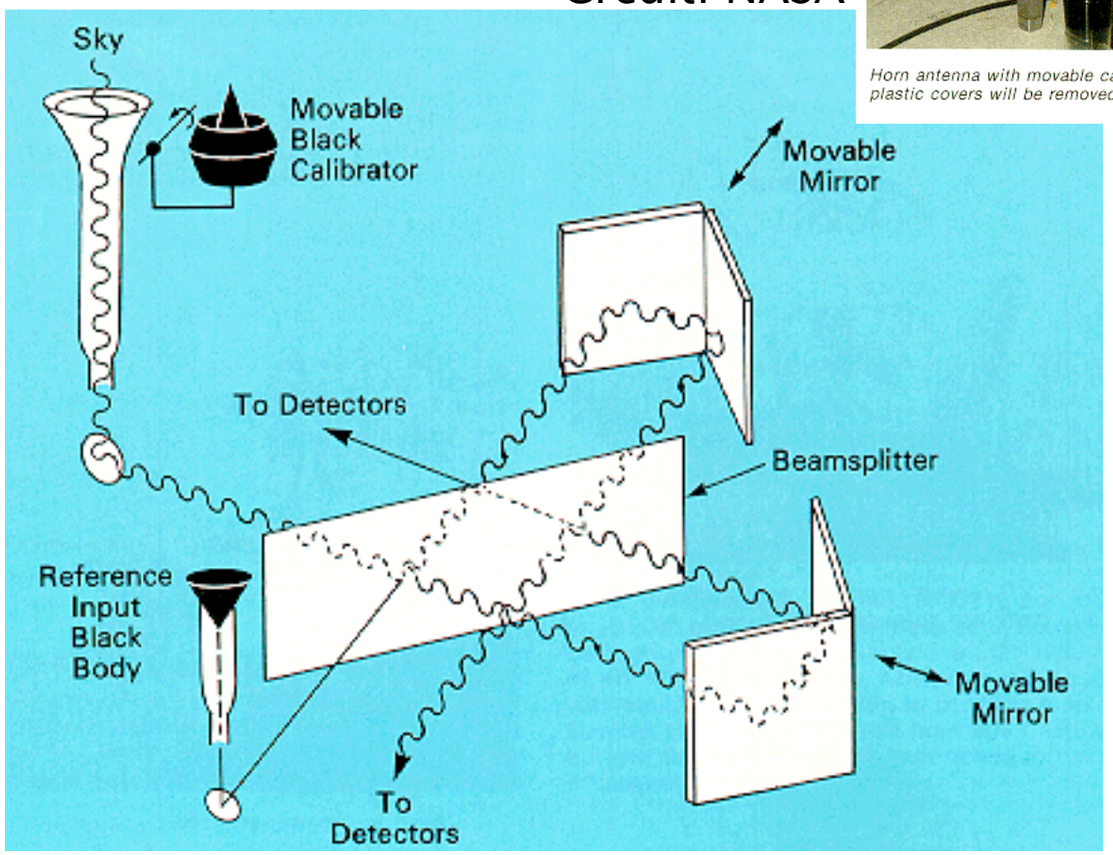

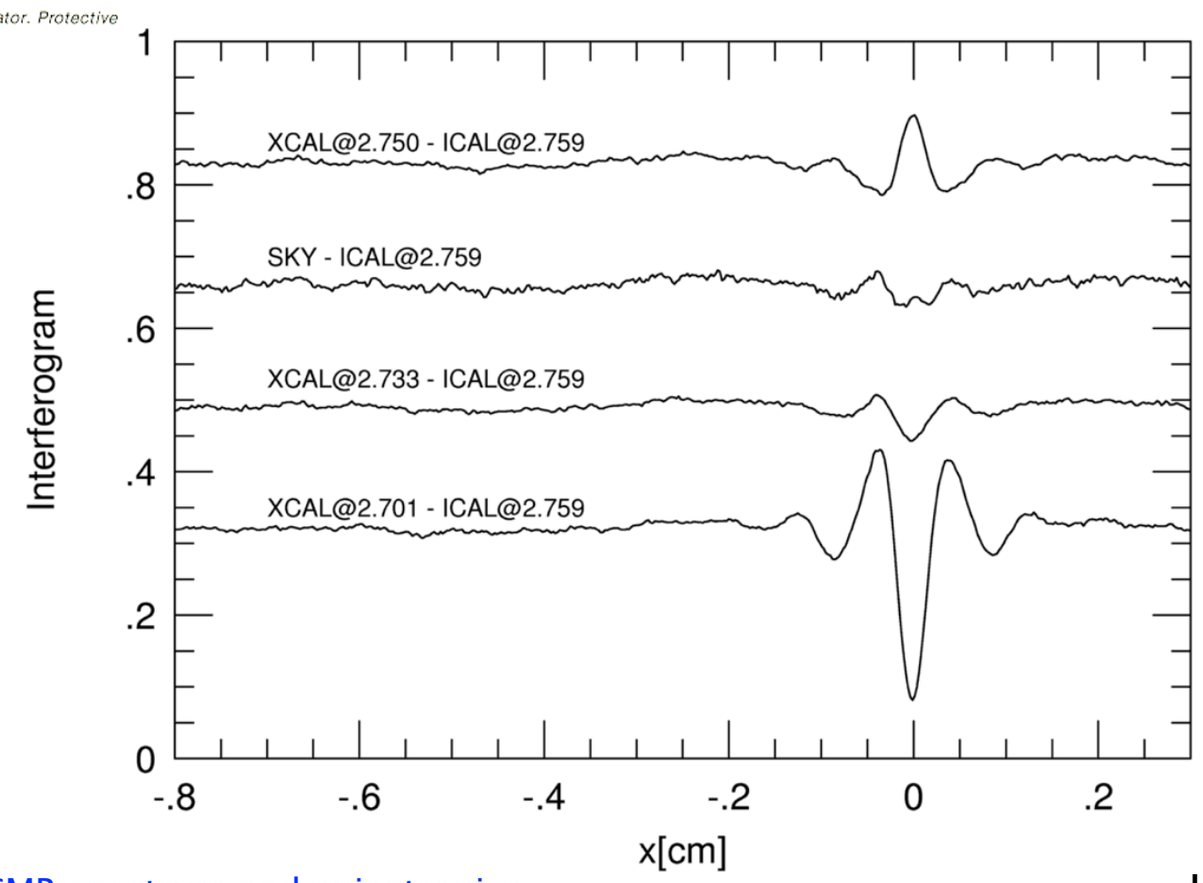

FIRAS Measurements

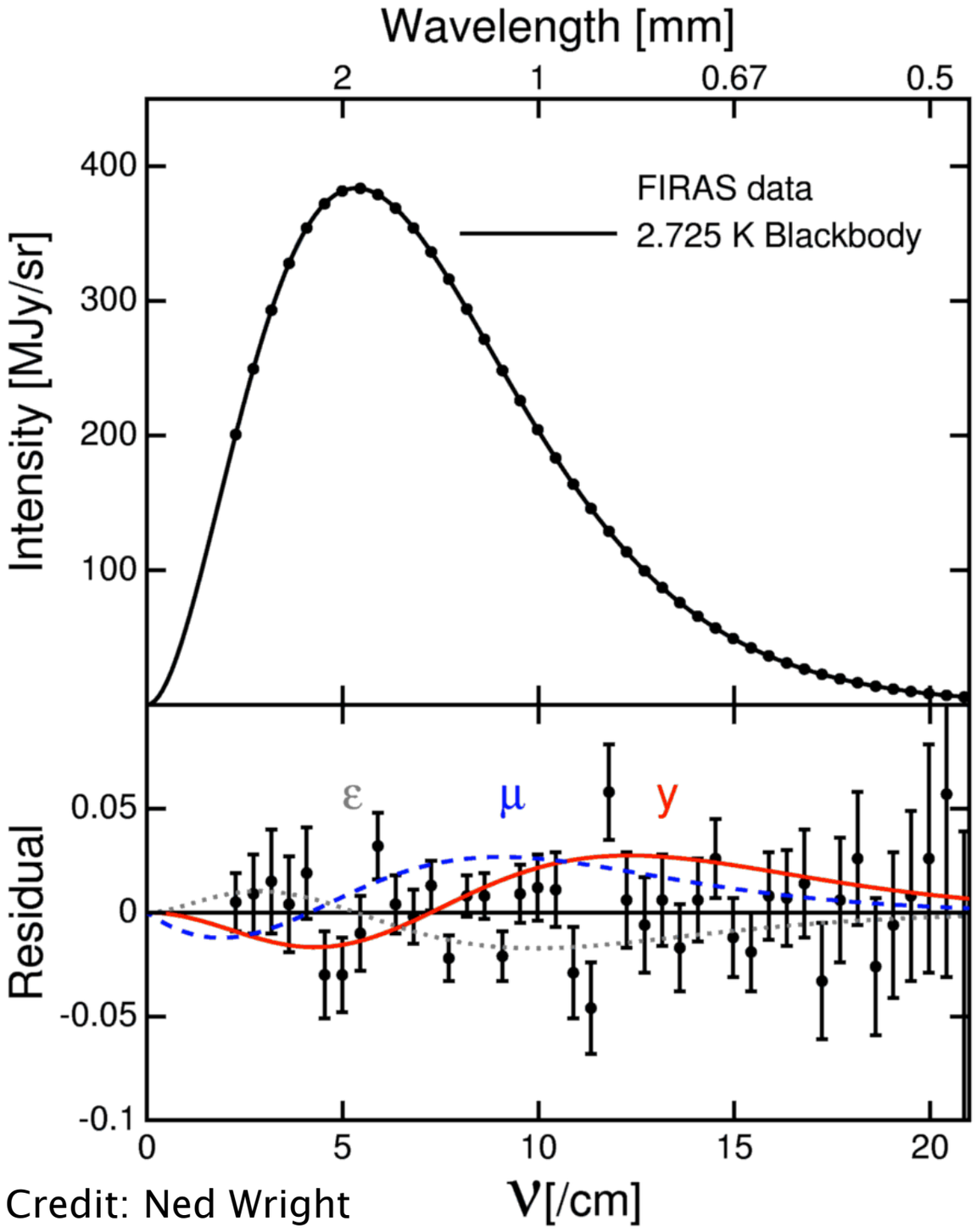

Credit: Ned Wright

Fundamental FIRAS measurement is the plot at the bottom: the difference between the CMB and the best-fitting blackbody. The top plot shows this residual added to the theoretical blackbody spectrum at the best fitting cold load temperature.

The three curves in the lower panel represents three likely non-blackbody spectra:

Red and blue curves show effect of hot electrons adding energy before and after recombination, the grey curve shows effect of a non-perfect blackbody as calibrator (less than 10^{-4})

DMR on COBE

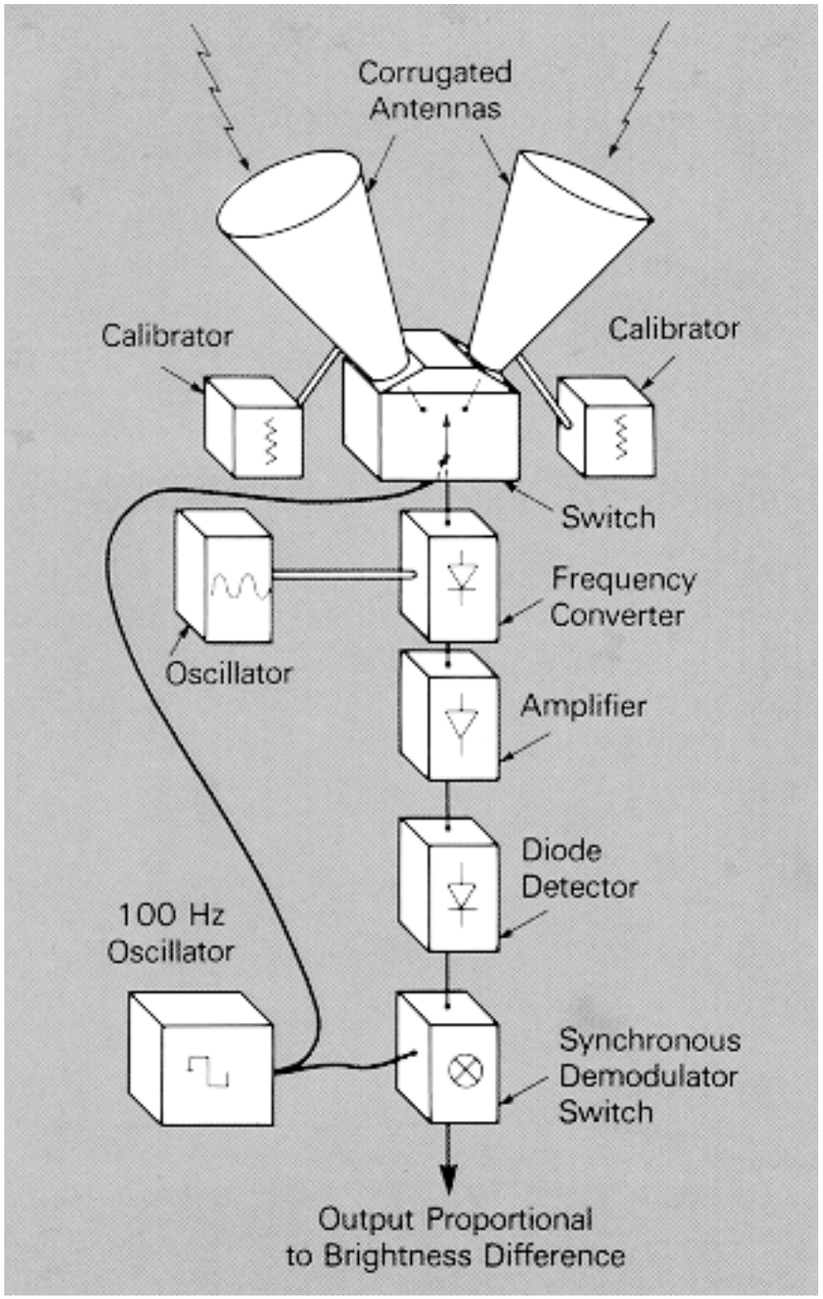

Credit: NASA

Differential Microwave Radiometer

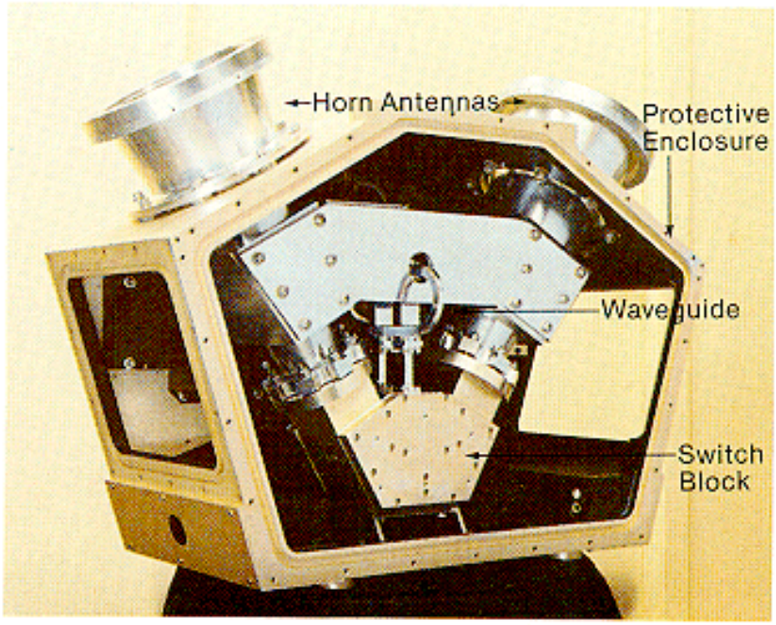

The 9.6 mm DMR receiver partially assembled. Corrugated cones are antennas.

- Differential radiometers measured at frequencies 31.5, 53 and 90 GHz, over a 4-year period
- Comparative measurements of the sky offer far greater sensitivity than absolute measurements

COBE DMR Measurements

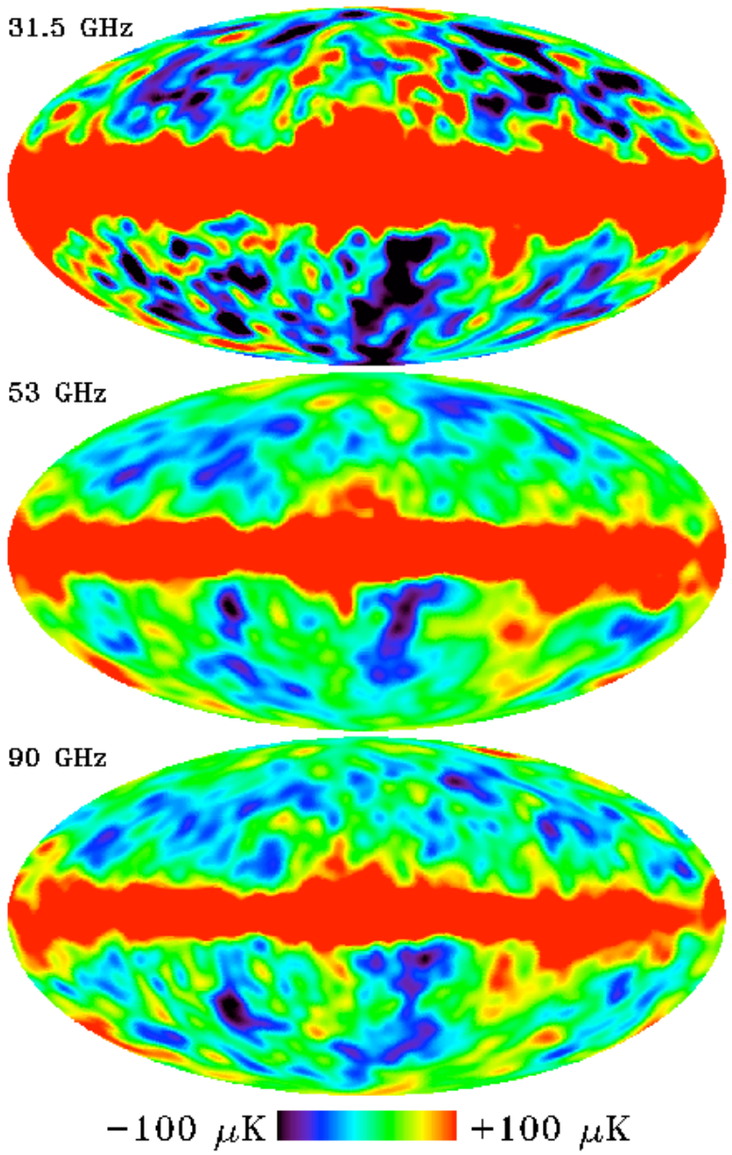

Credit: NASA

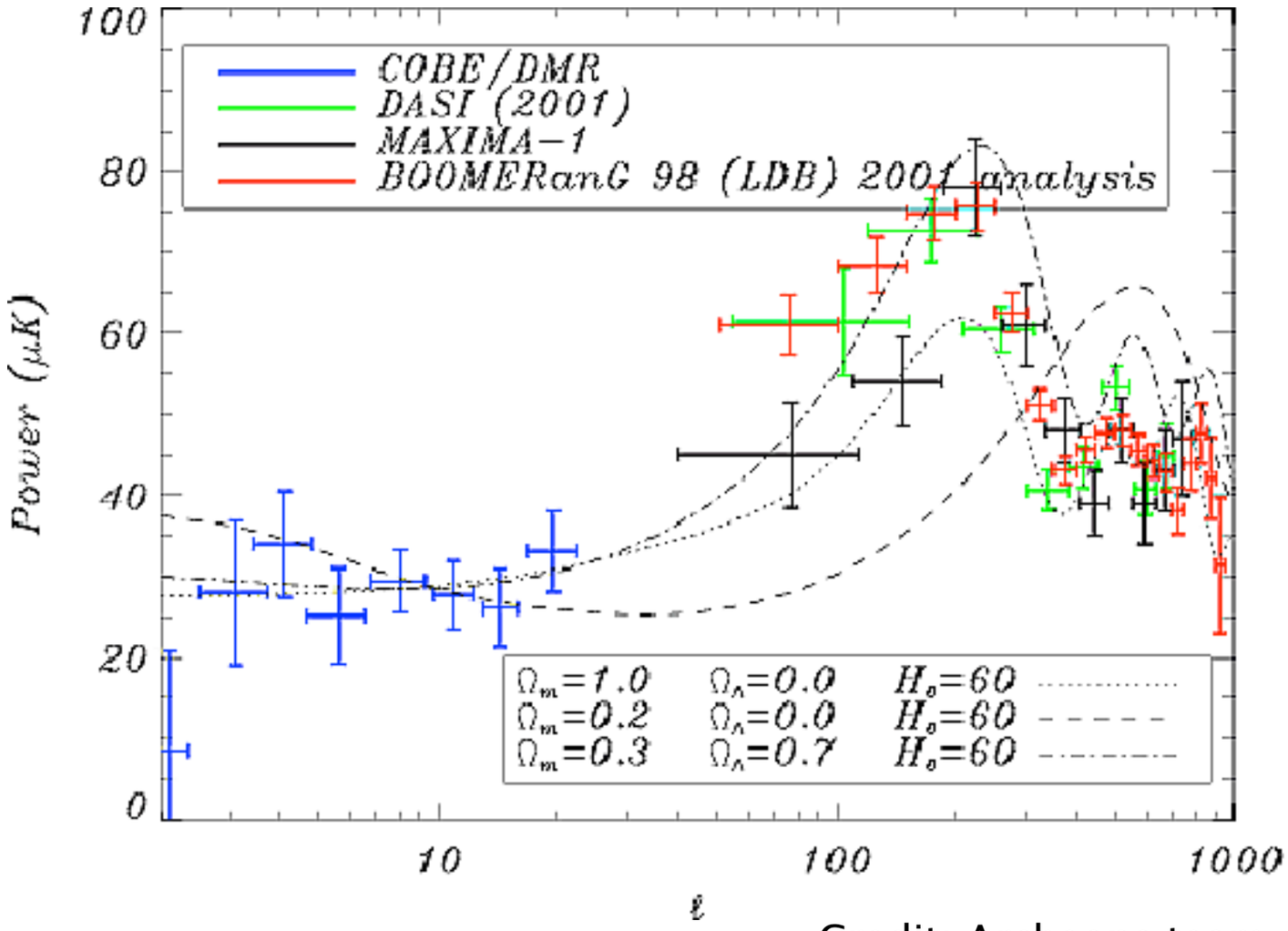

Credit: Archeops team

WMAP mission: 2001–2008

Credit: NASA

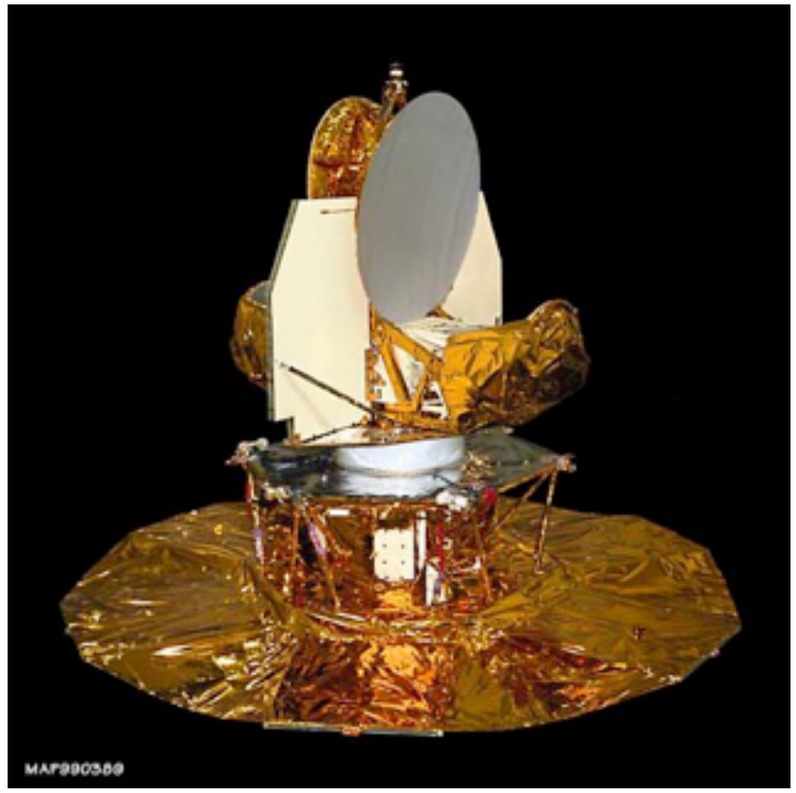

Note the same dual receivers as COBE. This design, plus the very stable conditions at the L2, minimizes the "1/f noise" in amplifiers and receivers.

Thus after 7 years, the data could still be added and noise lowered (of course, the improvement will be marginal).

WMAP results after 1st year

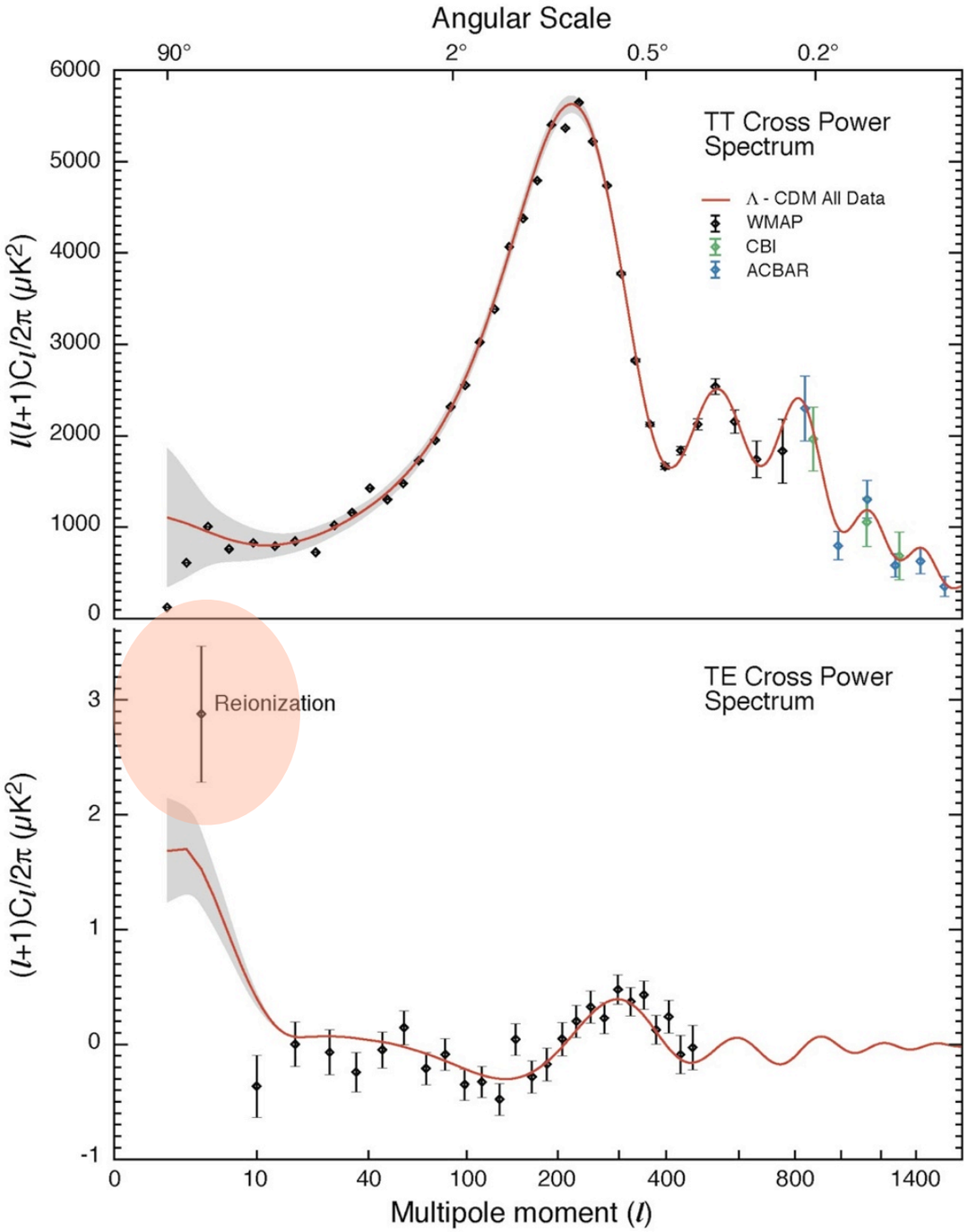

(Credit: WMAP Science Team)

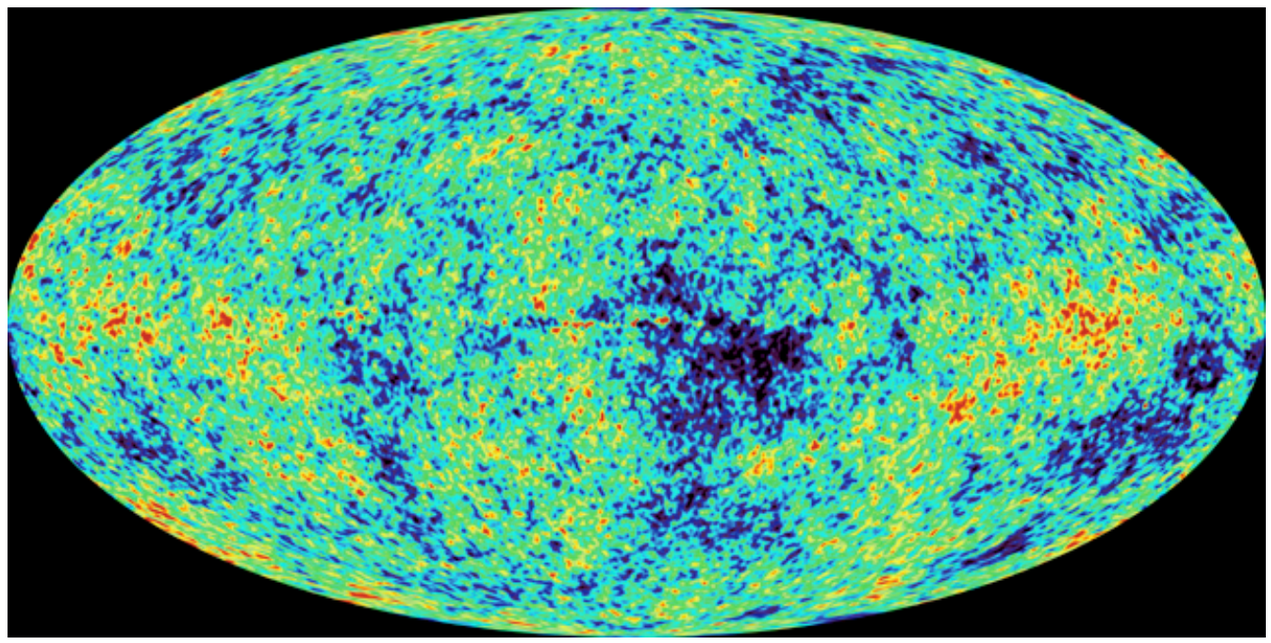

Internal Linear Combination map

WMAP revolutionizing CMB science

Resolution more than 20 times better with WMAP than COBE

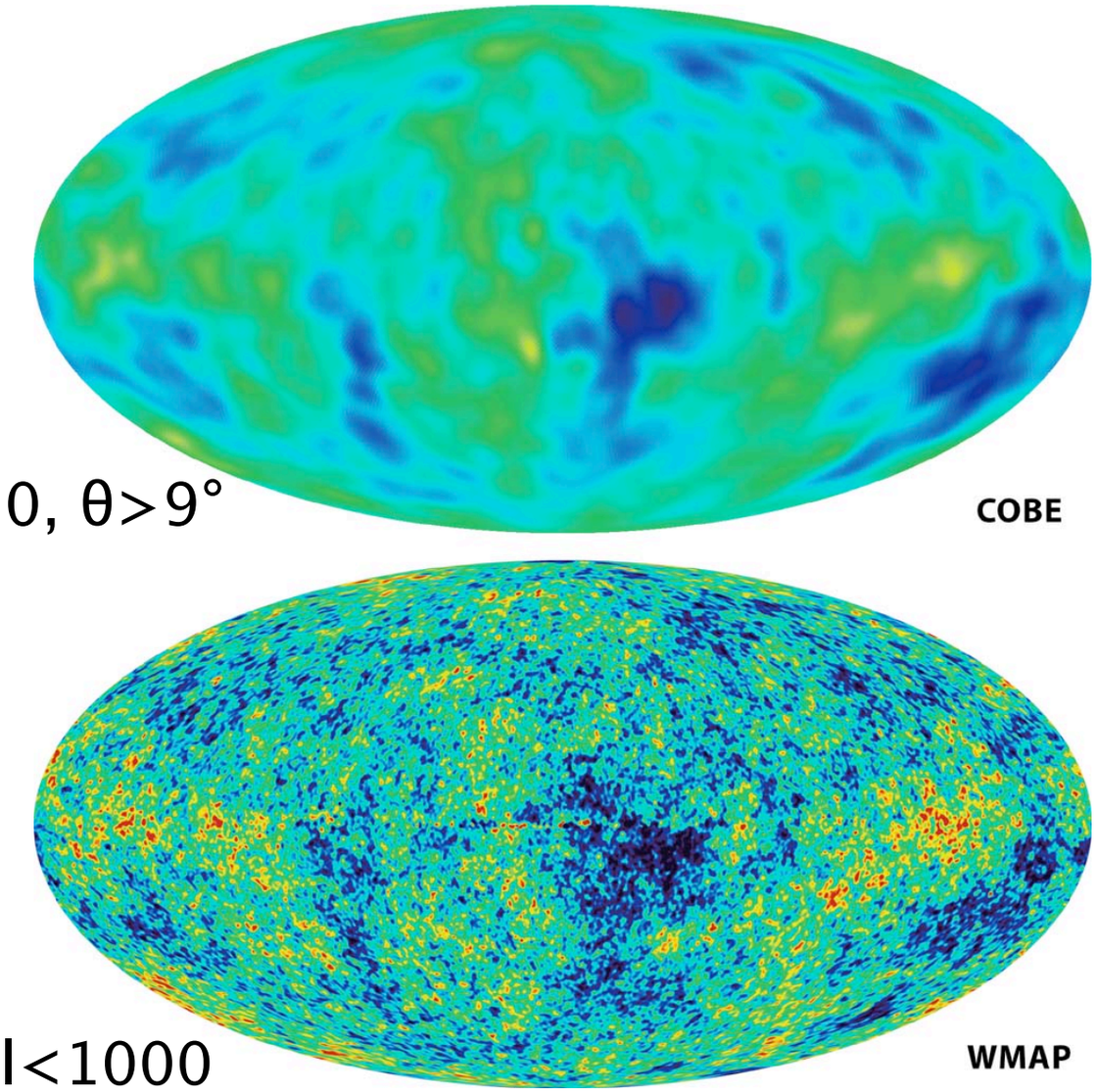

l<20, θ>9°

COBE

2<l<1000
0.02°<θ<90°

WMAP

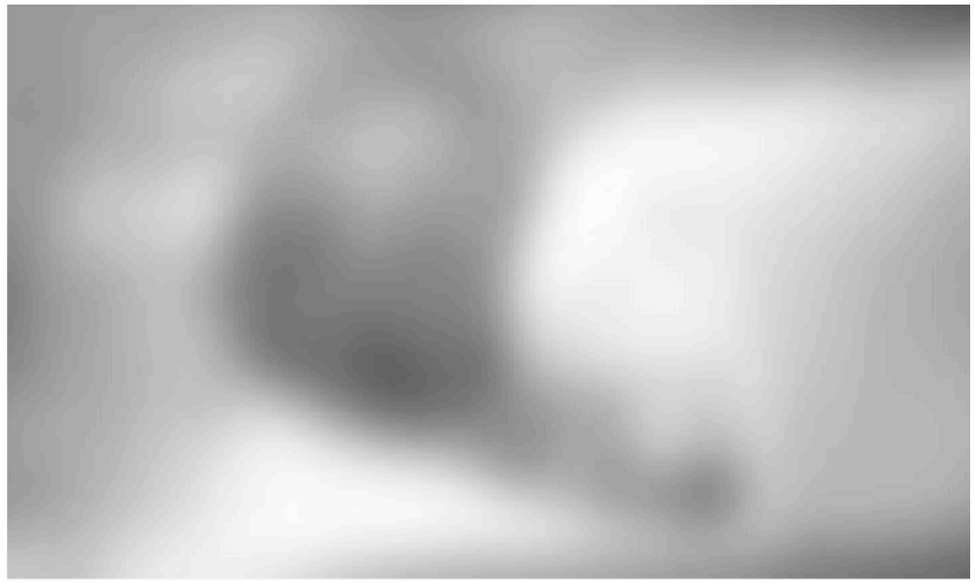

Credit: ??

Temperature anisotropies

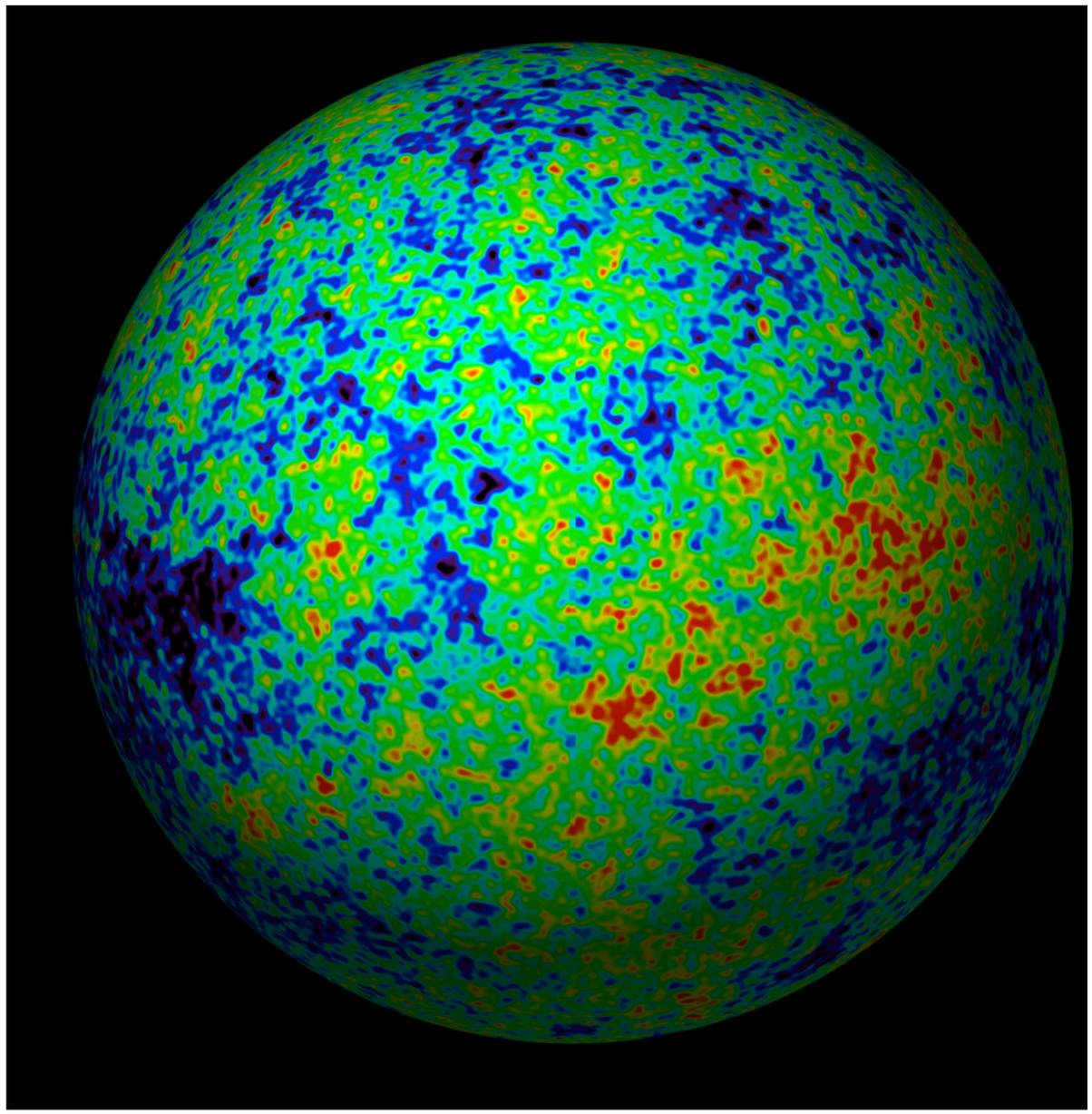

The Last Scattering Surface

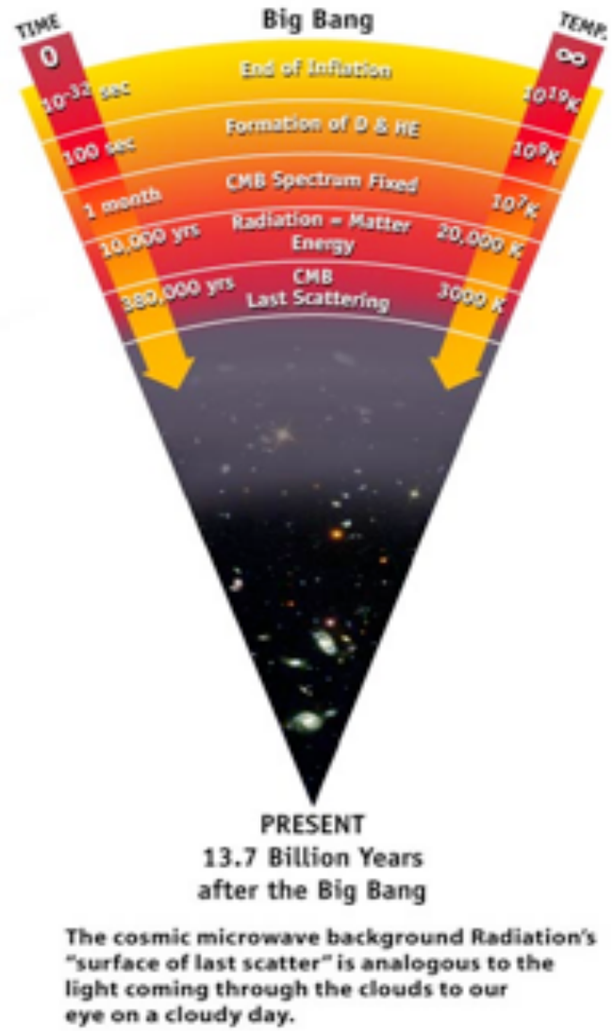

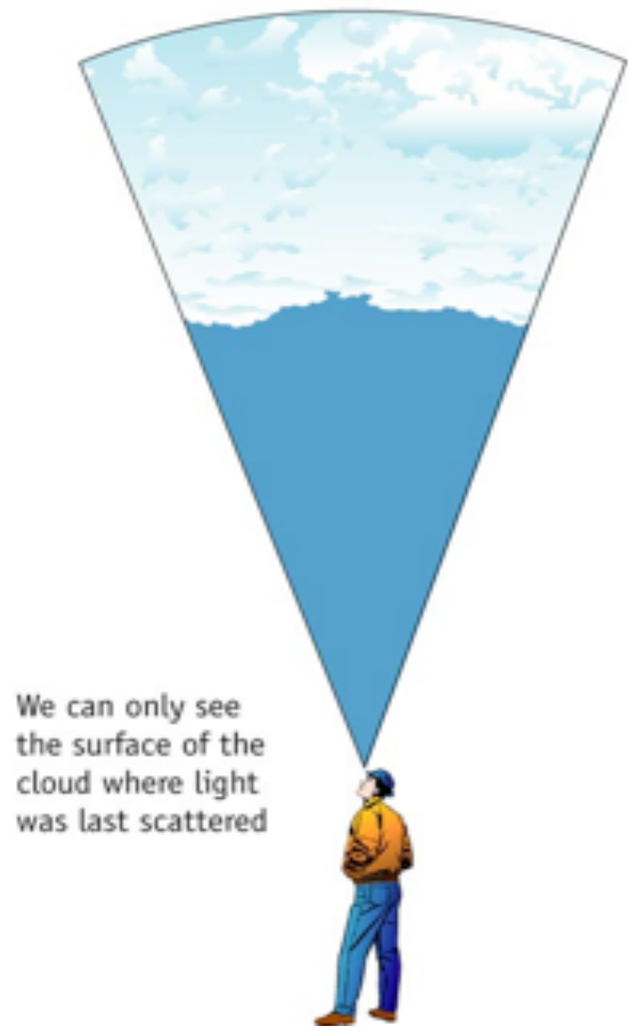

All photons have travelled the same distance since recombination.
We can think of the CMB being emitted from inside of a spherical surface, we're at the center. (This surface has a thickness)

LSS & recombination

The temperature of last scattering depends very weakly on the cosmological parameters (weaker than logarithmically).

It is mainly determined by the ionization potential of hydrogen and the photon-to-baryon ratio.

$N_e \sim 500$ cm^{-3} (roughly same as Galactic HII regions!)

$T_e = T_r = 2970$ K $= 0.26$ eV

$z_r = 1090$

Why this is so low compared to ionization potential of hydrogen, 13.6 eV?

Thickness of recombination era

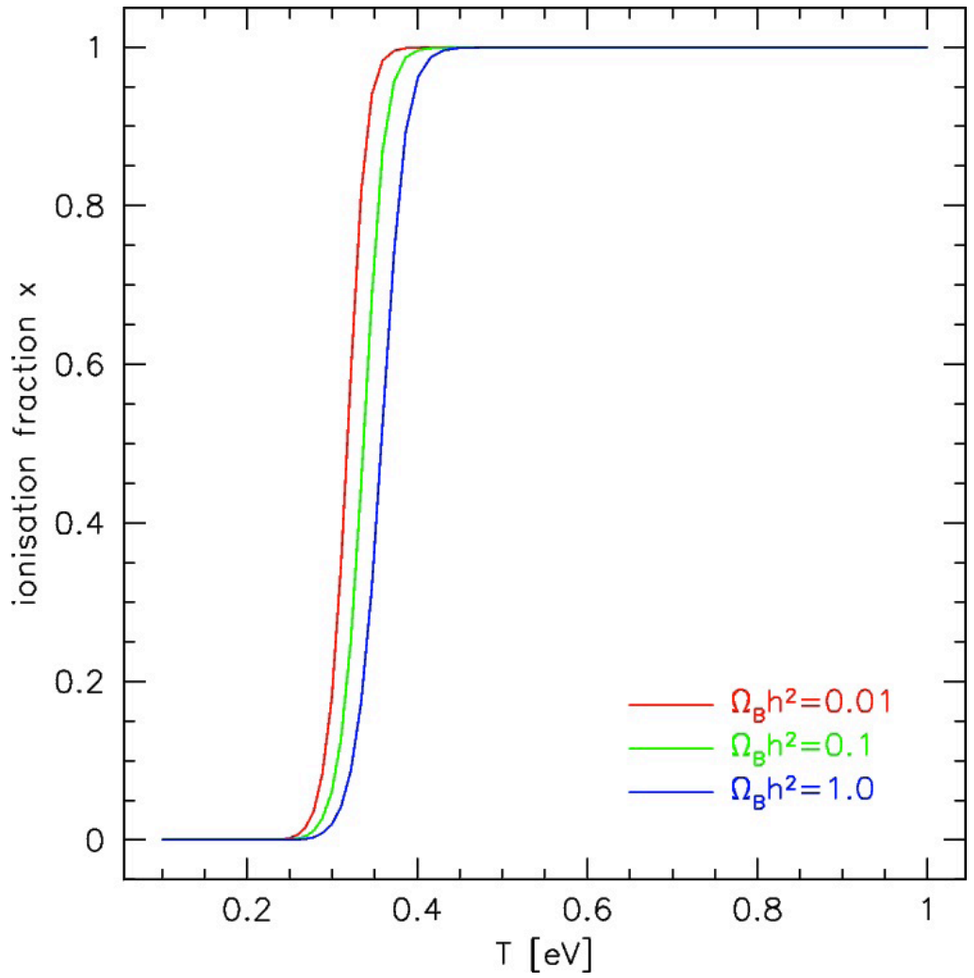

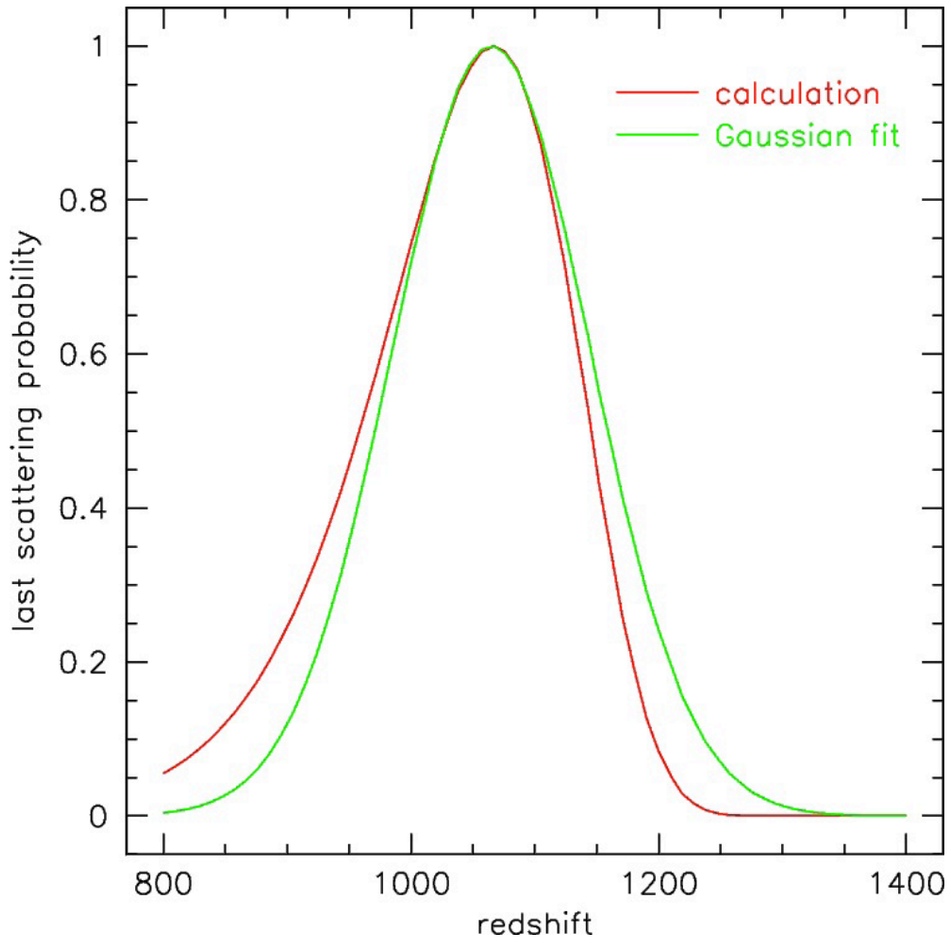

The visibility function is defined as the probability density that a photon is last scattered at redshift z: $g(z) \sim \exp(-\tau)\, d\tau/dz$

Probability distribution is well described by Gaussian with mean $z \sim 1100$ and standard deviation $\delta z \sim 80$.

Amplitude of temp. anisotropies

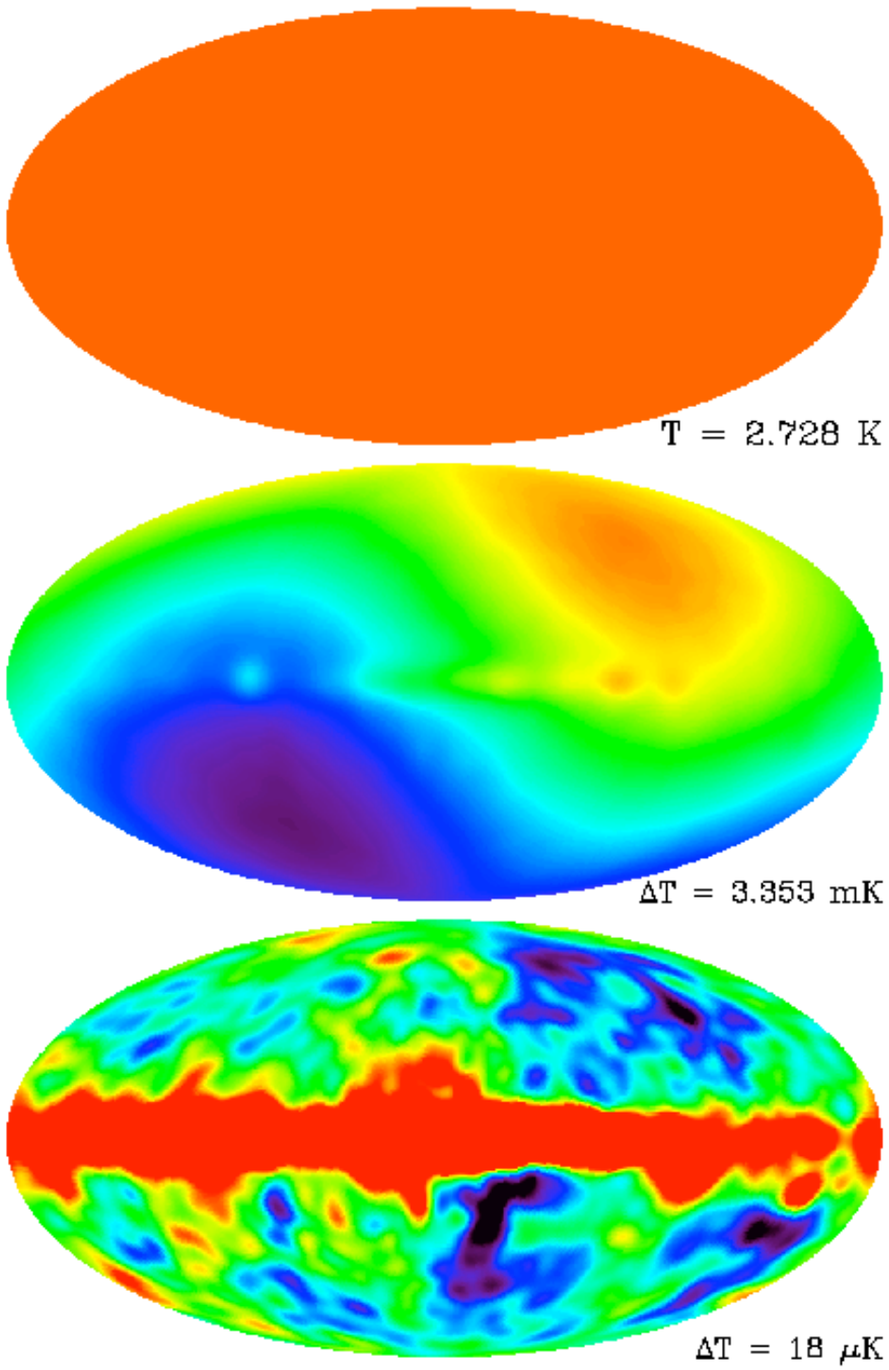

CMB is primarily a uniform glow across the sky!

Turning up the contrast, dipole pattern becomes prominent at a level of 10^{-3}. This is from the motion of the Sun relative to the CMB.

Enhancing the contrast further (at the level of 10^{-5}, and after subtracting the dipole, temperature anisotropies appear.

The CMB dipole

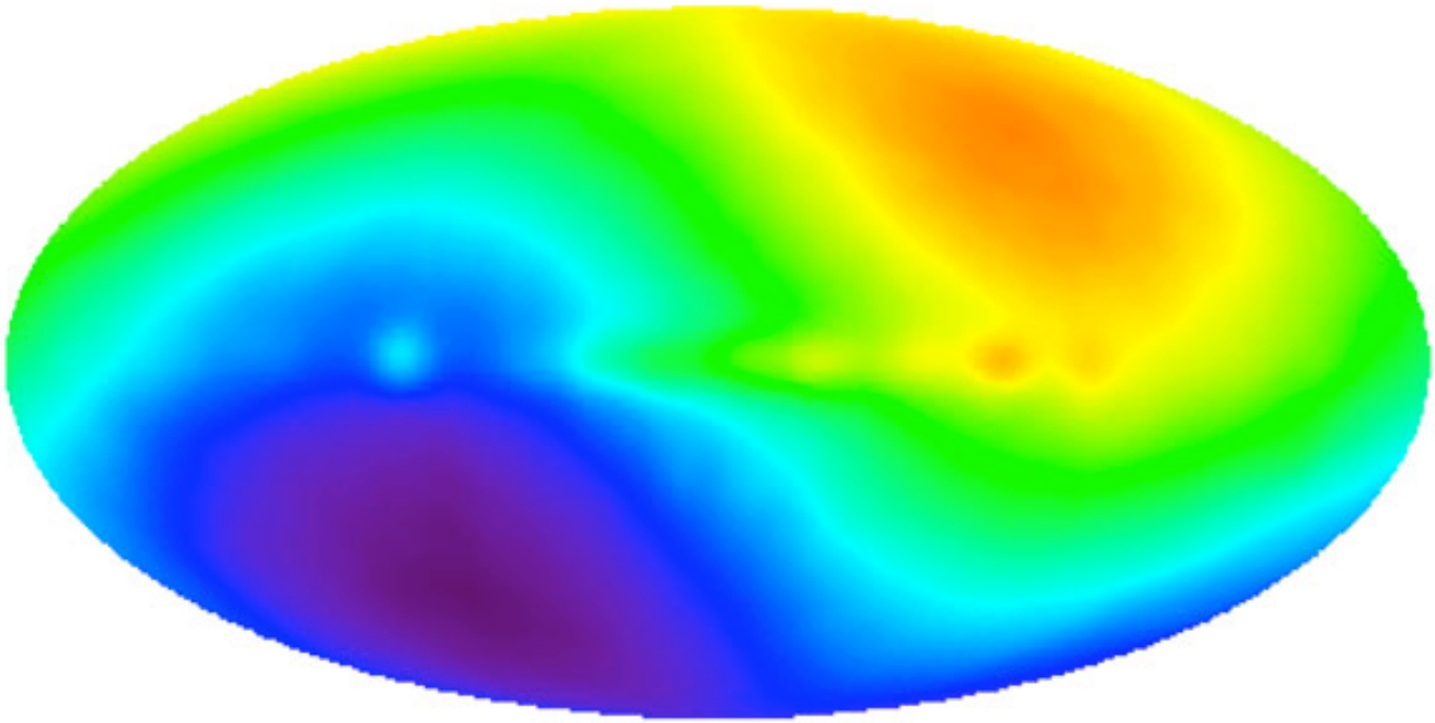

$I'(\nu')=(1+(v/c)\cos\theta)^3\, I(\nu)$
$\nu'=(1+(v/c)\cos\theta)\,\nu$
$T(\theta)=T\,(1+(v/c)\cos\theta)$

- Measured velocity: 390±30 km/s
- After subtracting out the rotation and revolution of the Earth, the velocity of the Sun in the Galaxy and the motion of the Milky Way in the Local Group one finds: v = 627 ± 22 km/s
- Towards Hydra-Centaurus, l=276±3° b=30±3°

Can we measure an intrinsic CMB dipole ?

CMB sky seen from WMAP

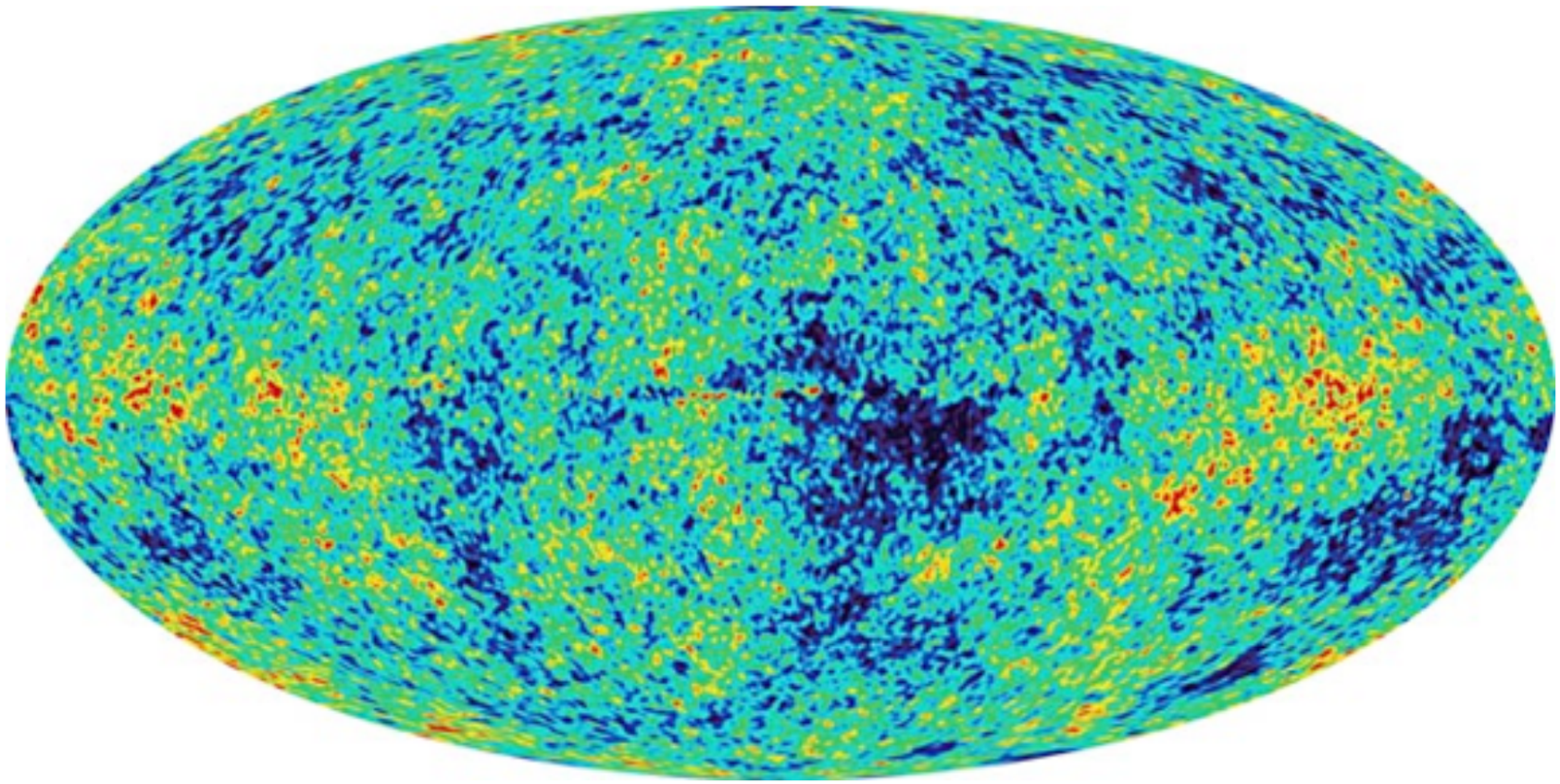

Measurement from WMAP, dipole and Galaxy subtracted.

Snapshot of the universe ages 380,000 years!

How to do science from this 2D map?

CMB data product from WMAP

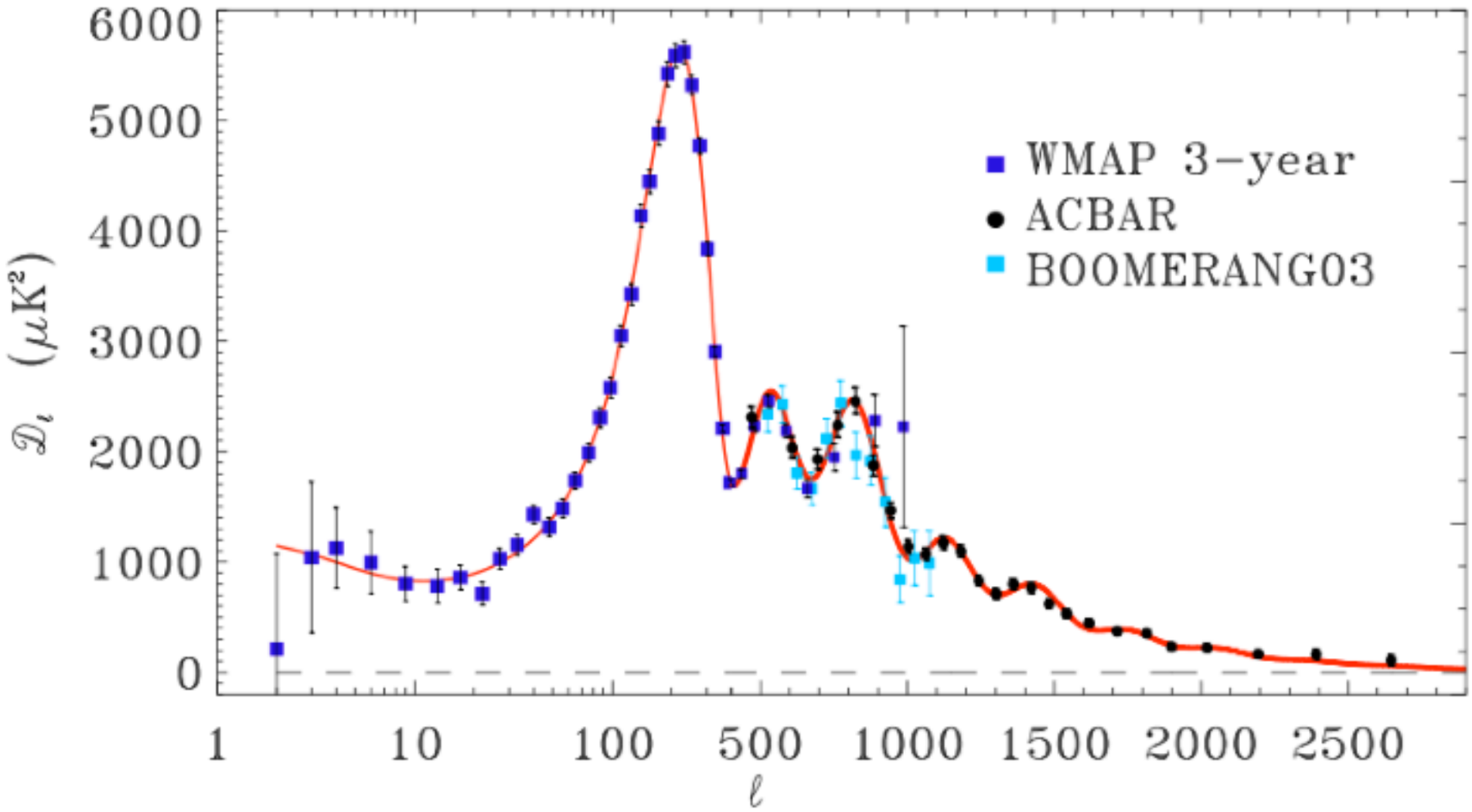

$$\langle [\delta T(\mathbf{n})]^2 \rangle = \sum_l \frac{2l+1}{4\pi} C_l \approx \int \frac{dl}{l} \frac{l(l+1)}{2\pi} C_l = \int \frac{dl}{l} D_l.$$

CMB temperature anisotropies

• The basic observable is the CMB intensity as a function of frequency and direction on the sky. Since the CMB spectrum is an extremely good black body with a fairly constant temperature across the sky, we generally describe this observable in terms of a temperature fluctuation

$$\frac{\Delta T}{T}(\theta,\phi) = \frac{T(\theta,\phi) - \bar{T}}{\bar{T}}$$

• The equivalent of the Fourier expansion on a sphere is achieved by expanding the temperature fluctuations in spherical harmonics

$$\frac{\Delta T}{T}(\theta,\phi) = \sum_{\ell=1}^{\infty} \sum_{m=-\ell}^{\ell} a_{\ell m} Y_m^{\ell}(\theta,\phi)$$

Analogy: Fourier series

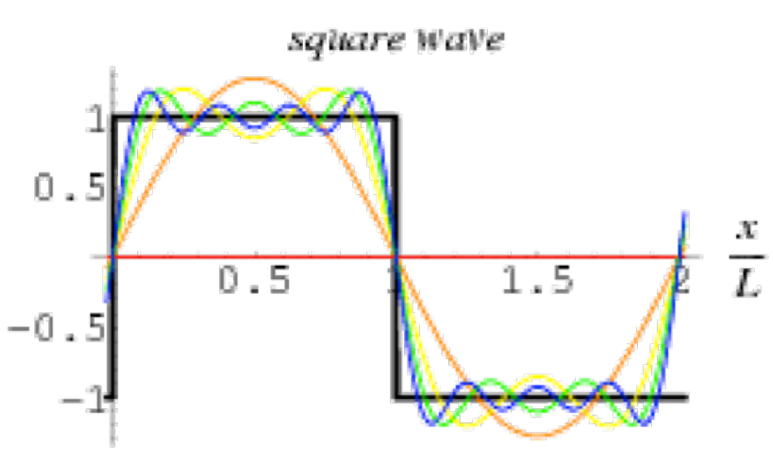

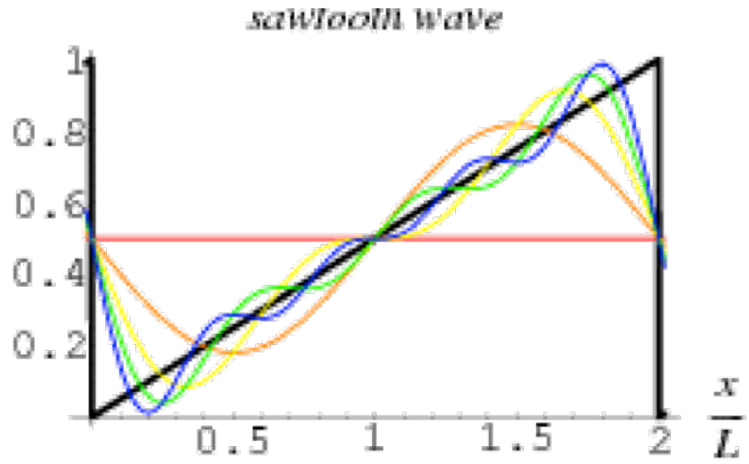

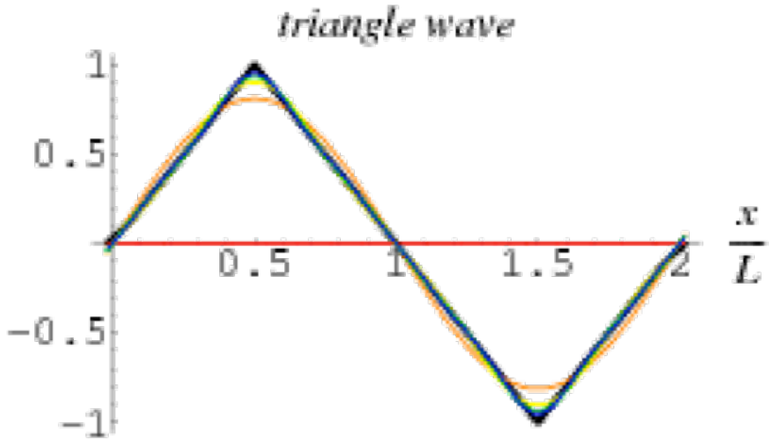

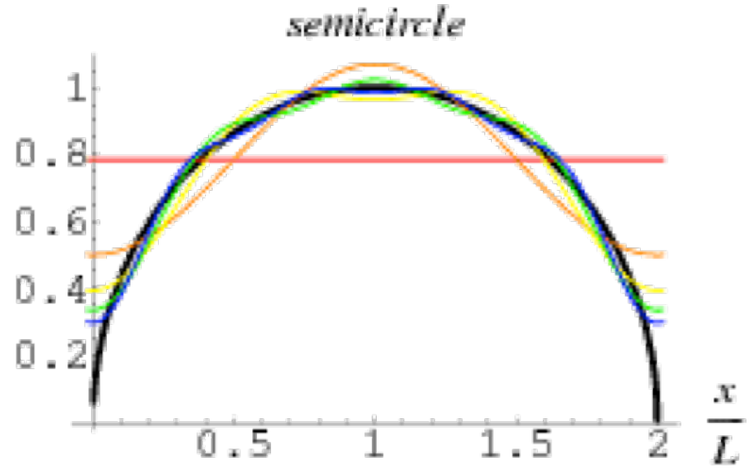

Sum sine waves of different frequencies to approximate any function.

Each has a coefficient, or amplitude.

Spherical harmonics

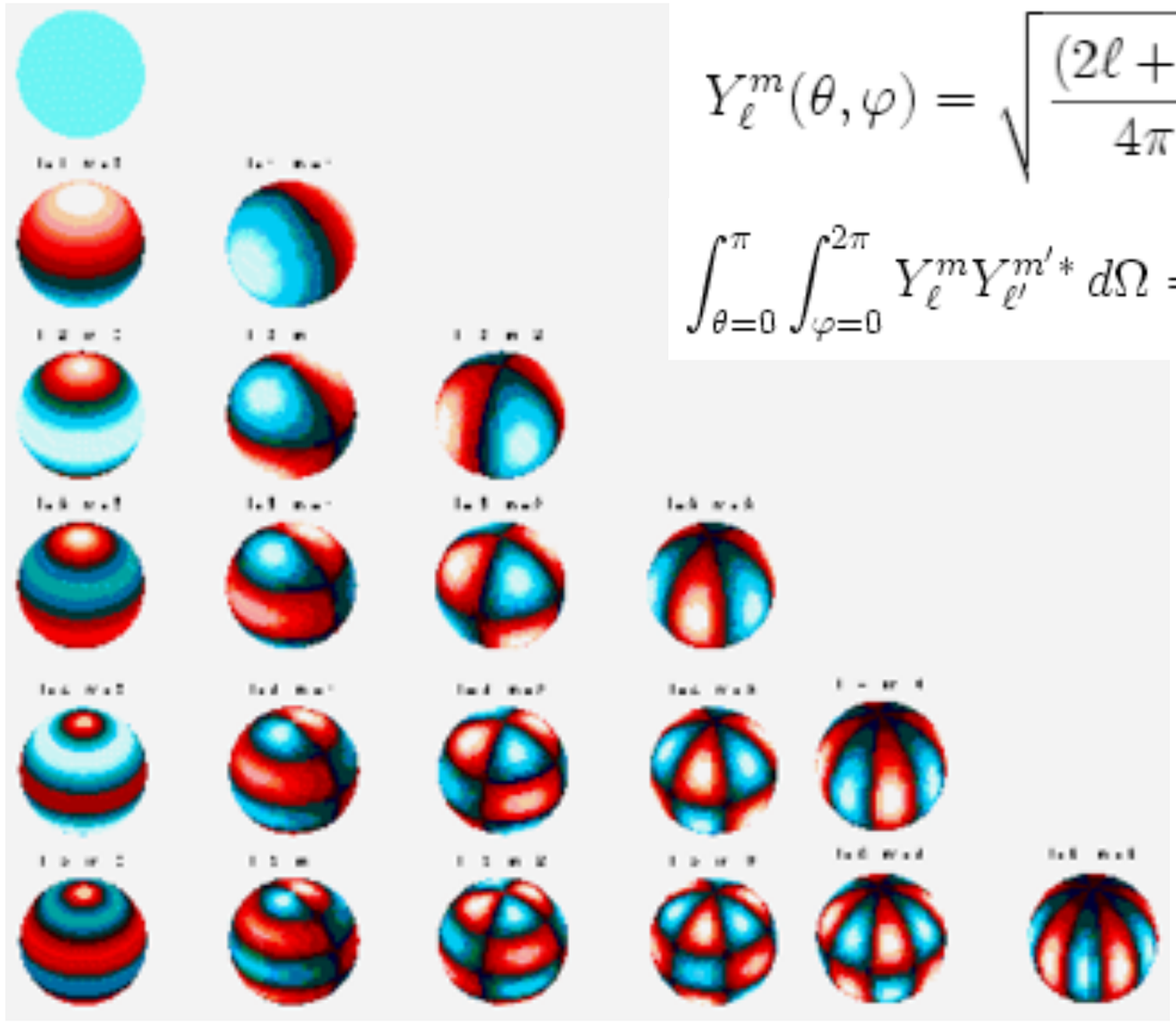

$$Y_\ell^m(\theta,\varphi) = \sqrt{\frac{(2\ell+1)}{4\pi}\frac{(\ell-m)!}{(\ell+m)!}} \cdot e^{im\varphi} \cdot P_\ell^m(\cos\theta)$$

$$\int_{\theta=0}^{\pi}\int_{\varphi=0}^{2\pi} Y_\ell^m Y_{\ell'}^{m'*}\, d\Omega = \delta_{\ell\ell'}\delta_{mm'} \qquad d\Omega = \sin\theta\, d\varphi\, d\theta$$

Visualizing the multipoles

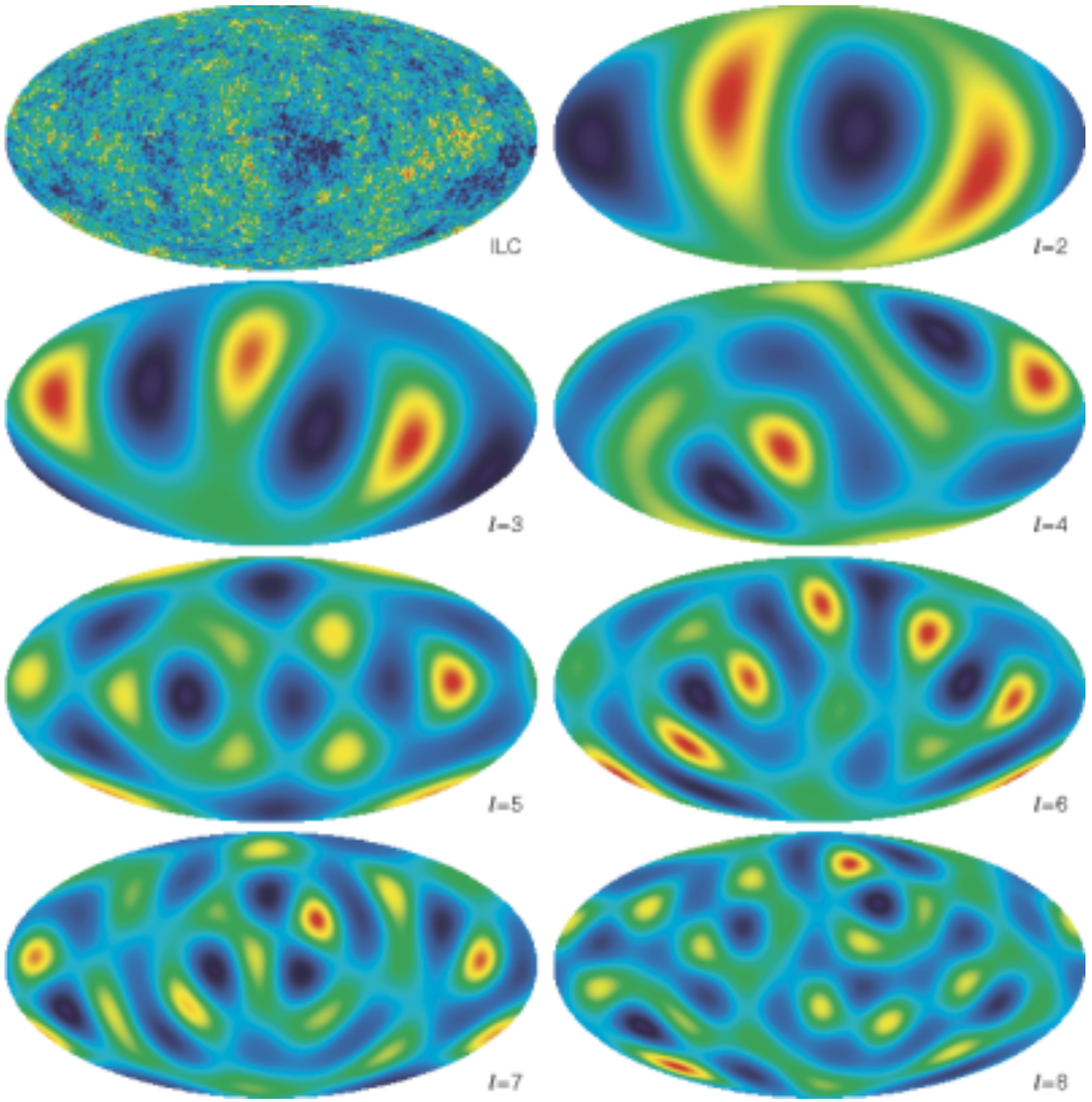

CMB power spectrum

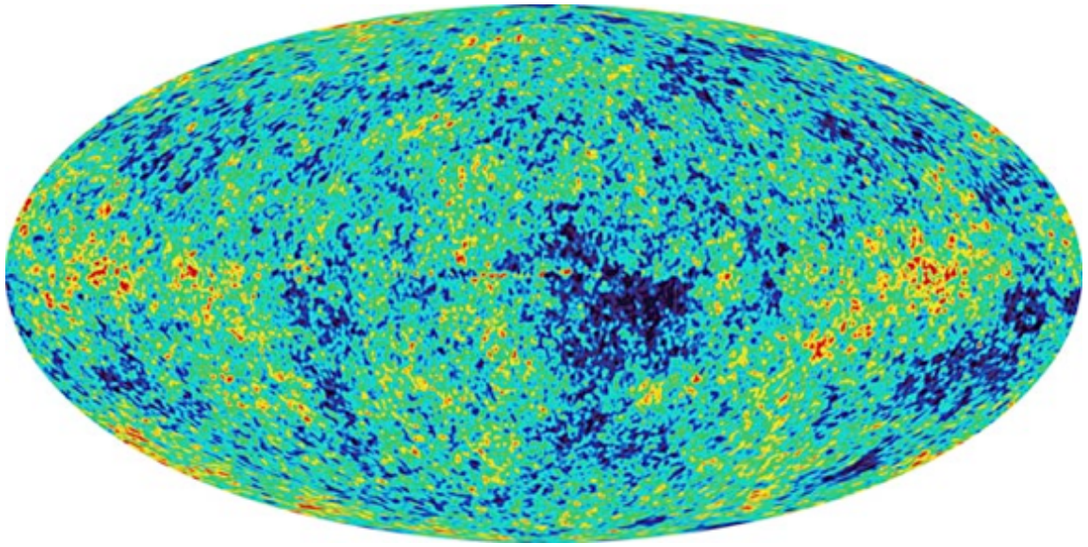

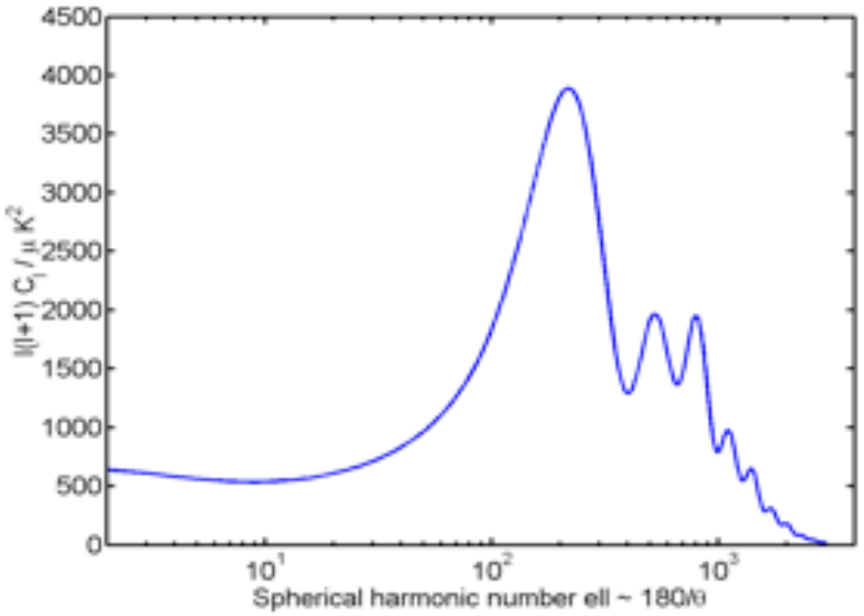

Use spherical harmonics in place of sine waves: $\frac{\Delta T}{T}(\theta,\phi) = \sum_{\ell=1}^{\infty} \sum_{m=-\ell}^{\ell} a_{\ell m} Y_m^{\ell}(\theta,\phi)$

Calculate coefficients, a_{lm}, and then the statistical average: $c_\ell = \langle |a_{\ell m}| \rangle^2$

Amplitude of fluctuations on each scale — that's what we plot.
(TT power spectrum)

Make your own CMB experiment!

- Design experiment to measure $\frac{\Delta T}{T}(\theta, \phi)$
- Find component amplitudes $a_{\ell m} = \int_\Omega \frac{\Delta T}{T}(\theta, \phi) Y^*_{\ell m}(\theta, \phi) d\Omega$
- Plot $c_\ell = \langle |a_{\ell m}| \rangle^2$ against l (where l is inverse of angular scale, $l \sim \pi / \theta$)

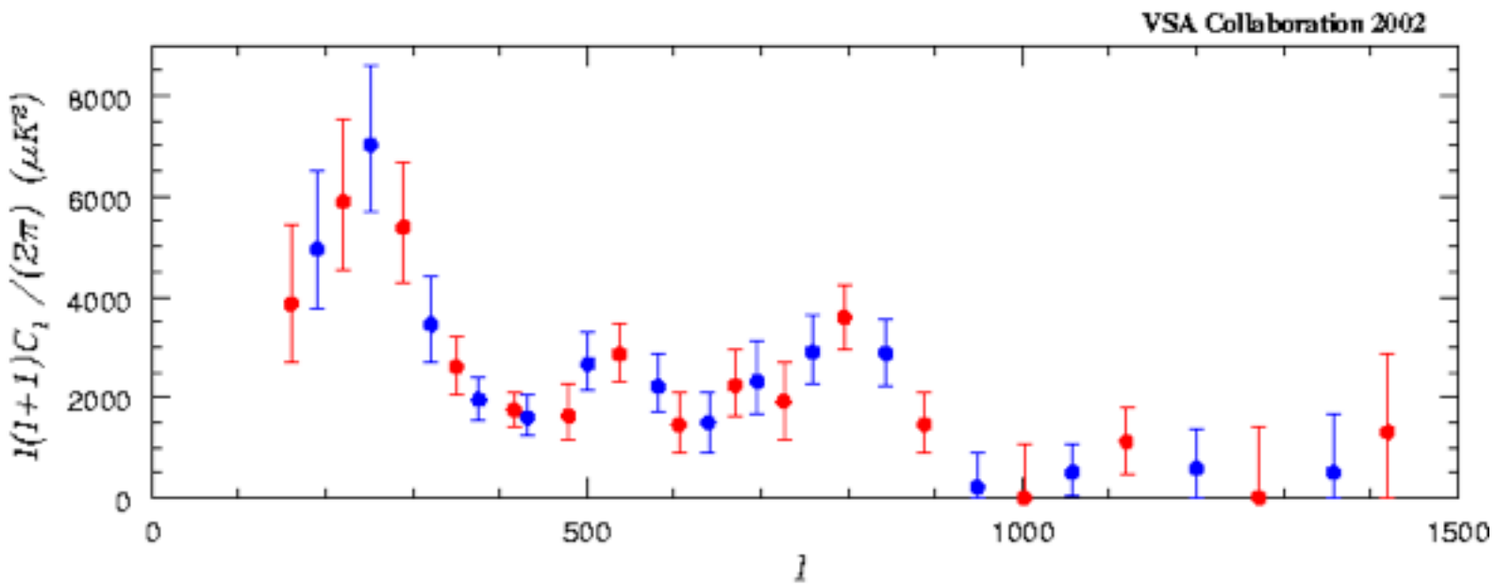

Generating theoretical C_l

INPUT

Favorite cosmological model:
Ω_m, Ω_Λ, σ_8, H_0, ..

??

Physics

powerful cosmological codes (CMBFast or CAMB)

OUTPUT

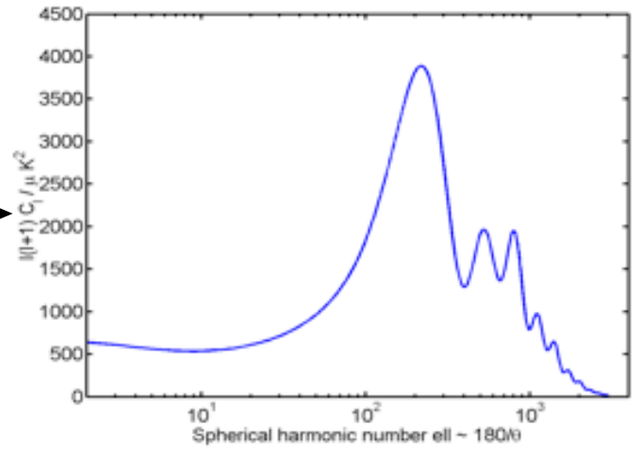

Fit to data

Power at different scales

What does it mean for cosmology?

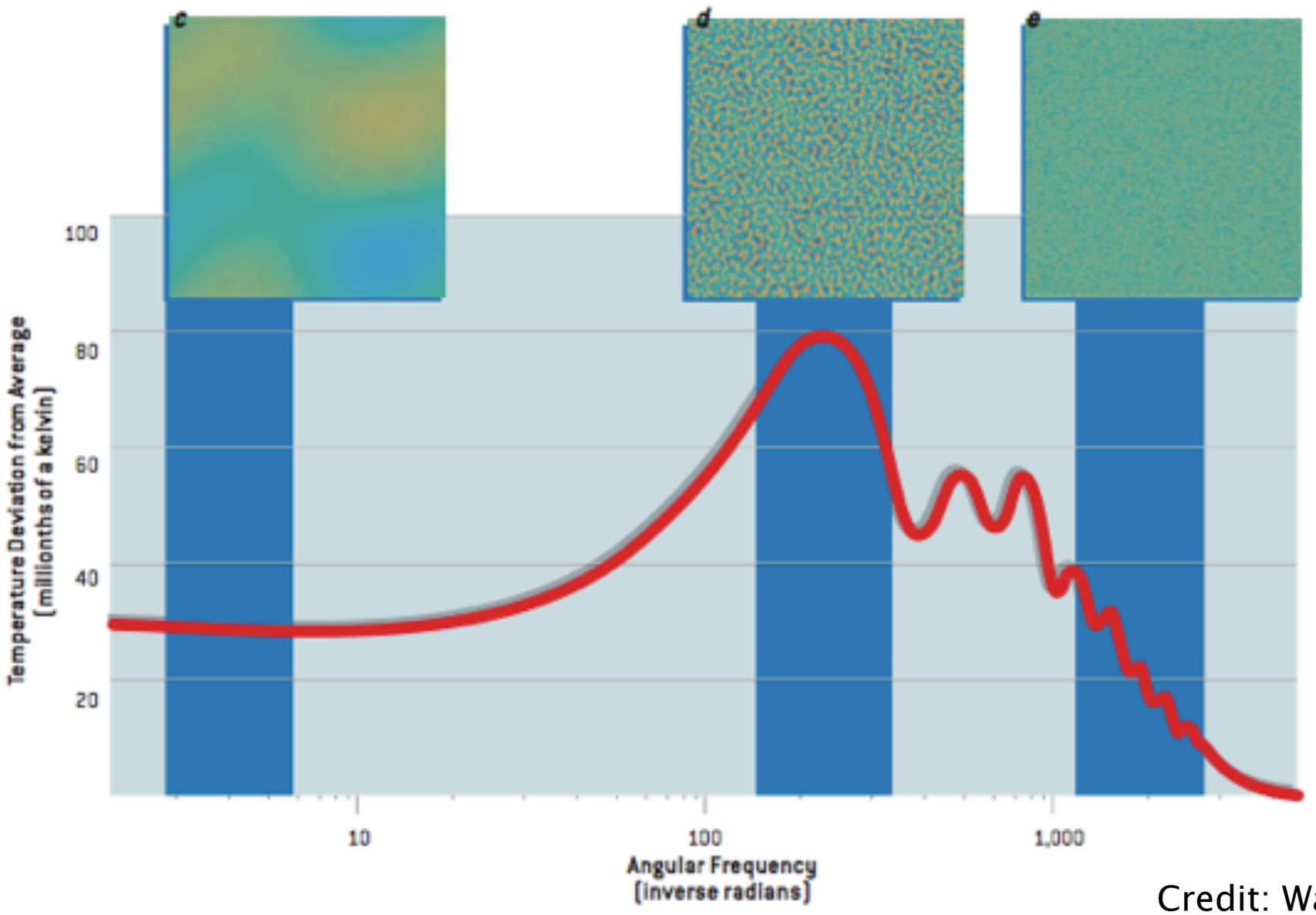

Credit: Wayne Hu

Cosmic and sample variance

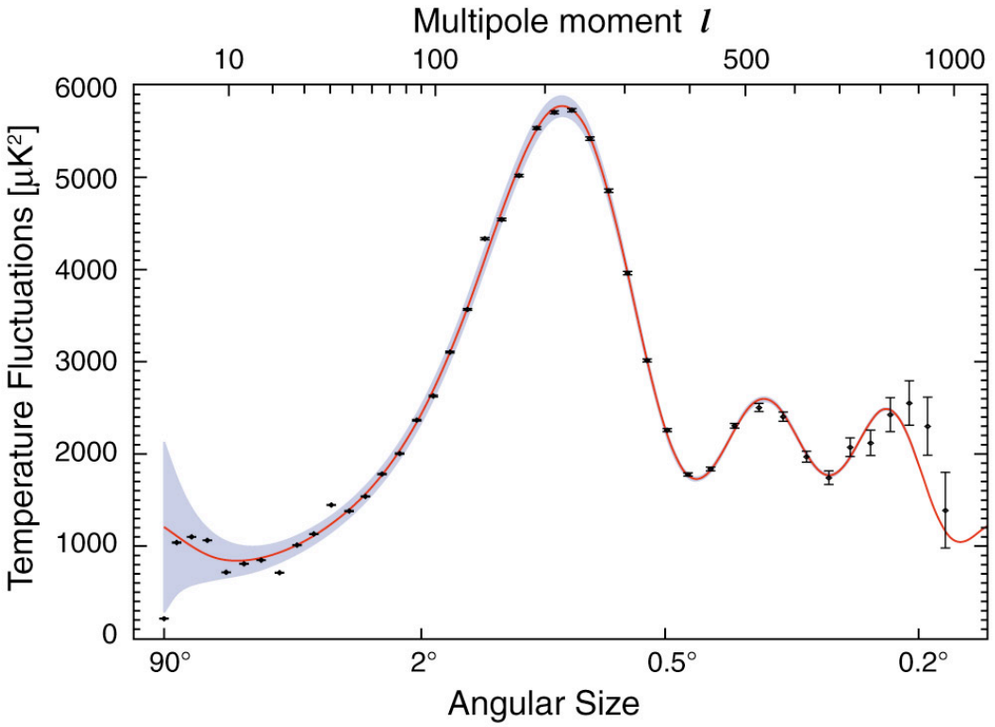

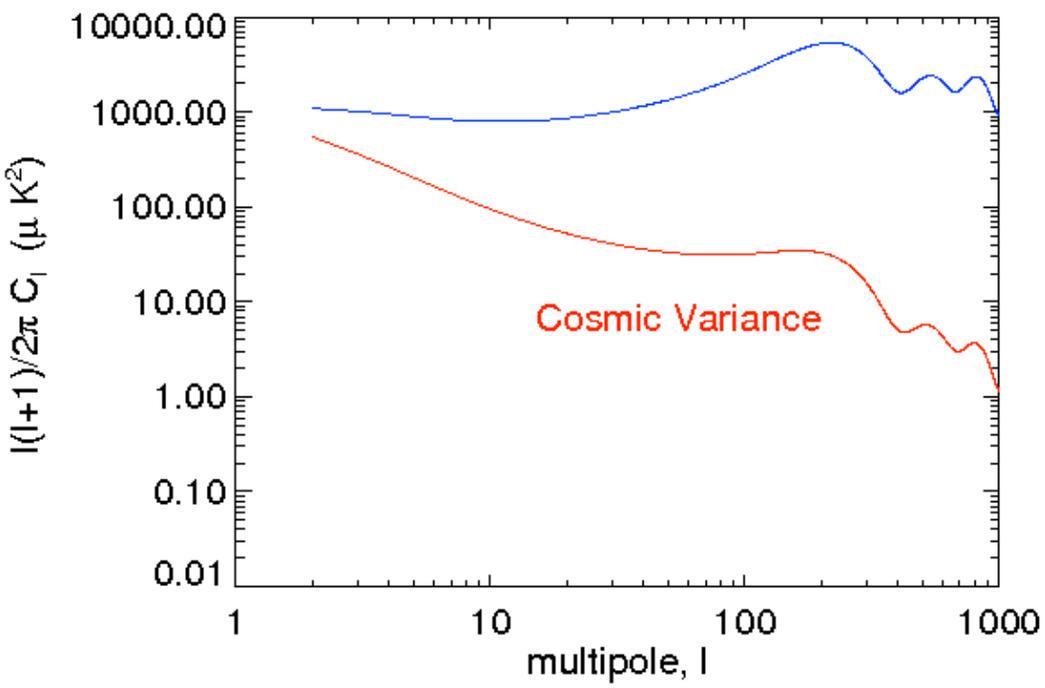

- **Cosmic variance**: on scale *l*, there are only *~l(l+1)* independent modes (only one sky!)

$$\Delta C_\ell = \sqrt{\frac{2}{2\ell+1}} C_\ell$$

- This leads to an inevitable error, in the predicted amplitudes at low *l*, even for very specific cosmological models

- Averaging over *l* in bands of $\Delta l \approx 1$ makes the error scale as l^{-1}

- If the fraction of sky covered is f, then the errors increase by a factor $f^{-1/2}$ and the resulting variance is called **sample variance** (f=0.65 for the PLANCK satellite)

Primordial temp. anisotropies

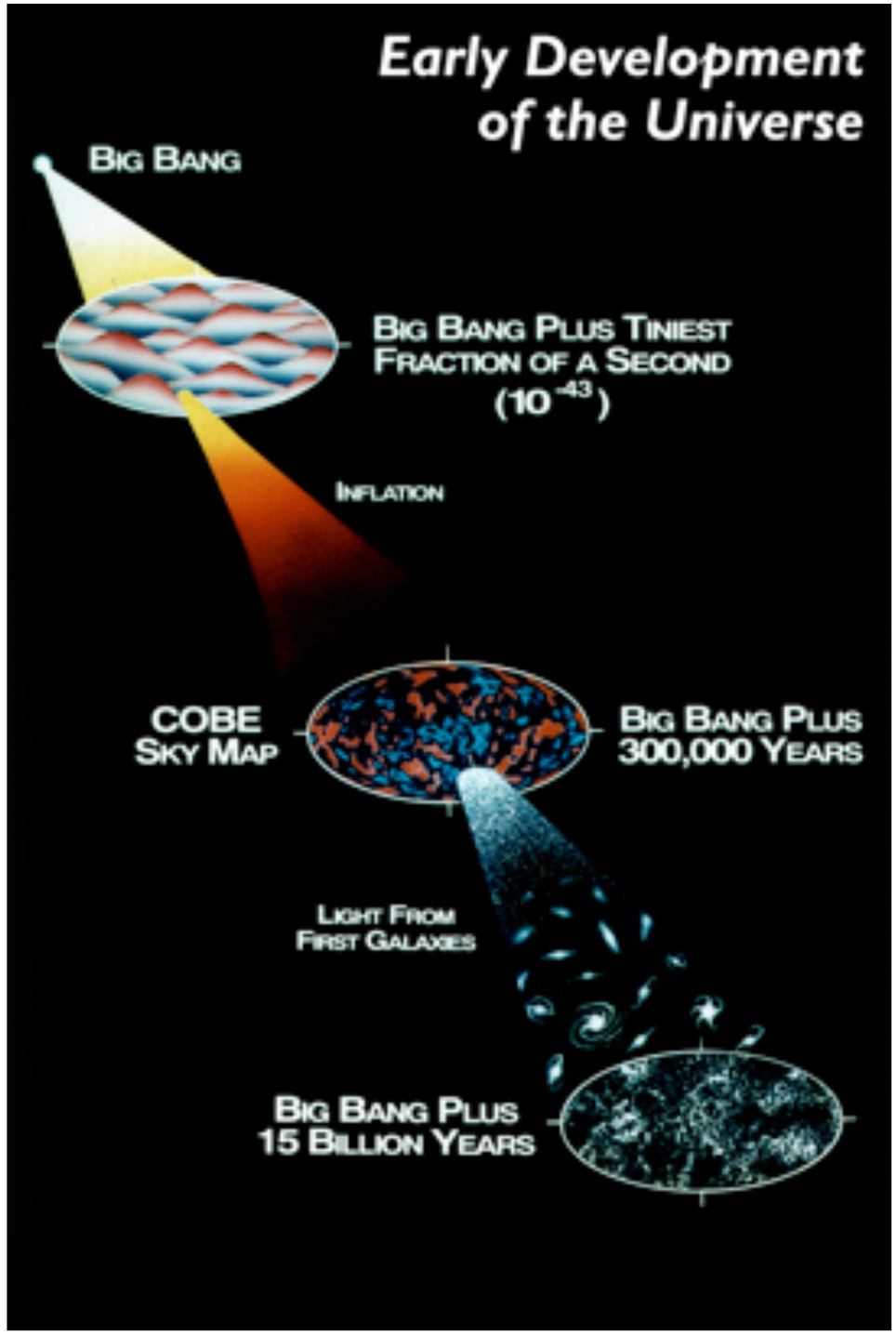

At recombination, when the CMB was released, structure had started to form

This created the “hot” and “cold” spots in the CMB

These were the seeds of structure we see today

Please don’t confuse between the “creation” of the CMB photons, and their “release” from the last scattering surface!

CMB photons are created at much earlier epoch through matter/anti-matter annihilation, and thus, were formed as gamma rays (now cooled down to microwave)

Sources of ΔT

(Secondaries we'll cover in the next lecture)

Table 1. Sources of temperature fluctuations.

PRIMARY	Gravity	
	Doppler	
	Density fluctuations	
	Damping	
	Defects	Strings
		Textures
SECONDARY	Gravity	Early ISW
		Late ISW
		Rees-Sciama
		Lensing
	Local reionization	Thermal SZ
		Kinematic SZ
	Global reionization	Suppression
		New Doppler
		Vishniac
"TERTIARY" (foregrounds & headaches)	Extragalactic	Radio point sources
		IR point sources
	Galactic	Dust
		Free-free
		Synchrotron
	Local	Solar system
		Atmosphere
		Noise, *etc.*

Max Tegmark (astro-ph/9511148)

Power spectrum

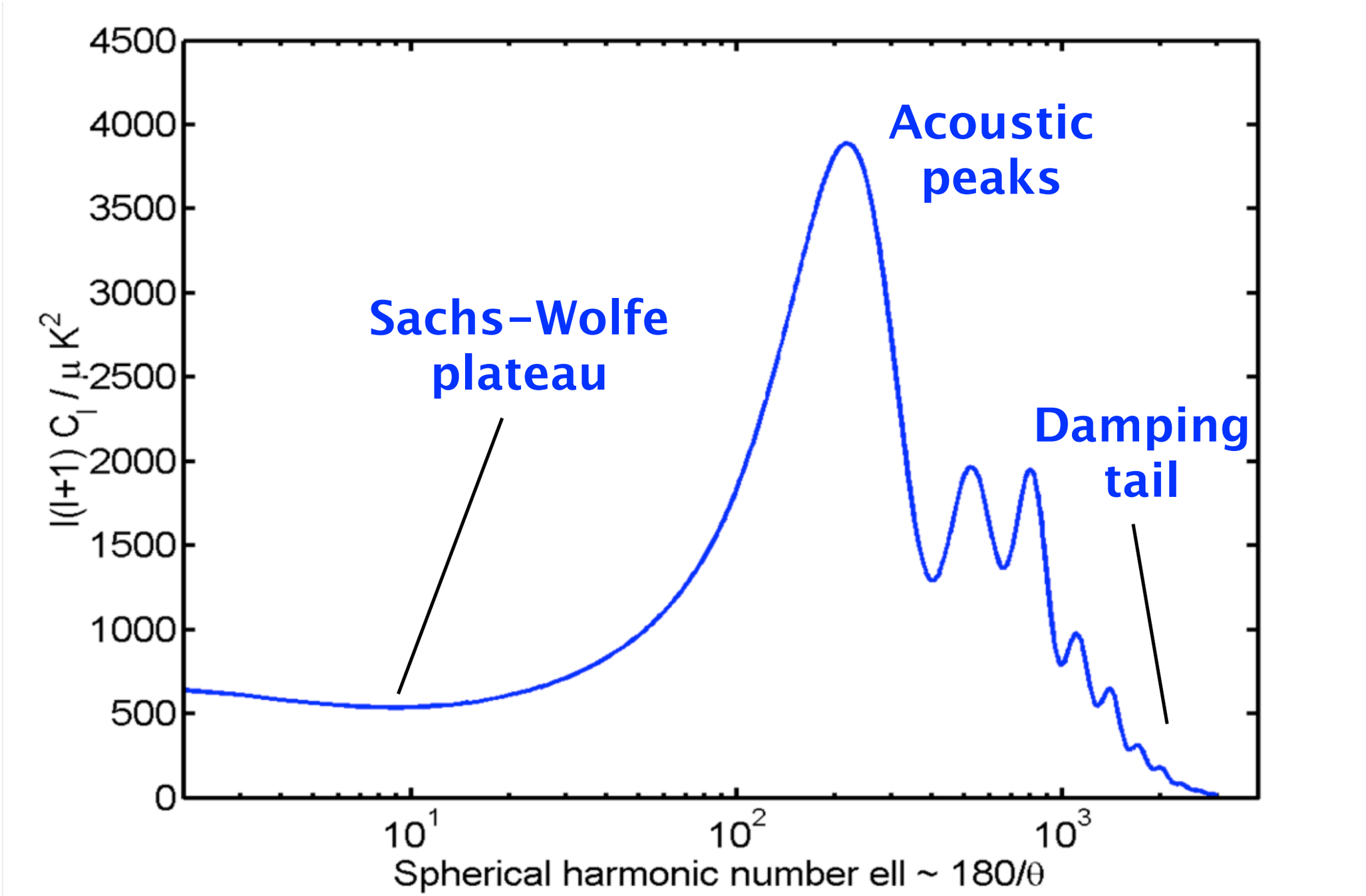

Sources of primary anisotropies

Quantum density fluctuations in the dark matter were amplified by inflation.
Gravitational potential wells (or “hills”) developed, baryons fell in (or moved away).

Various related physical processes affected the CMB photons:

- **Perturbations in the gravitational potential (Sachs-Wolfe effect):** photons that last scattered within high-density regions have to climb out of potential wells and are thus redshifted

- **Intrinsic adiabatic perturbations:** in high-density regions, the coupling of matter and radiation will also compress the radiation, giving a higher temperature

- **Velocity (Doppler) perturbations:** photons last-scattered by matter with a non-zero velocity along the line-of-sight will receive a Doppler shift

Sachs-Wolfe effect

$\Delta\nu/\nu \sim \Delta T/T \sim \Phi/c^2$

Additional effect of time dilation while potential evolves (see White & Hu 1997):

$$\frac{\Delta T}{T} \sim \frac{1}{3}\frac{\Delta\Phi}{c^2}$$

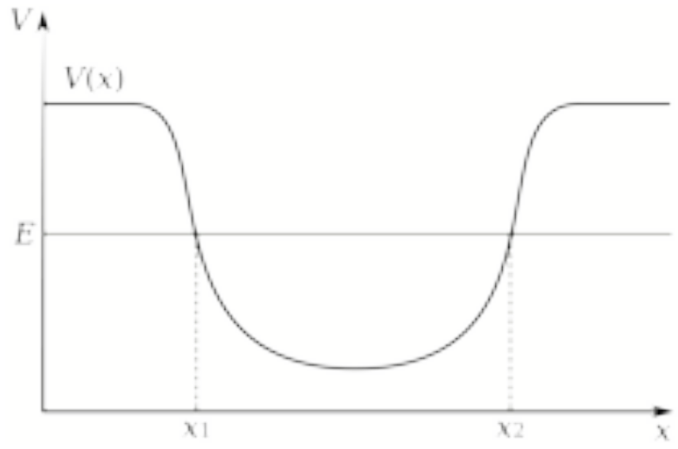

For power-law index of primary density perturbations (n_s=1, Harrison-Zel'dovich spectrum), the Sachs-Wolfe effect produces a flat power spectrum: $C_l^{SW} \sim 1/l(l+1)$

Secondary integrated Sachs-Wolfe effect after recombination: photon falls in potential well, gains energy; photon climbs out, loses energy

No net change in energy, unless the potential changes while the photon is inside (late ISW).

Power at low multipoles *(l≤100)*

The horizon scale at the surface of last scattering (z ~ 1100) corresponds roughly to 2°. At scales larger than this (l ≥ 100), we thus see the power spectrum imprinted during the inflationary epoch, unaffected by later, causal, physical processes.

Due to the limit of cosmic variance, the measurements by COBE some ~25 years ago was already of adequate accuracy!

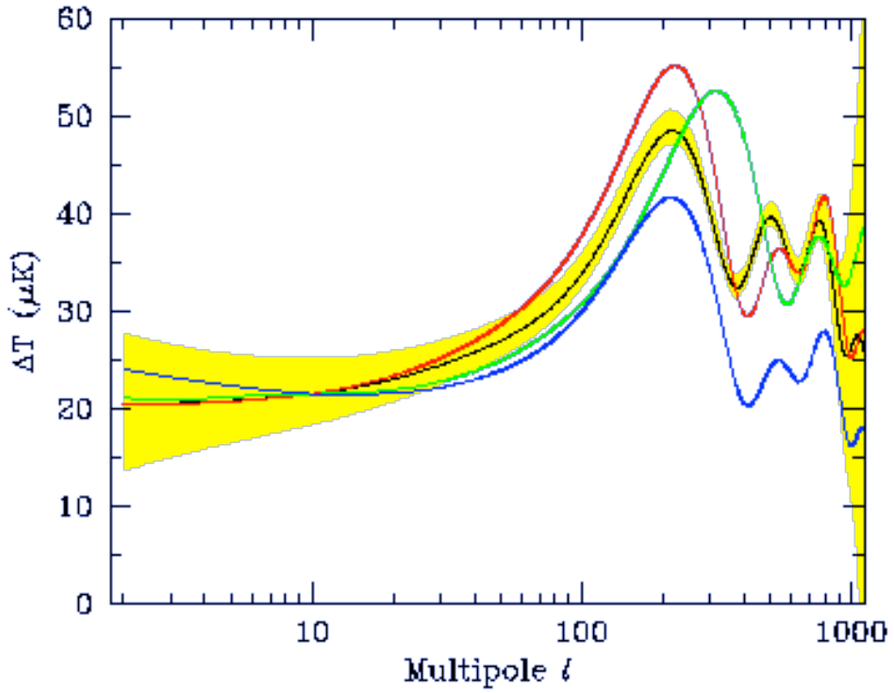

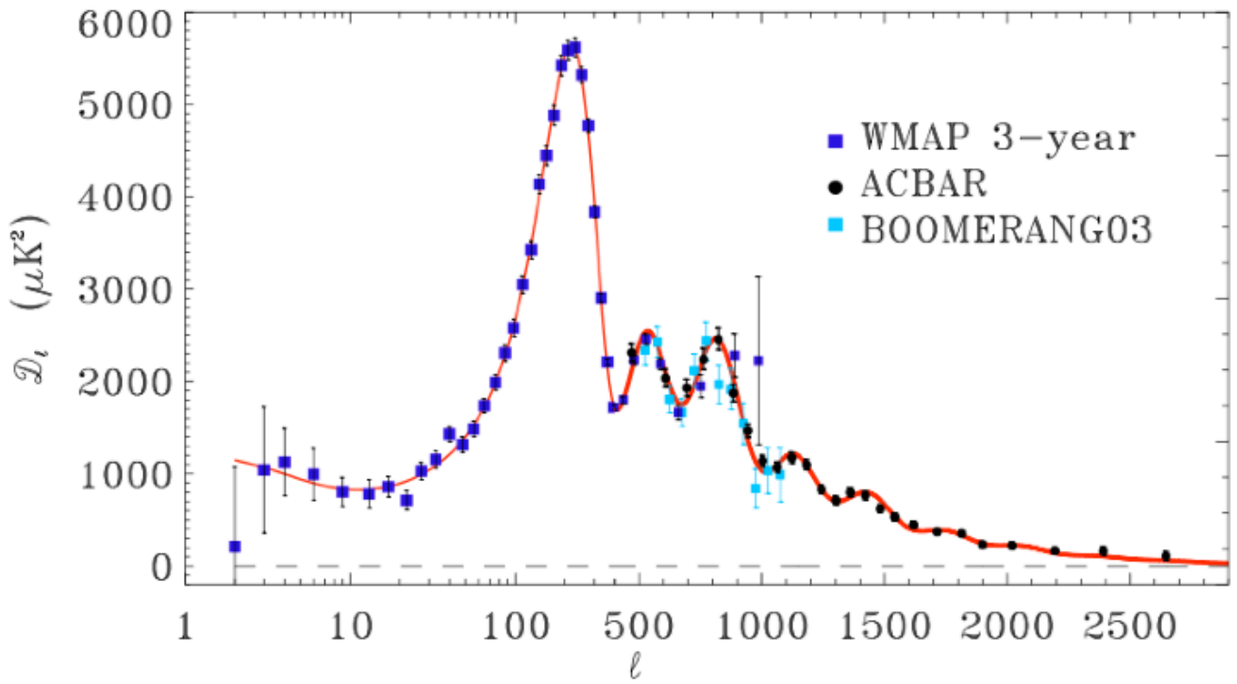

Acoustic oscillations

- Baryons fall into dark matter potential wells: Photon baryon fluid heats up
- Radiation pressure from photons resists collapse, overcomes gravity, expands: Photon-baryon fluid cools down
- Oscillating cycles on all scales. Sound waves stop oscillating at recombination when photons and baryons decouple.

Credit: Wayne Hu

Springs: photon pressure

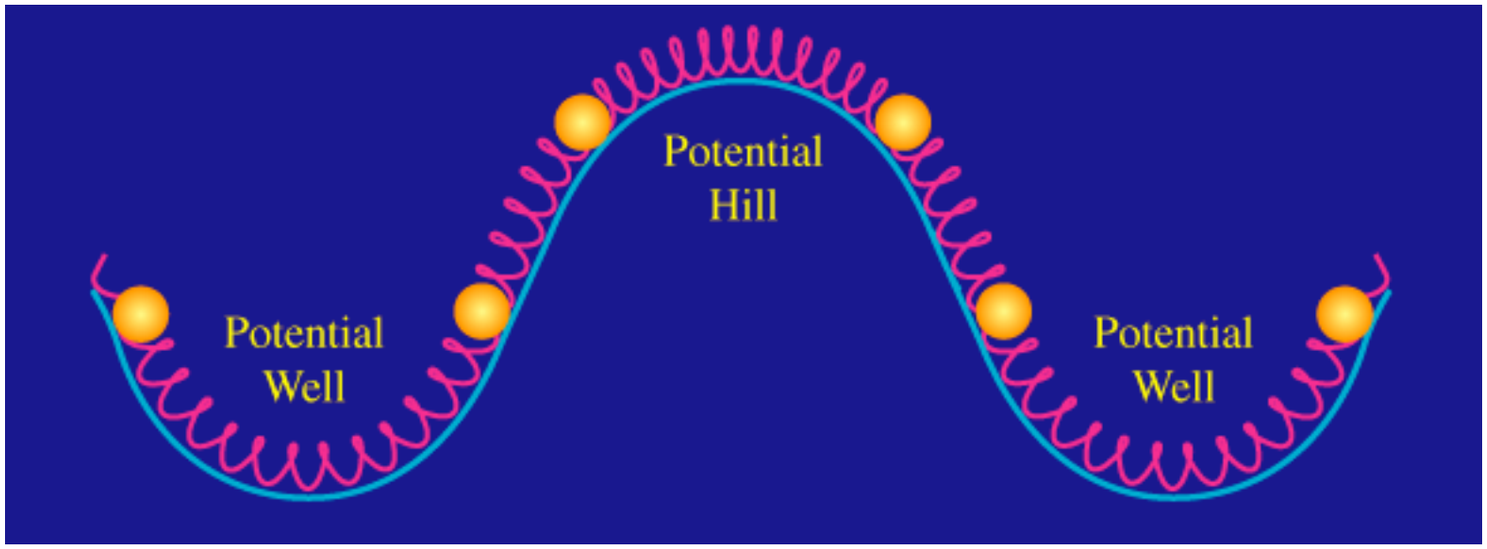

Balls: baryon mass

Acoustic peaks

Oscillations took place on all scales. We see temperature features from modes which had reached the extrema

- Maximally compressed regions were hotter than the average
  Recombination happened later, corresponding photons experience less red-shifting by Hubble expansion: HOT SPOT

- Maximally rarified regions were cooler than the average
  Recombination happened earlier, corresponding photons experience more red-shifting by Hubble expansion: COLD SPOT

Harmonic sequence, like waves in pipes or strings:

2nd harmonic: mode compresses and rarifies by recombination
3rd harmonic: mode compresses, rarifies, compresses

➡ 2nd, 3rd, .. peaks

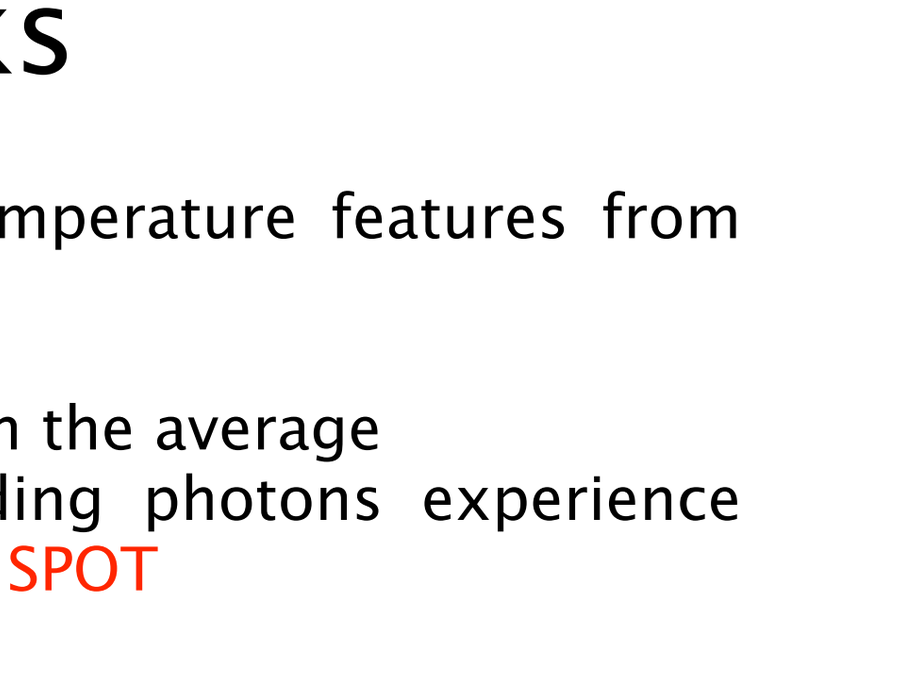

Harmonic sequence

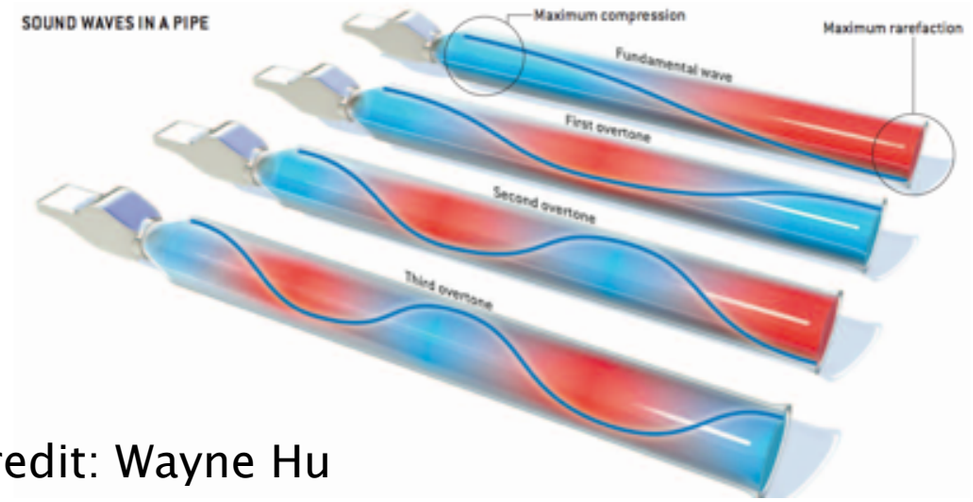

Credit: Wayne Hu

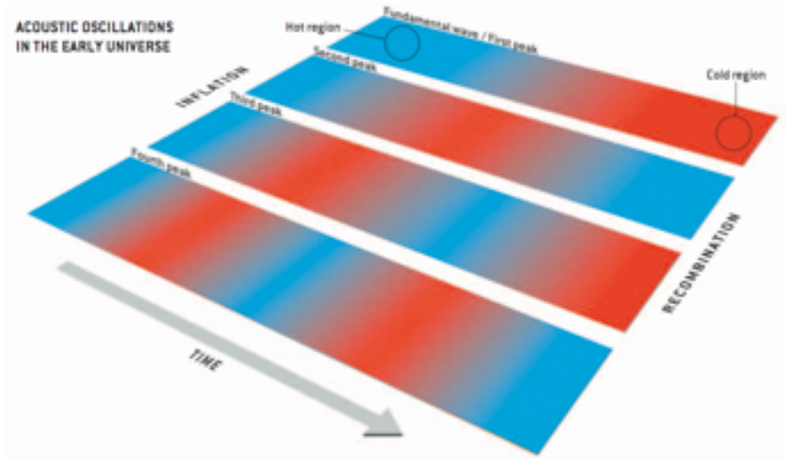

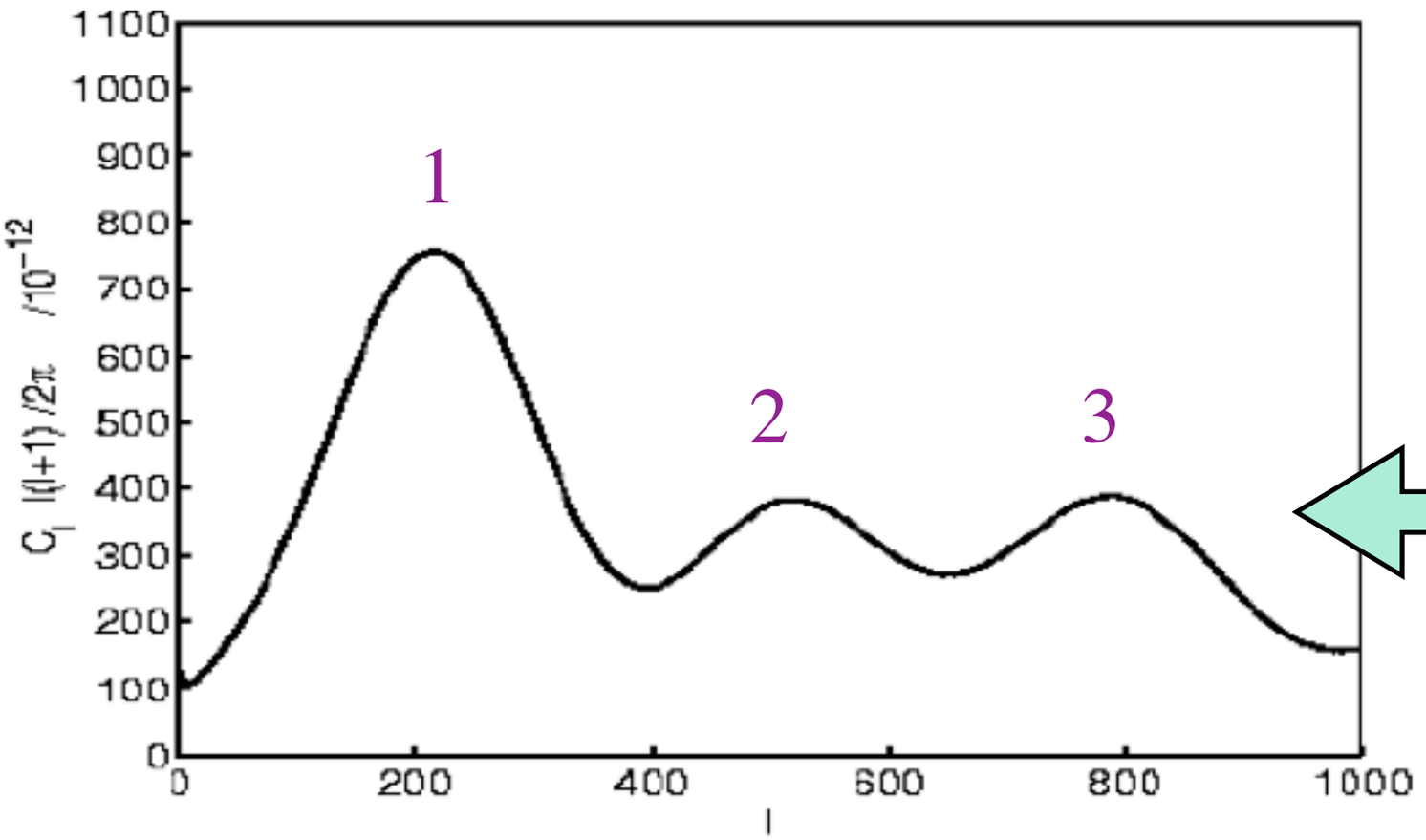

Modes with half the wavelengths osccilate twice as fast ($\nu = c/\lambda$).

Peaks are equally spaced in ℓ

Doppler shifts

Times in between maximum compression/rarefaction, modes reached maximum velocity

This produced temperature enhancements via the Doppler effect (non-zero velocity along the line of sight)

This contributes power in between the peaks

➡ **Power spectrum does not go to zero**

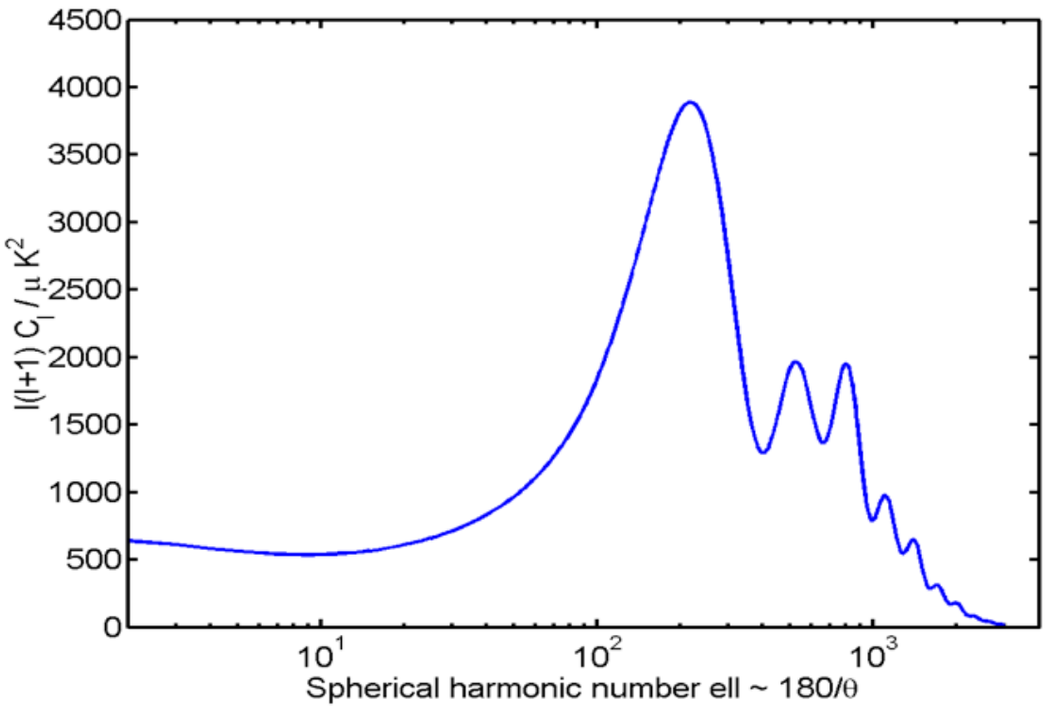

Damping and diffusion

- Photon diffusion (Silk damping) suppresses fluctuations in the baryon-photon plasma

- Recombination does not happen instantaneously and photons execute a random walk during it. Perturbations with wavelengths which are shorter than the photon mean free path are damped (the hot and cold parts mix up)

This is same as a low-resolution instrument blurs all the details!

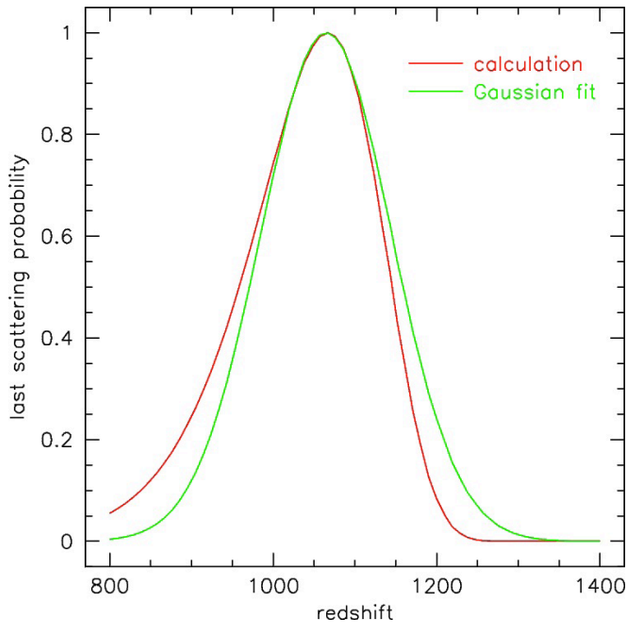

Thickness of the LSS

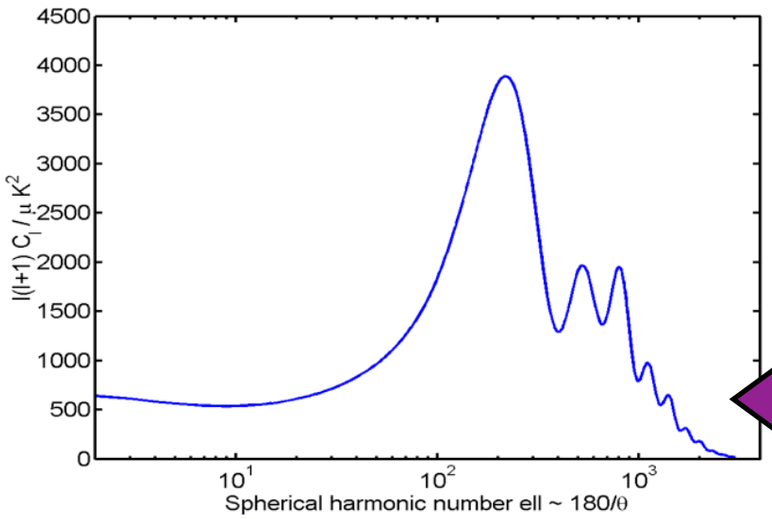

Power falls off

Power spectrum summary

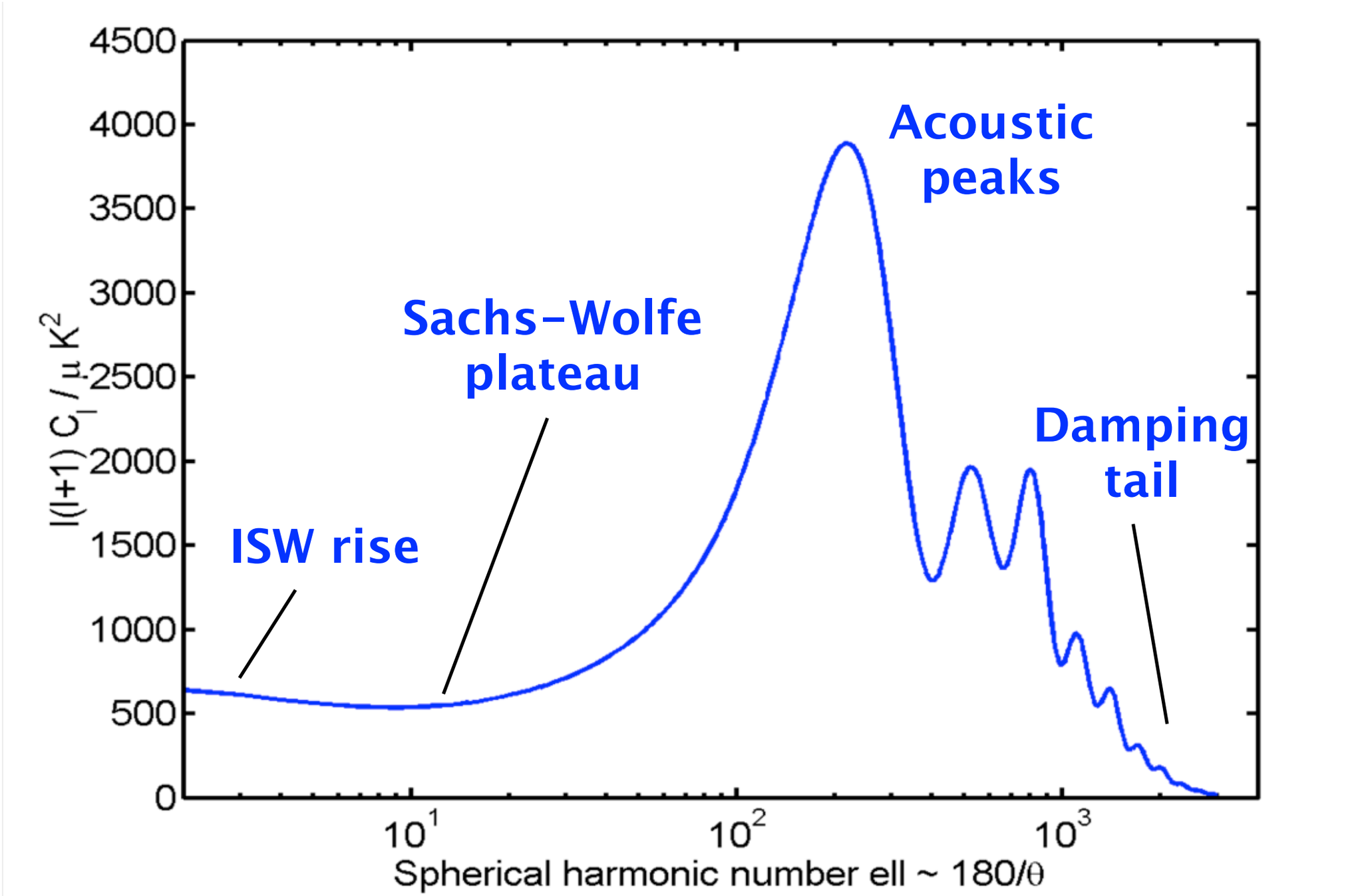

Which way the peaks move?

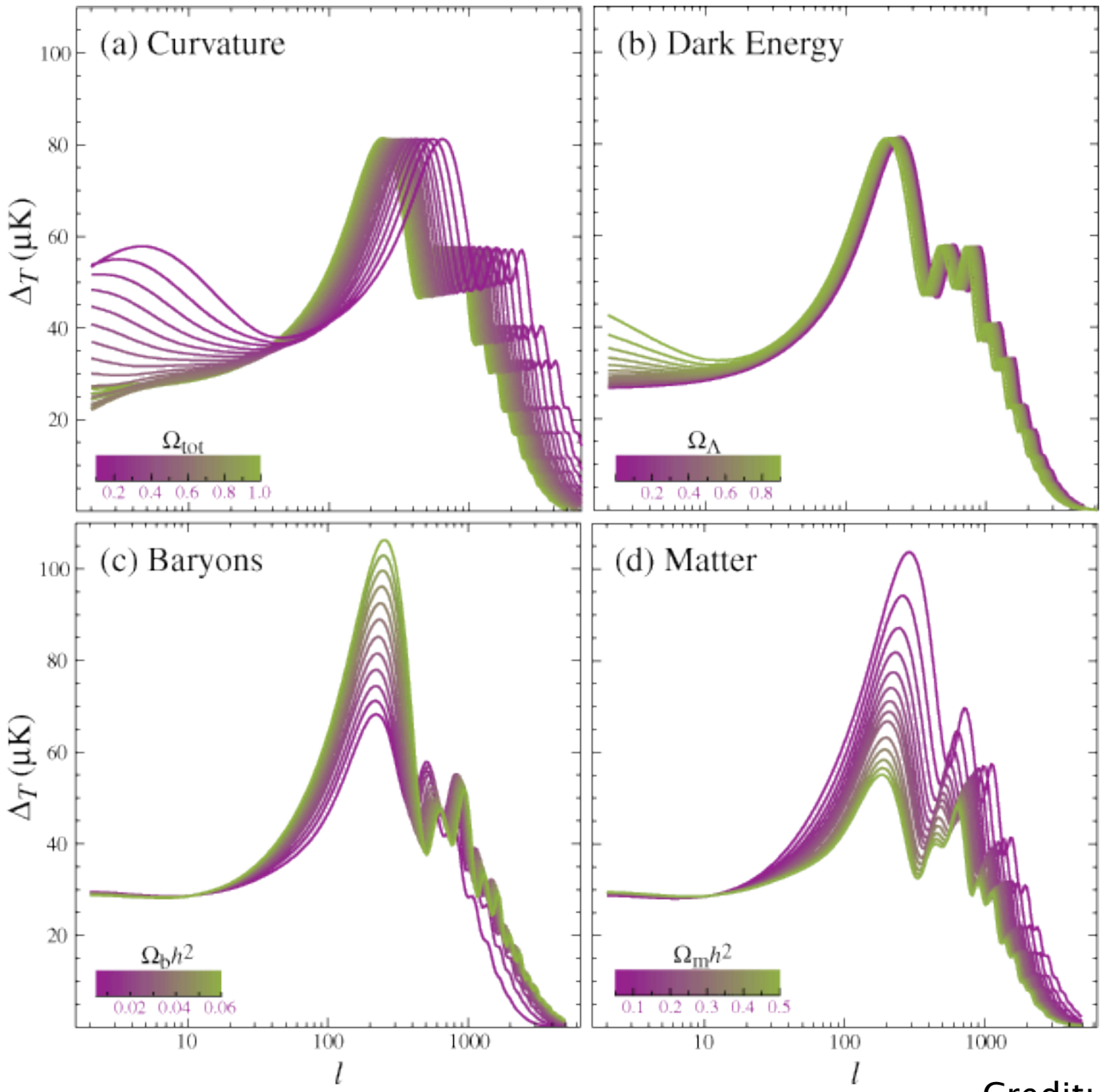

Credit: Wayne Hu

Baryon loading

The presence of more baryons increases the amplitude of the oscillations (baryons drag the fluid into potential wells).

Perturbations are then compressed more before radiation pressure can revert the motion.

This causes an alternation in the odd and even peak heights that can be used to measure the abundance of cosmic baryons.

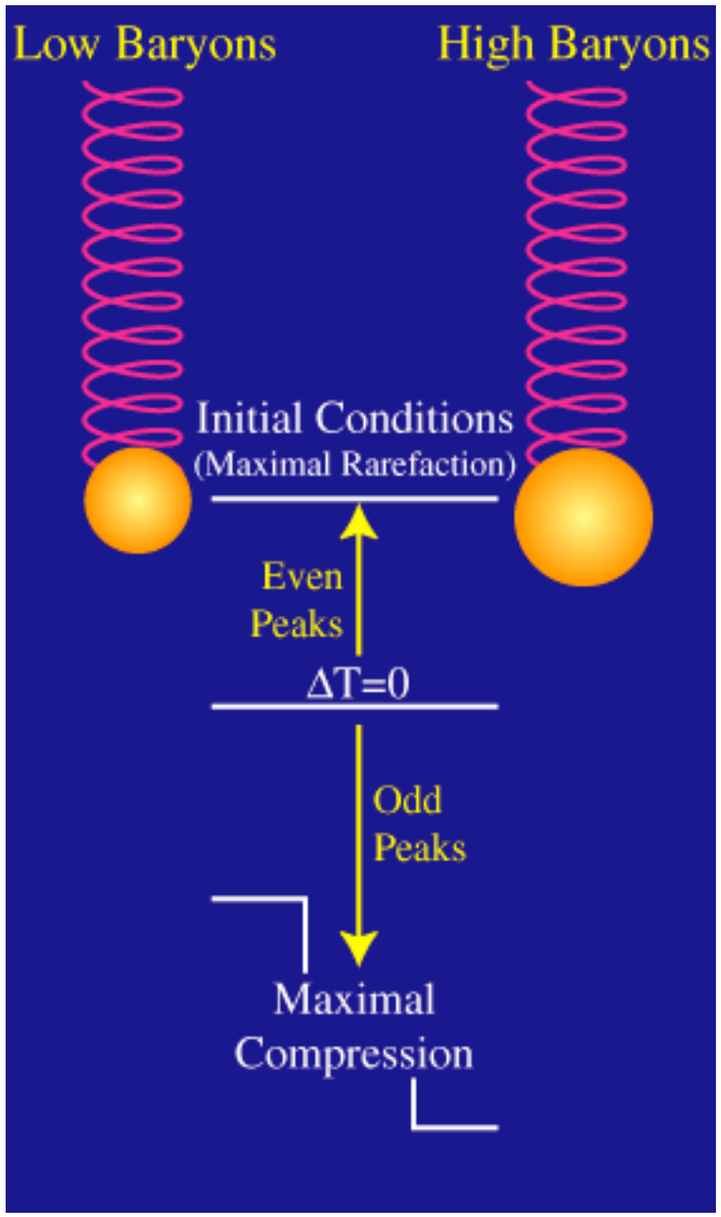

Credit: Wayne Hu

Baryons in the power spectrum

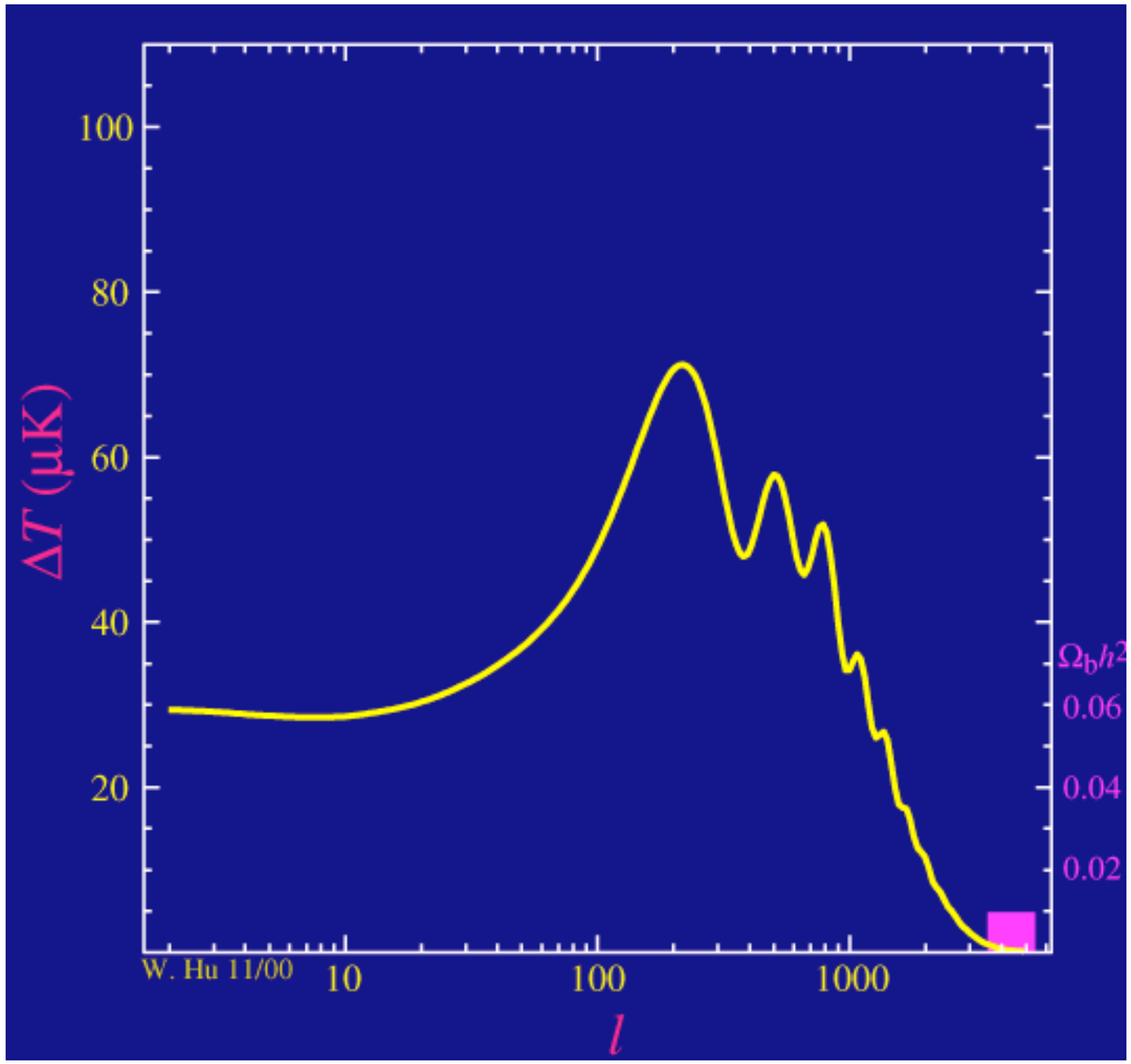

Credit: Wayne Hu

Power spectrum shows baryon enhance every other peak, which helps to distinguish baryons from cold dark matter

DM in the power spectrum

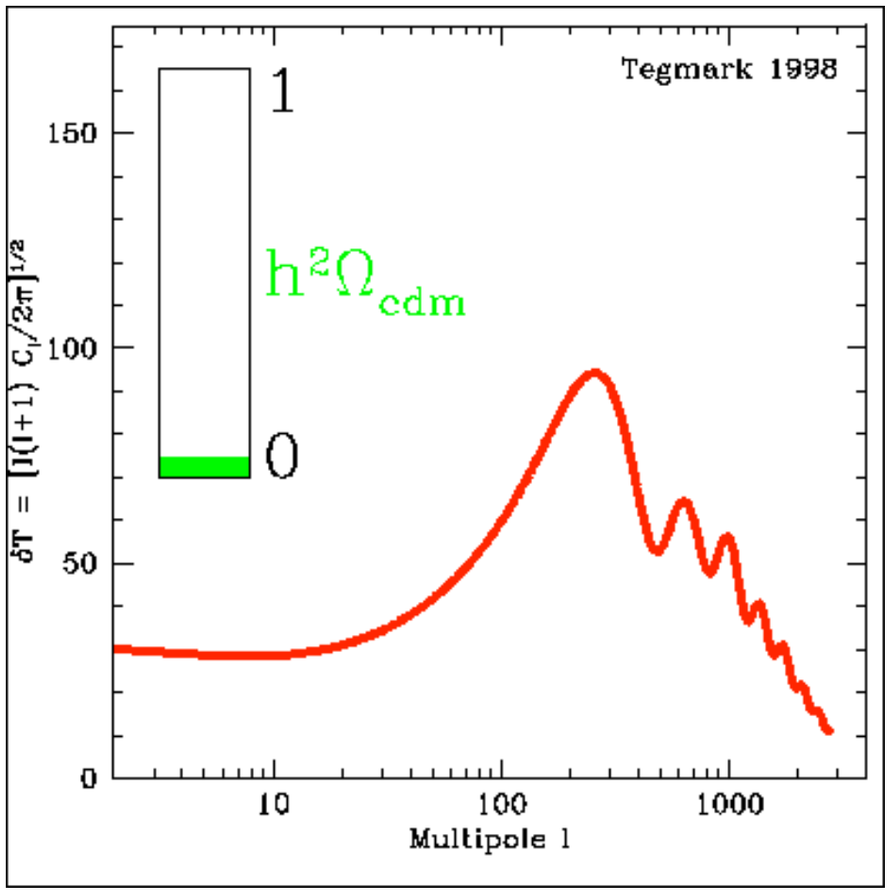

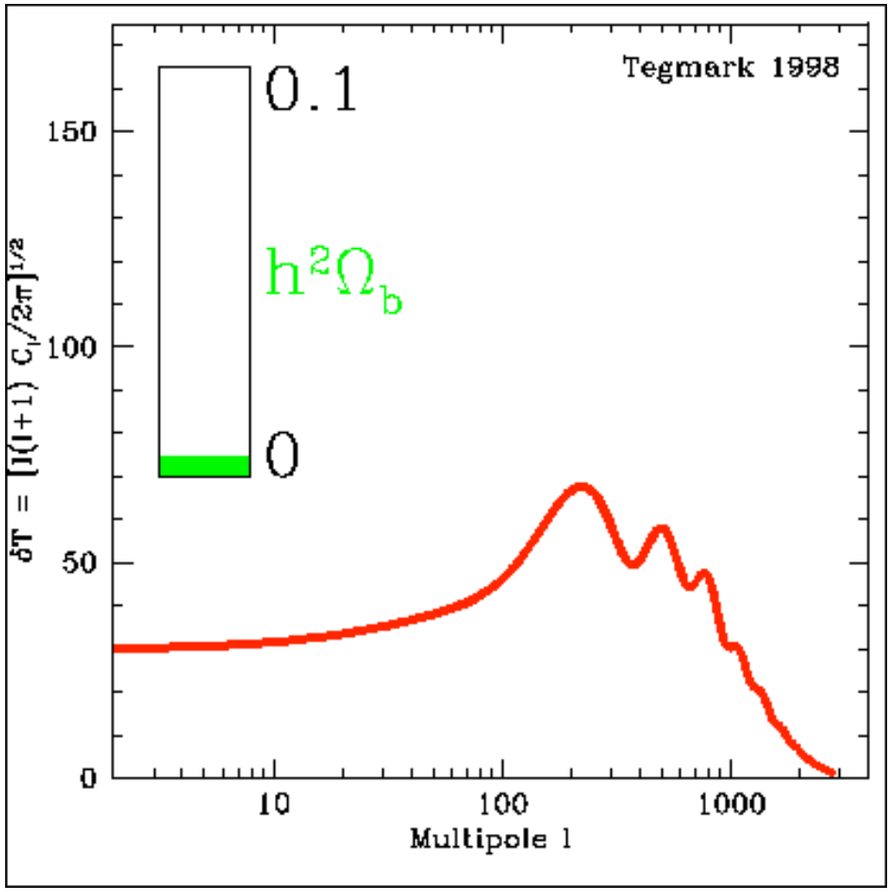

Cold dark matter

Baryons

Credit: Max Tegmark

Effect of curvature

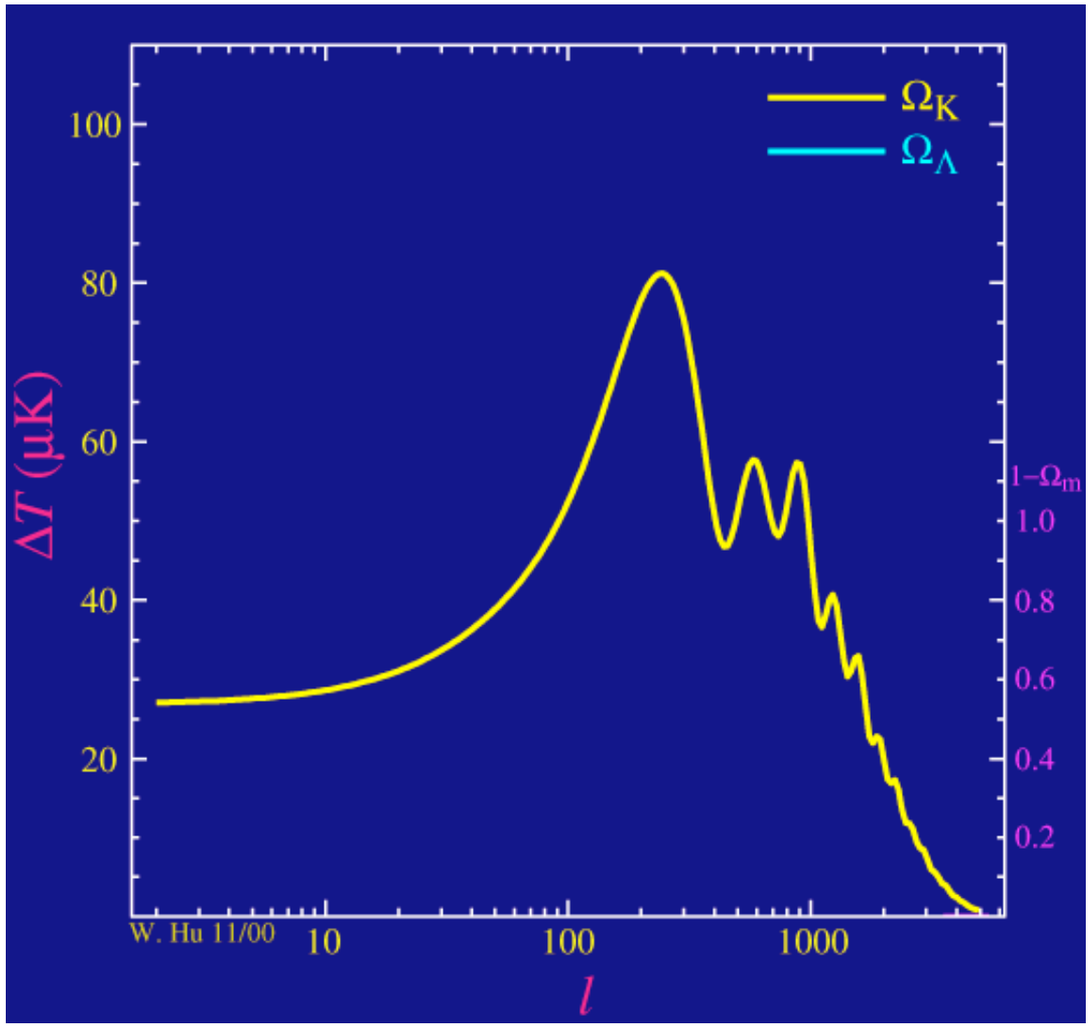

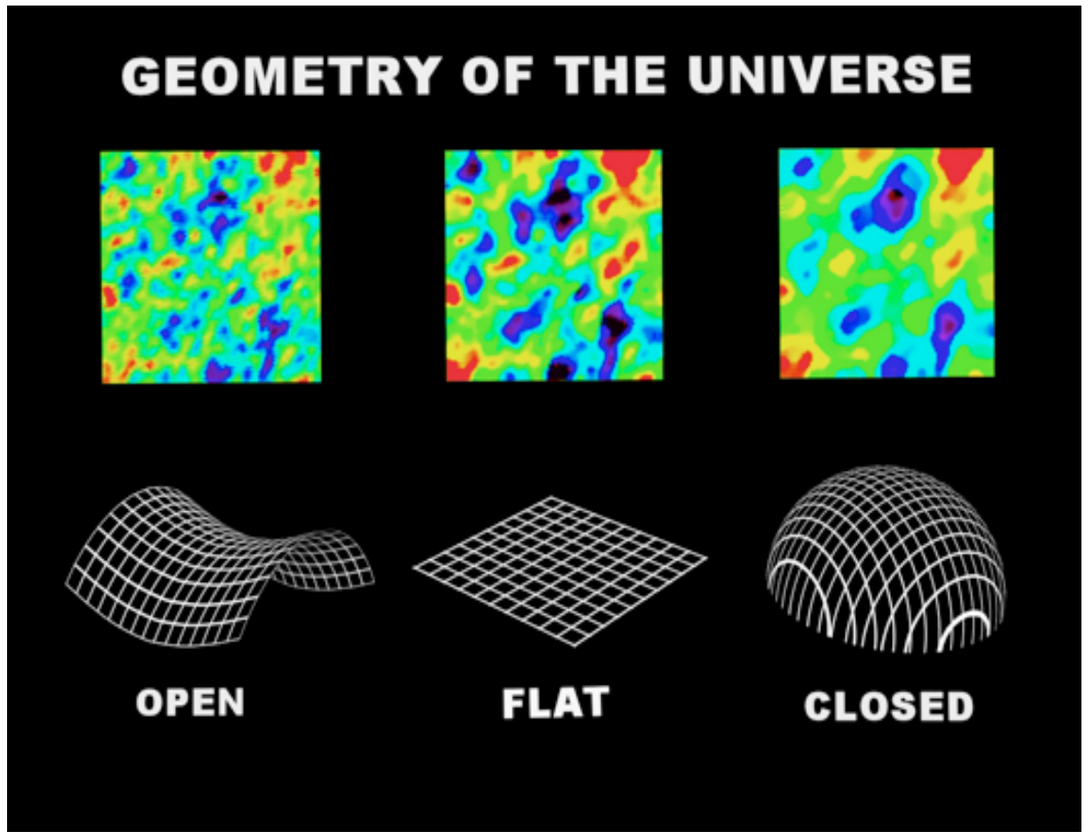

Ω_k does not change the amplitude of the power spectrum, rather it shifts the peaks sideways. This follows from the conversion of the physical scales (on the LSS) to angular scales (that we observe), which depends on the geometry.

Curvature (cosmological constant, Ω_Λ) also causes ISW effect on large scales, by altering the growth of structures in the path of CMB photons.

Effect of re-ionization

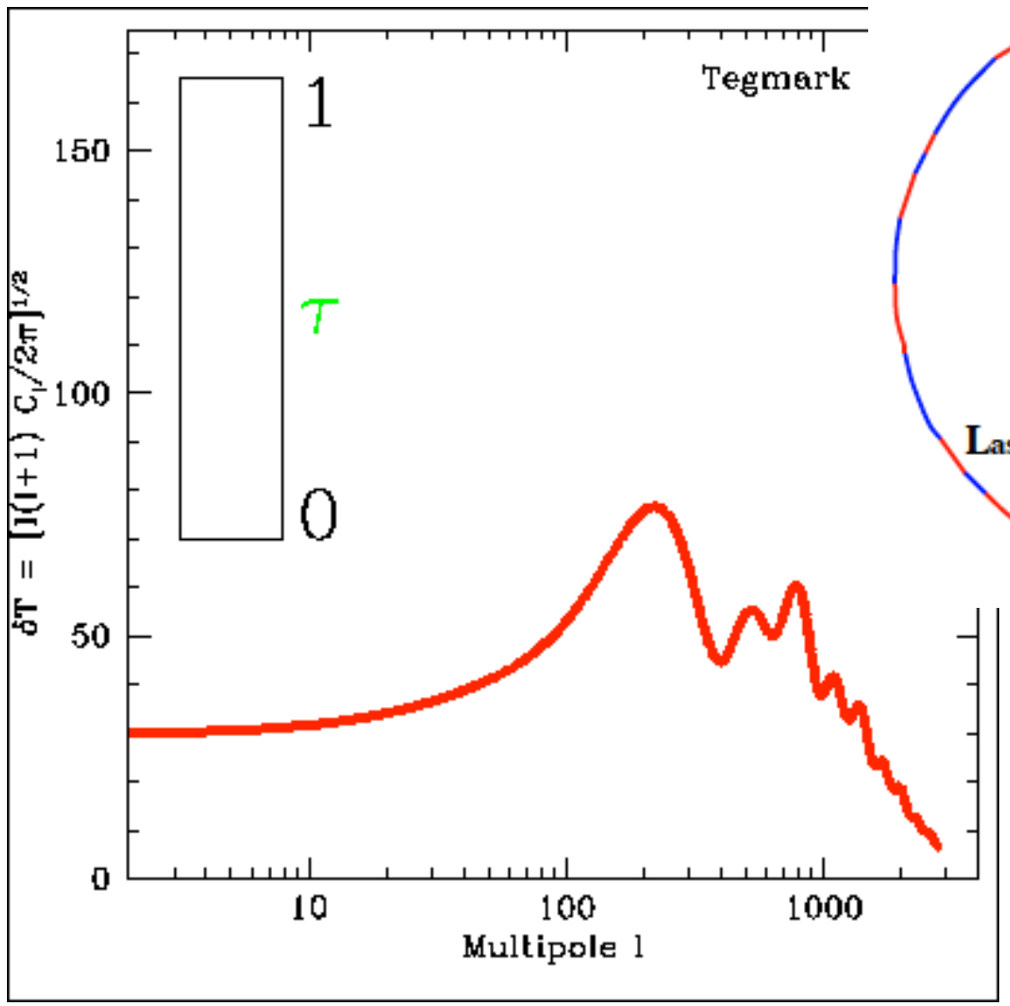

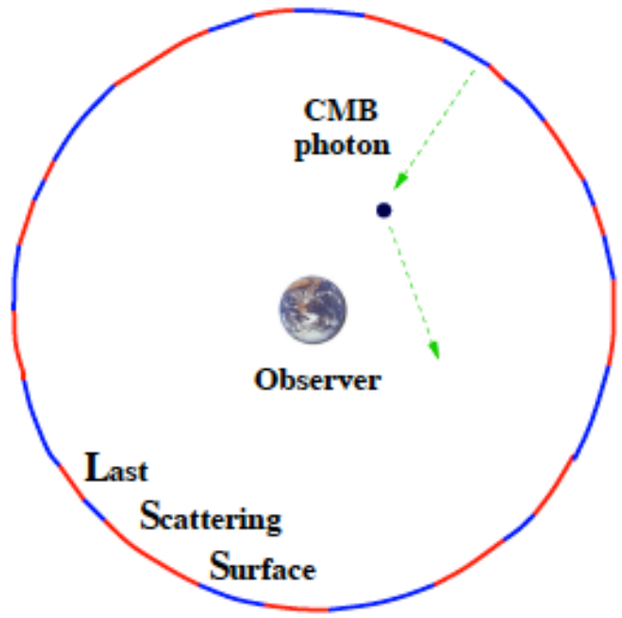

$$\frac{\Delta T}{T_0}(\theta) = e^{-\tau_\nu} \left.\frac{\Delta T}{T_0}(\theta)\right|_{orig.} + \left.\frac{\Delta T}{T_0}(\theta)\right|_{new}$$

"suppression (blurring)" & "generation"

Thomson scattering smears-out the features in the power spectrum, causing peaks at all scales by a constant factor $e^{-\tau}$

(it also generates new anisotropies due to Doppler motion and the Ostriker-Vishniac effect – next lecture!)

CMB parameter cheat sheet

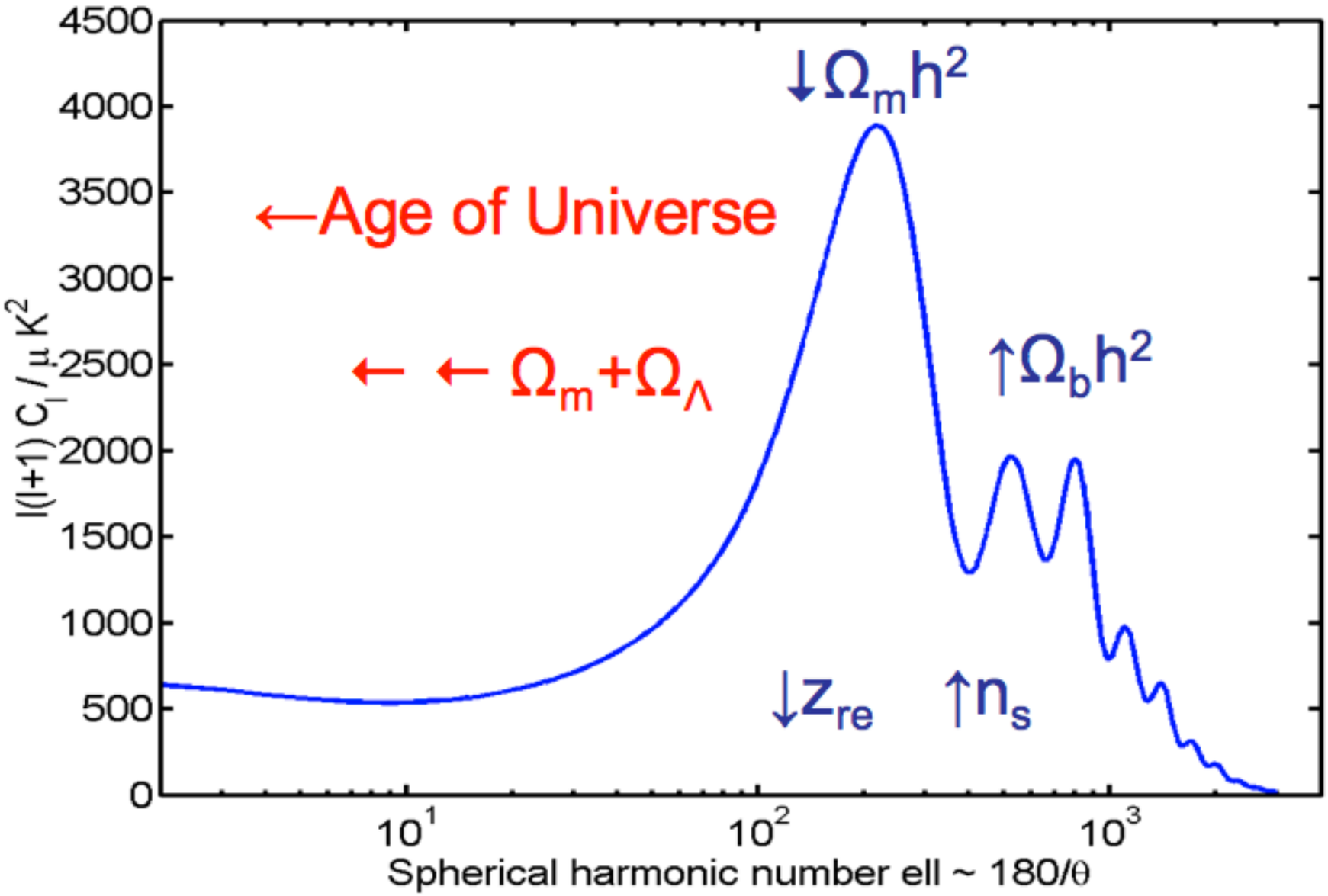

Outline of the CMB exercise

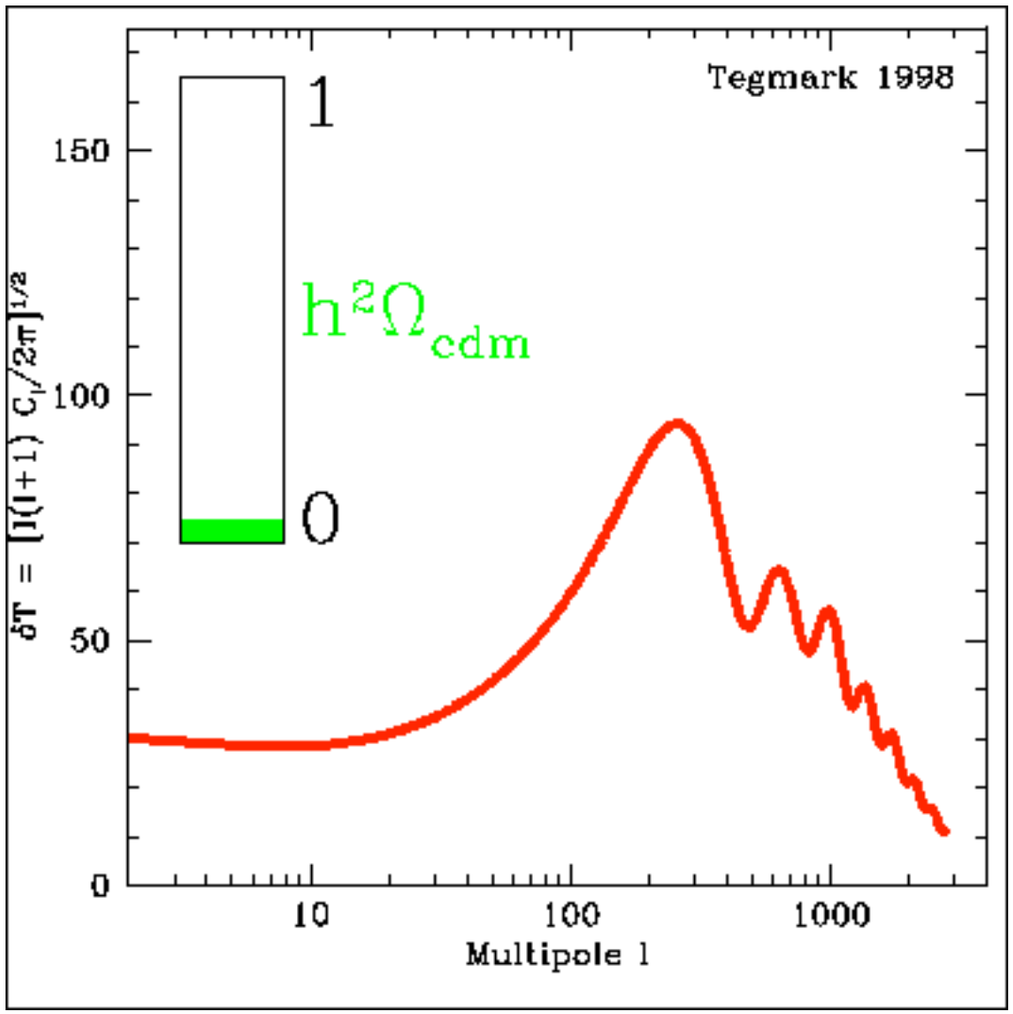

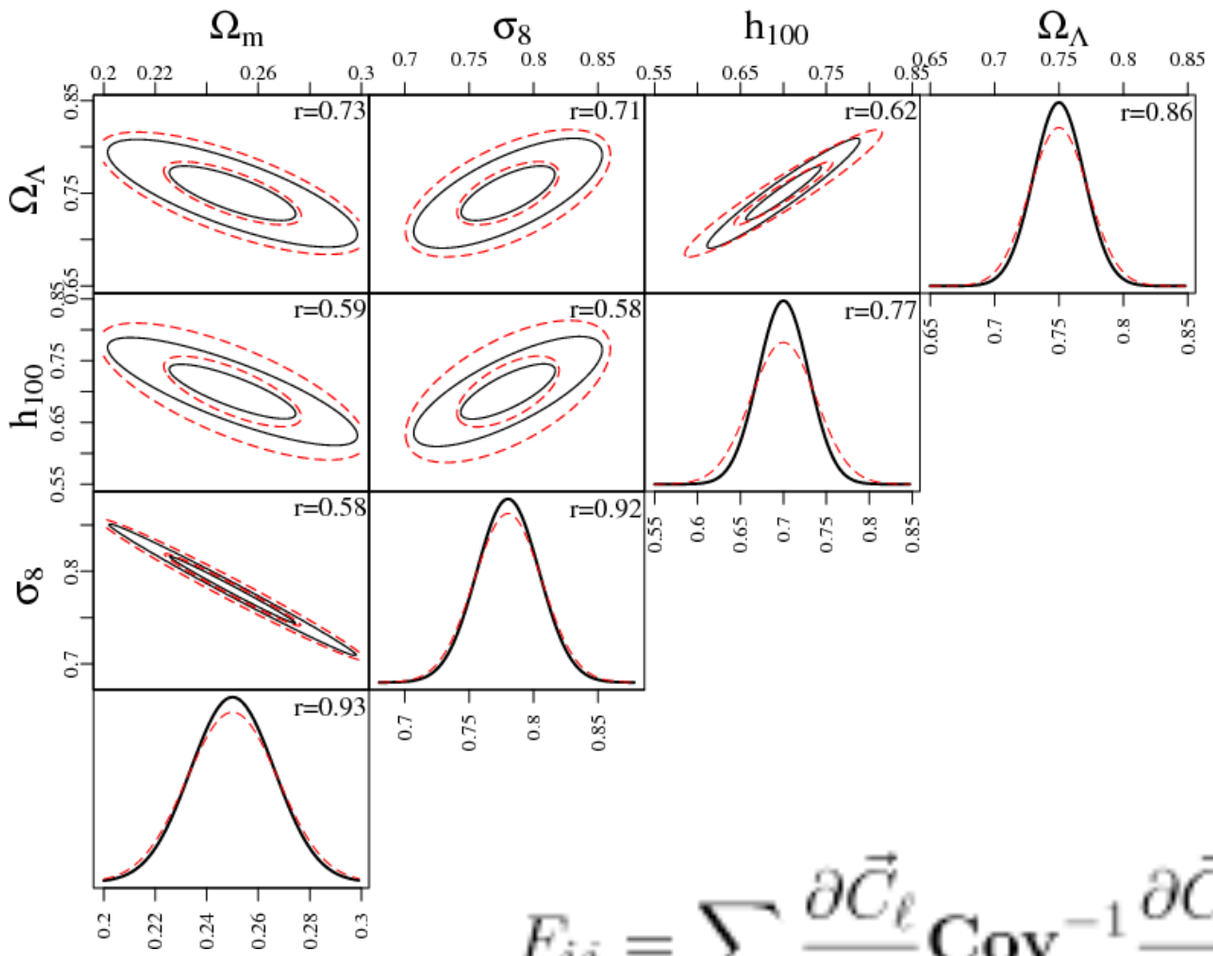

$$F_{ij} = \sum_\ell \frac{\partial \vec{C}_\ell}{\partial s_i} \mathbf{Cov}^{-1} \frac{\partial \vec{C}_\ell}{\partial s_j}$$

We will use online CMB tools, e.g.
http://lambda.gsfc.nasa.gov/toolbox/tb_cmbfast_form.cfm

Online C_l calculators

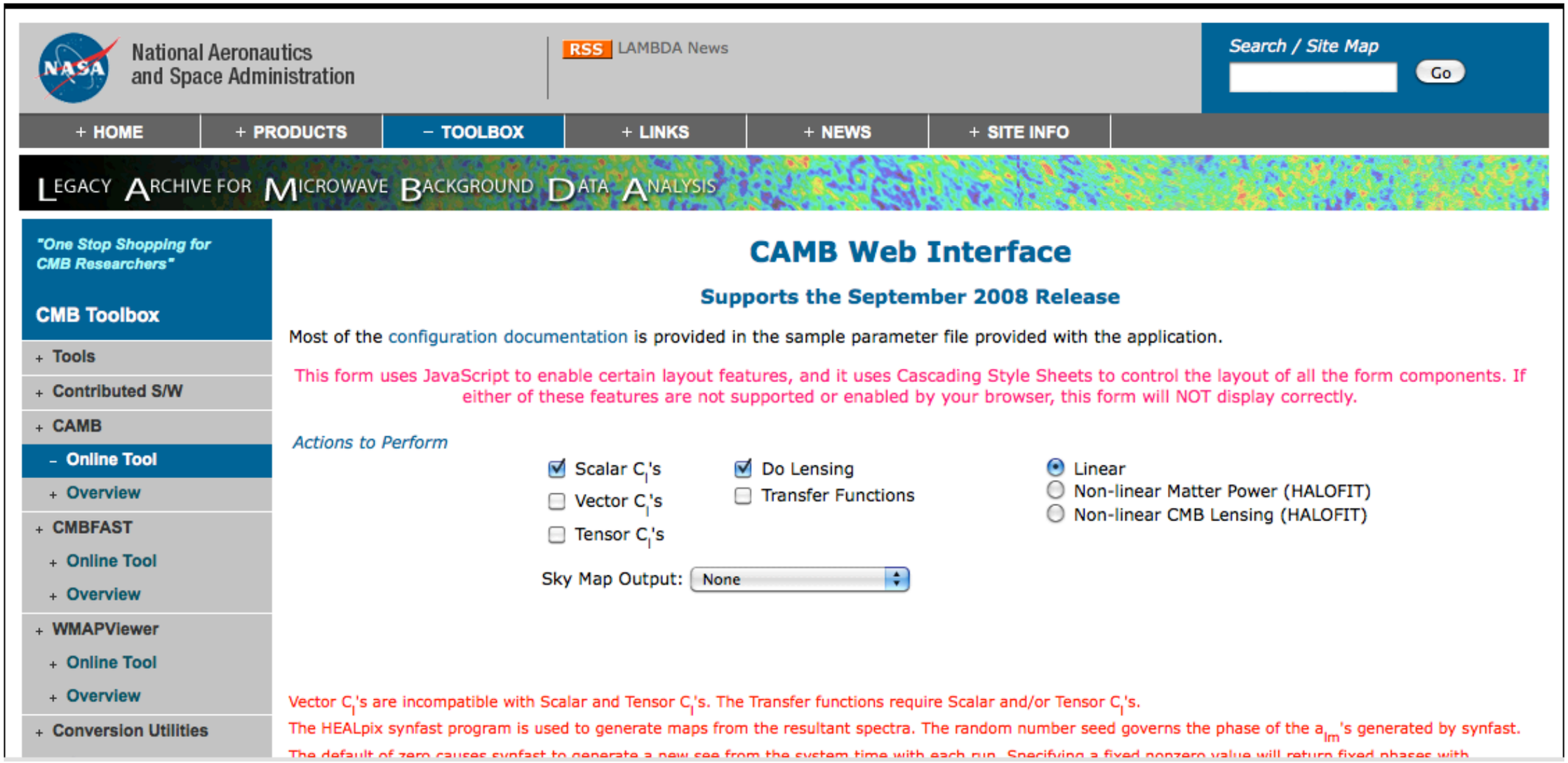

CMB Toolbox: http://lambda.gsfc.nasa.gov/toolbox/

CAMB website: http://camb.info/
CMBFast website: http://www.cmbfast.org/

Parameter estimation (Exercise!)

$$I_{ij} \equiv \frac{\partial^2 \mathcal{L}}{\partial\theta_i \partial\theta_j} = \sum_{\ell=2}^{\ell_{\max}} (2\ell+1) \left[C_\ell + \frac{4\pi\sigma^2}{N} e^{\theta_b^2 \ell(\ell+1)} \right]^{-2} \left(\frac{\partial C_\ell}{\partial\theta_i} \right) \left(\frac{\partial C_\ell}{\partial\theta_j} \right).$$

Cosmic variance

Noise per beam

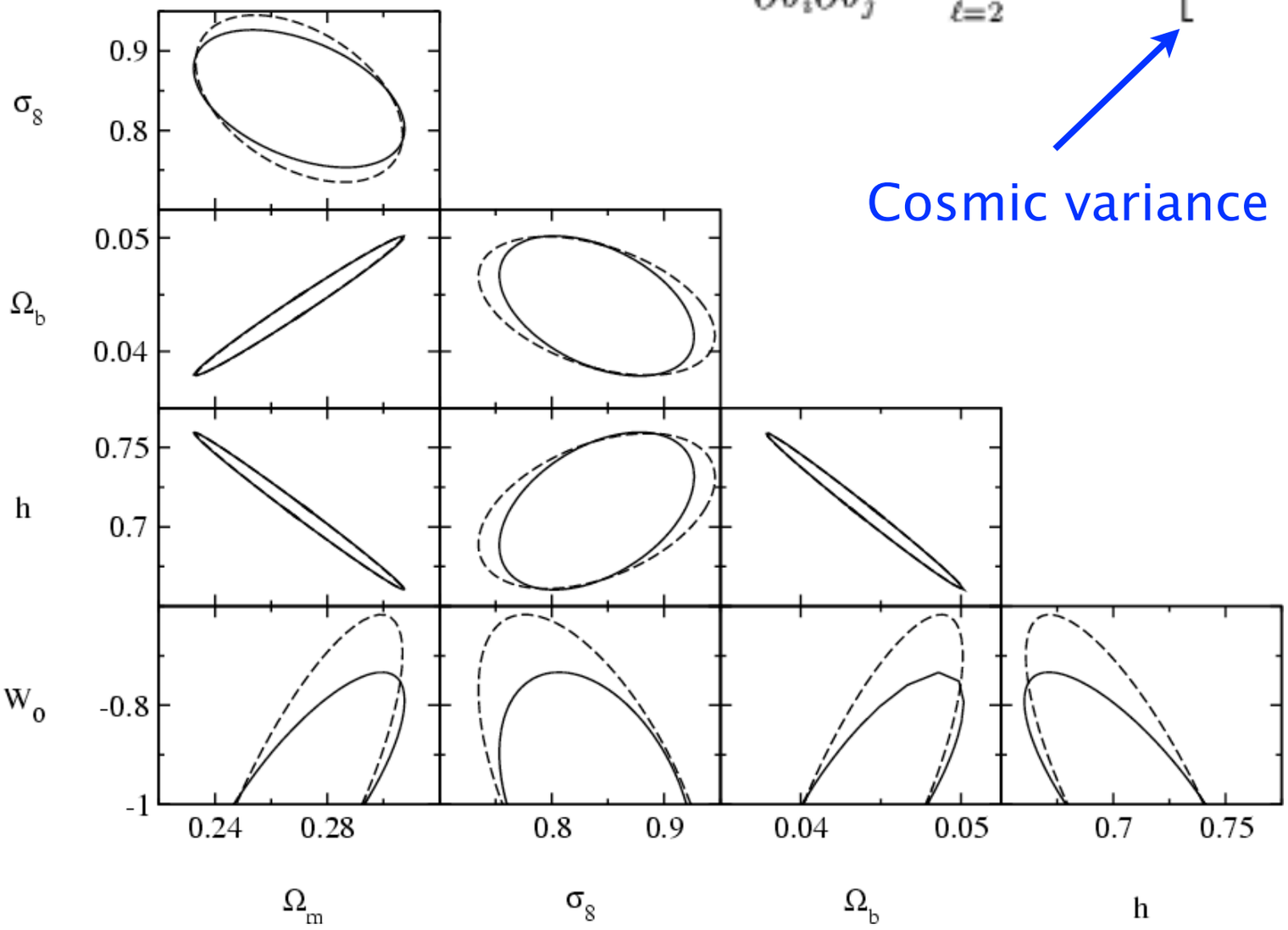

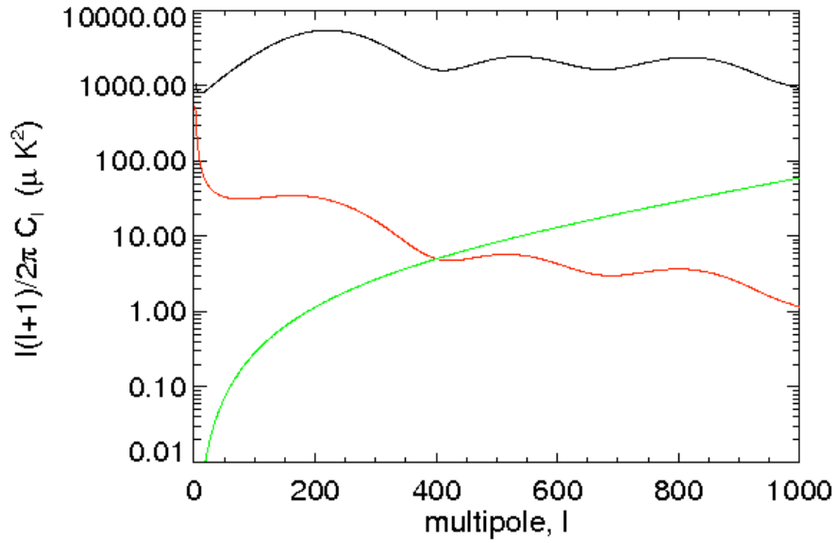

Plot your own power spectra (two for each parameter), and sum up the terms!

WMAP cosmology after 7 years

WMAP Cosmological Parameters Model: lcdm+sz+lens Data: wmap7			
$10^2\Omega_b h^2$	$2.258^{+0.057}_{-0.056}$	$1-n_s$	0.037 ± 0.014
$1-n_s$	$0.0079 < 1-n_s < 0.0642$ (95% CL)	$A_{\rm BAO}(z=0.35)$	$0.463^{+0.021}_{-0.020}$
C_{220}	5763^{+38}_{-40}	$d_A(z_{\rm eq})$	14281^{+158}_{-161} Mpc
$d_A(z_*)$	14116^{+160}_{-163} Mpc	$\Delta^2_{\mathcal{R}}$	$(2.43 \pm 0.11) \times 10^{-9}$
h	0.710 ± 0.025	H_0	71.0 ± 2.5 km/s/Mpc
$k_{\rm eq}$	$0.00974^{+0.00041}_{-0.00040}$	$\ell_{\rm eq}$	137.5 ± 4.3
ℓ_*	302.44 ± 0.80	n_s	0.963 ± 0.014
Ω_b	0.0449 ± 0.0028	$\Omega_b h^2$	$0.02258^{+0.00057}_{-0.00056}$
Ω_c	0.222 ± 0.026	$\Omega_c h^2$	0.1109 ± 0.0056
Ω_Λ	0.734 ± 0.029	Ω_m	0.266 ± 0.029
$\Omega_m h^2$	$0.1334^{+0.0056}_{-0.0055}$	$r_{\rm hor}(z_{\rm dec})$	285.5 ± 3.0 Mpc
$r_s(z_d)$	153.2 ± 1.7 Mpc	$r_s(z_d)/D_v(z=0.2)$	$0.1922^{+0.0072}_{-0.0073}$
$r_s(z_d)/D_v(z=0.35)$	$0.1153^{+0.0038}_{-0.0039}$	$r_s(z_*)$	$146.6^{+1.5}_{-1.6}$ Mpc
R	1.719 ± 0.019	σ_8	0.801 ± 0.030
$A_{\rm SZ}$	$0.97^{+0.68}_{-0.97}$	t_0	13.75 ± 0.13 Gyr
τ	0.088 ± 0.015	θ_*	0.010388 ± 0.000027
θ_*	0.5952 ± 0.0016 °	t_*	379164^{+5187}_{-5243} yr
$z_{\rm dec}$	1088.2 ± 1.2	z_d	1020.3 ± 1.4
$z_{\rm eq}$	3196^{+134}_{-133}	$z_{\rm reion}$	10.5 ± 1.2
z_*	$1090.79^{+0.94}_{-0.92}$		

Check the WMAP website

LEGACY ARCHIVE FOR MICROWAVE BACKGROUND DATA ANALYSIS

"One Stop Shopping for CMB Researchers"

Data Products

- + Mission Data
  - + WMAP
    - – Overview
    - + Products
    - + Documents
    - + Software
    - + Images
    - + Education
  - + COBE
  - + Relikt
  - + IRAS
  - + SWAS
- + CMB Related Data
  - + Space Missions
  - + Suborbital CMB
  - + Foreground
  - + LSS Links

Wilkinson Microwave Anisotropy Probe

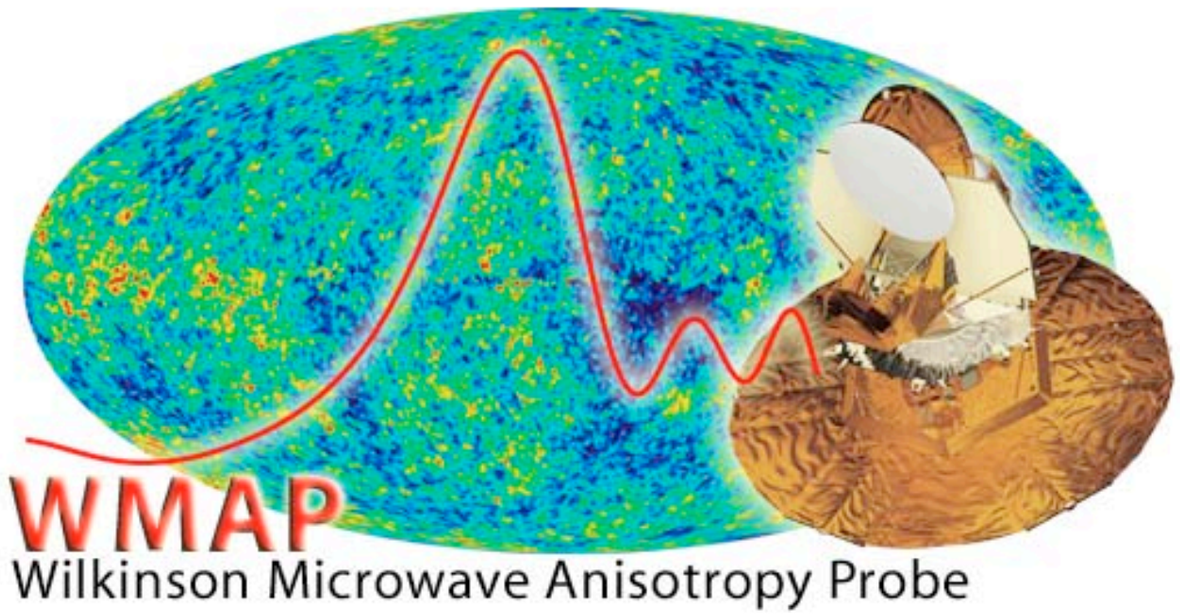

SEVEN-YEAR PAPERS
SEVEN-YEAR DATA
COSMOLOGICAL PARAMETERS TABLE
FIVE-YEAR DATA
THREE-YEAR DATA
FIRST-YEAR DATA
WMAP MISSION SITE

WMAP Overview

The WMAP (Wilkinson Microwave Anisotropy Probe) mission is designed to determine the geometry, content, and evolution of the universe via a 13 arcminute FWHM resolution full sky map of the temperature anisotropy of the cosmic microwave background radiation. The choice of orbit,

2009-2014: The Planck satellite

Credit: ESA

PLANCK launch May 2009

Credit: ESA

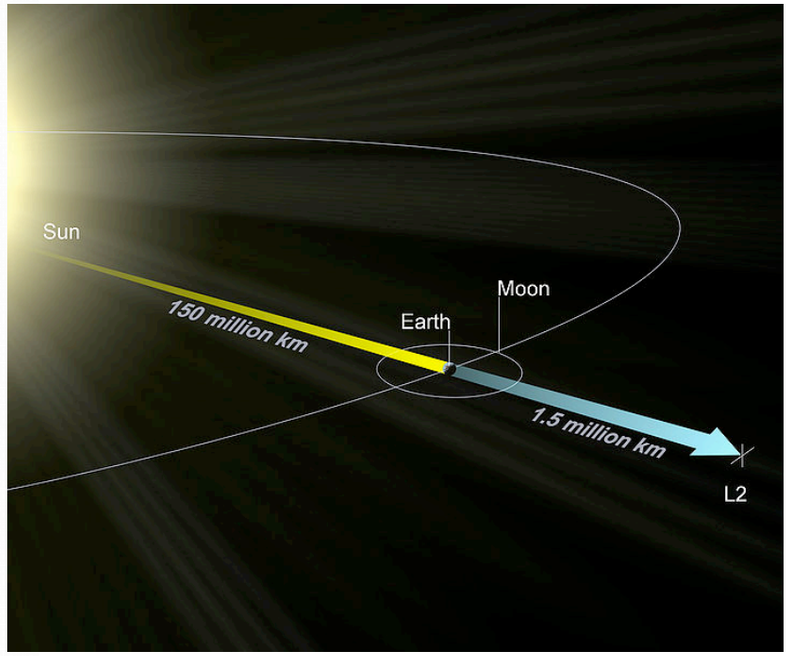

Destination L2: the second Lagrangian point

(getting crowded there!)

PLANCK scanning the sky!

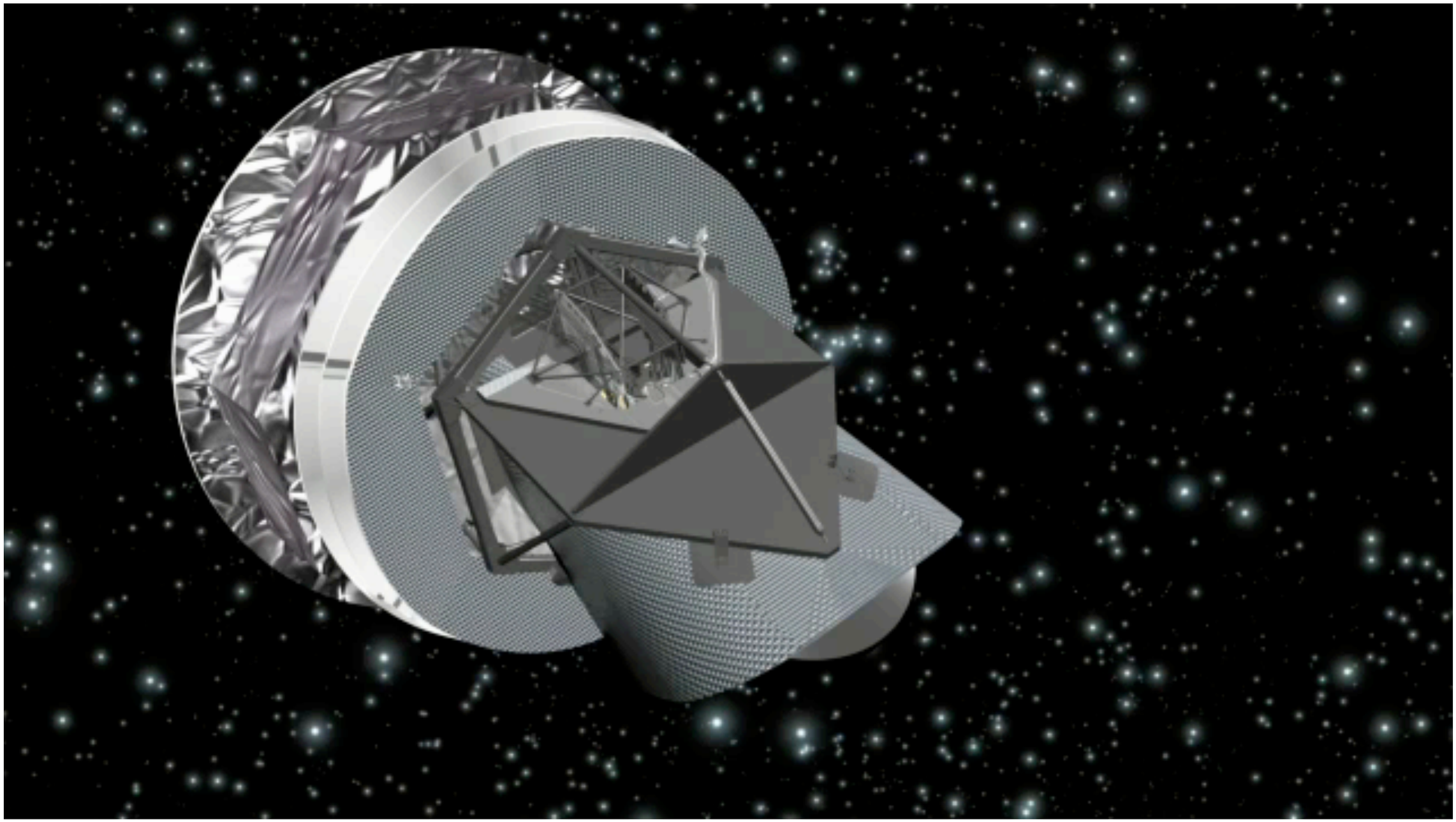

Credit: ESA

Planck data compared to WMAP

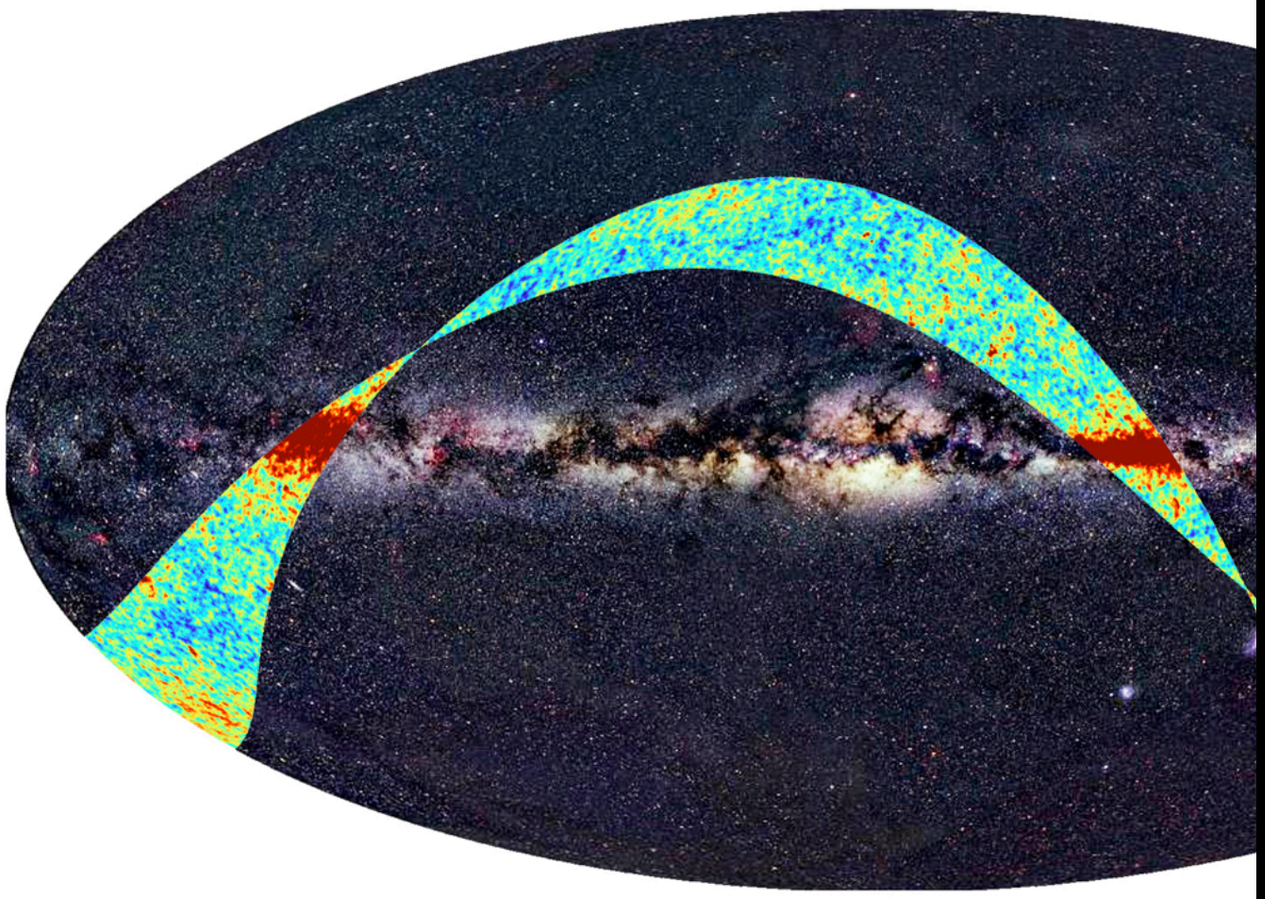

Planck science team
Credit: Ian Morison

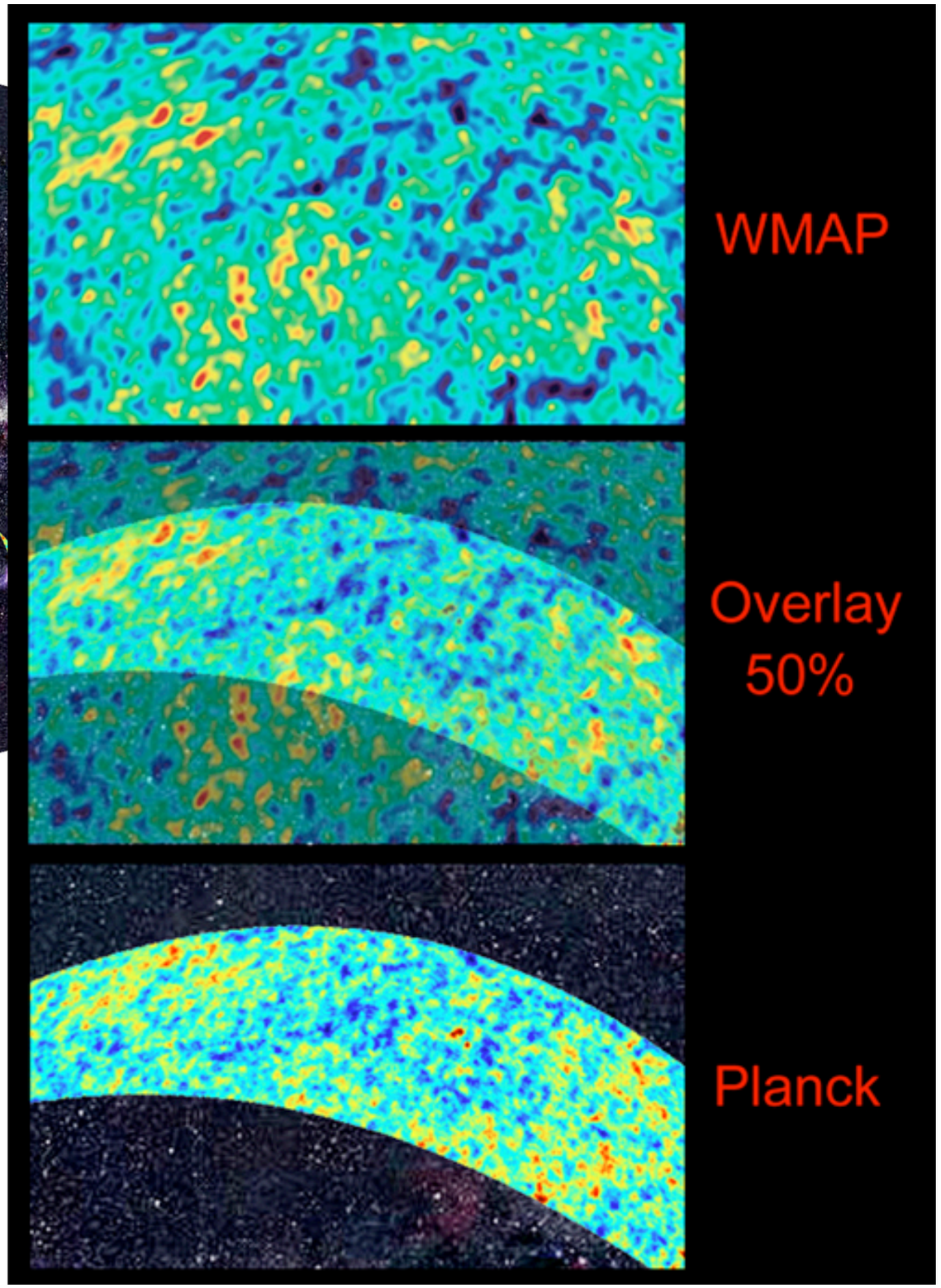

Precision cosmology with PLANCK

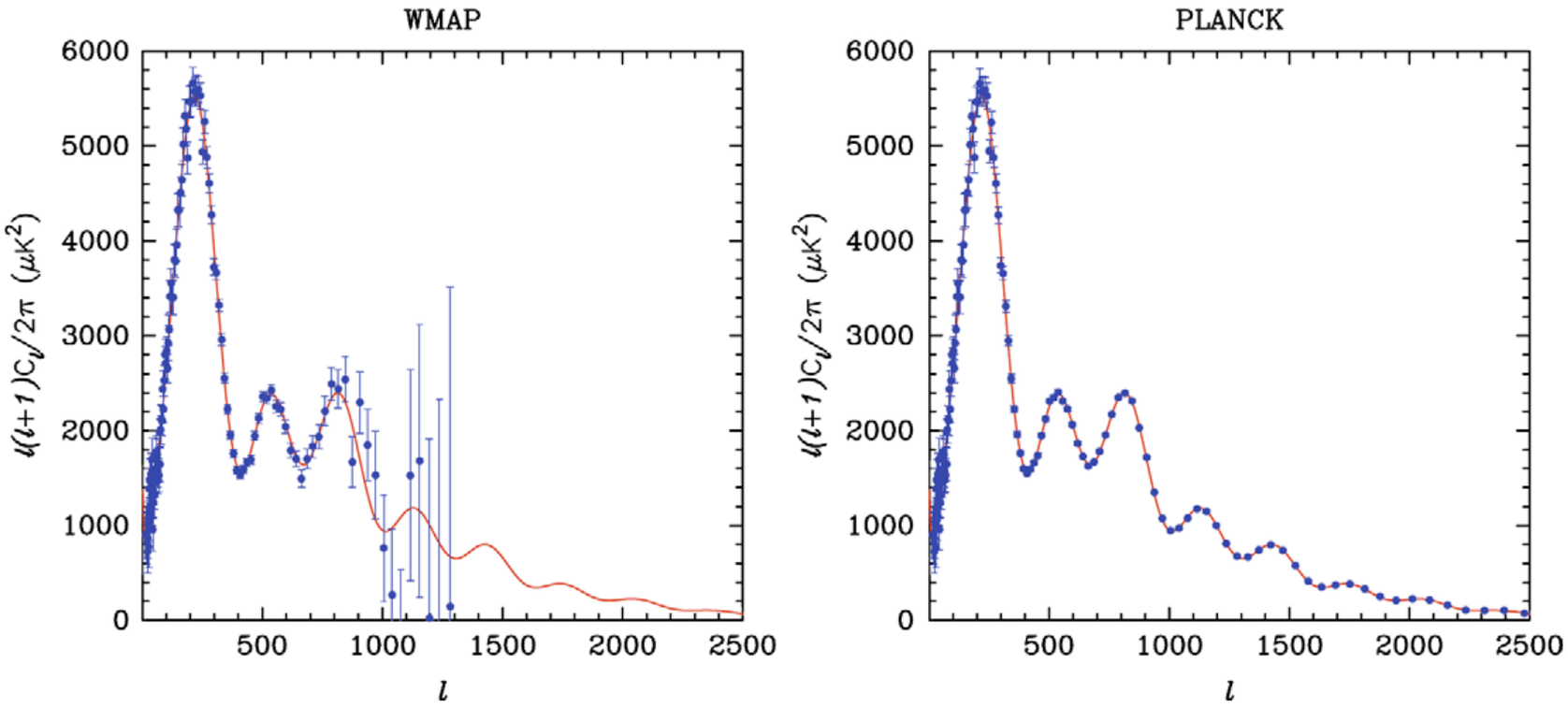

- Much better resolution (5′ compared to 14′ for WMAP), combined with μK sensitivity (about an order of magnitude lower than WMAP at 100 GHz)

- Much wider frequency coverage (30–857 GHz) – better foreground removal

- By-product: all-sky cluster catalogue, radio source catalogue, Galactic foreground maps

Measurement of EE and BB modes

Polarization measurement is PLANCK's holy grail (next lecture)

TE power

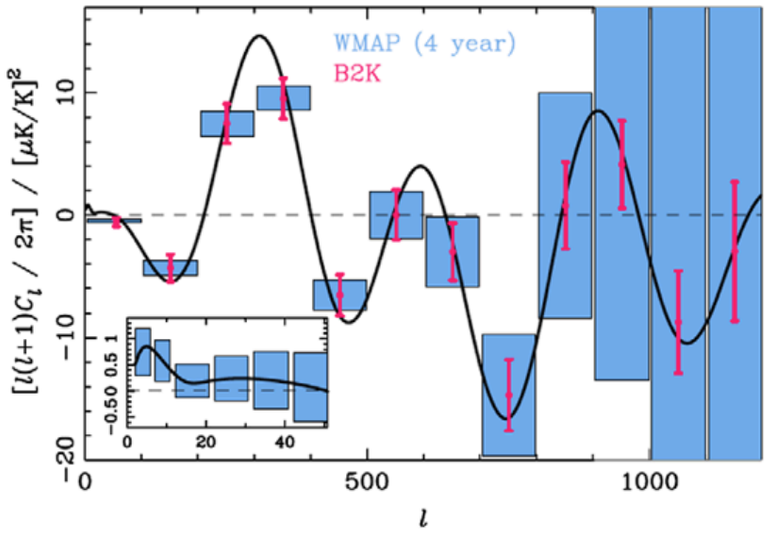

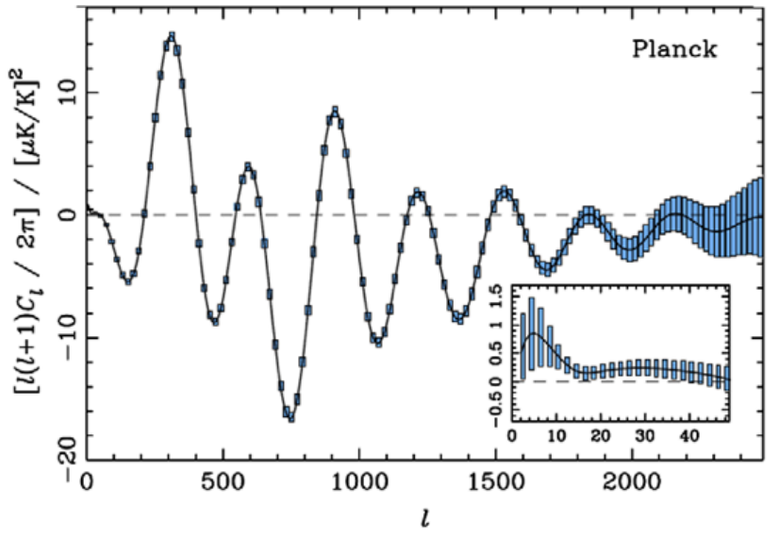

EE power

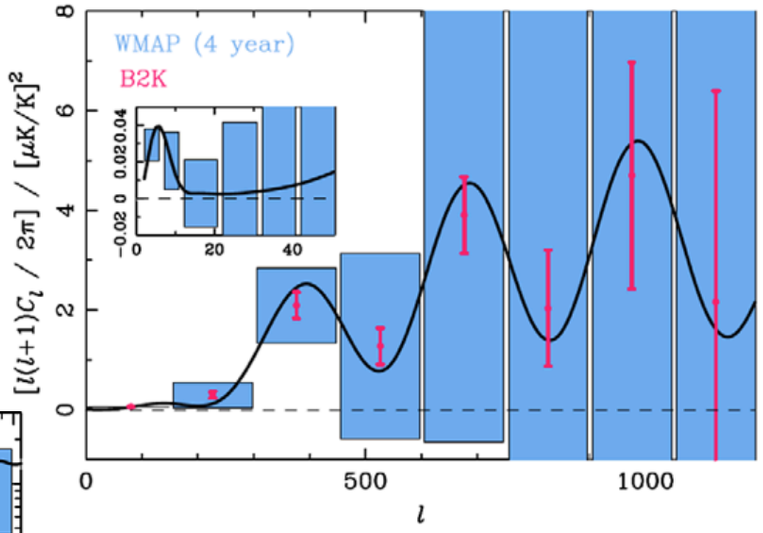

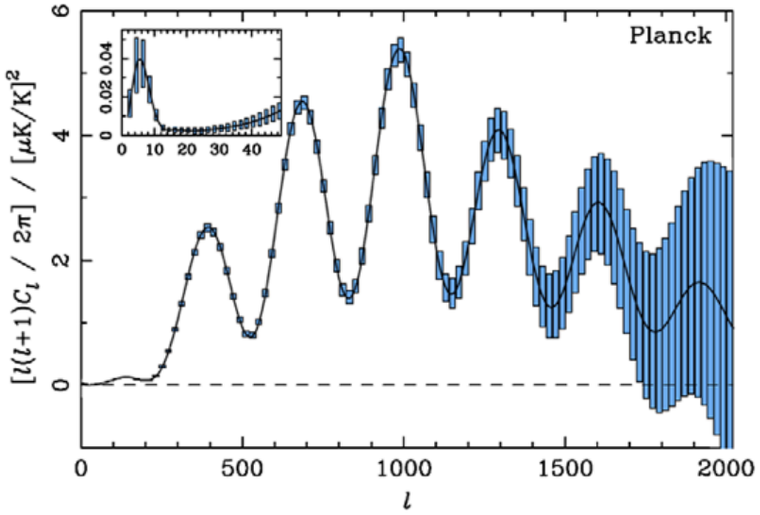

WMAP **PLANCK**

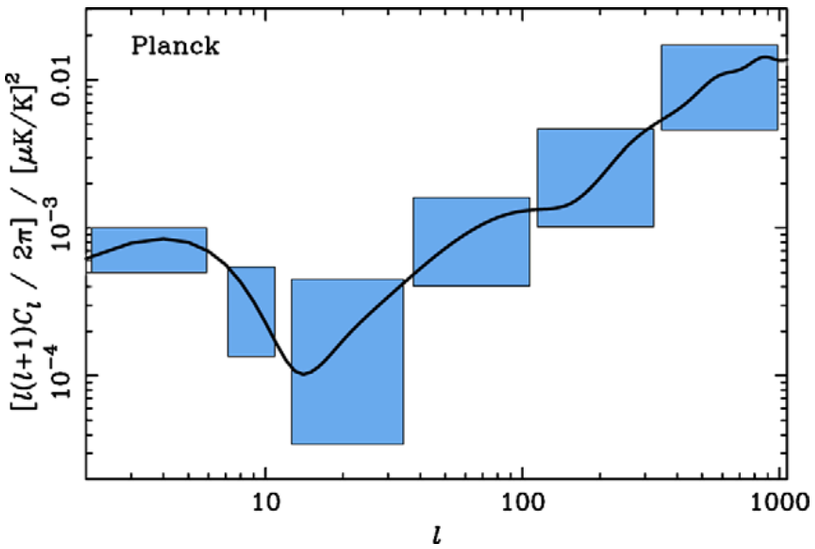

Measurement of the BB power spectrum!

Credit: Planck bluebook

Early science results

25 papers published early this year on instrument, Galactic foregrounds and compact objects (including SZ clusters)

Planck Early Results: The Early Release Compact Source Catalogue

Planck Collaboration: P. A. R. Ade[71], N. Aghanim[46], M. Arnaud[58], M. Ashdown[56,79], J. Aumont[46], C. Baccigalupi[69], A. Balbi[27], A. J. Banday[77,7,63], R. B. Barreiro[52], J. G. Bartlett[3,54], E. Battaner[81], K. Benabed[47], A. Benoît[47], J.-P. Bernard[77,7], M. Bersanelli[25,40], R. Bhatia[32], A. Bonaldi[36], L. Bonavera[69,5], J. R. Bond[6], J. Borrill[62,73], F. R. Bouchet[47], M. Bucher[3], C. Burigana[39], R. C. Butler[39], P. Cabella[27], C. M. Cantalupo[62], B. Cappellini[40], J.-F. Cardoso[59,3,47], A. Catalano[3,57], L. Cayón[18], A. Challinor[80,56,10], A. Chamballu[44], R.-R. Chary[45]*, X. Chen[45], L.-Y Chiang[49], C. Chiang[17], P. R. Christensen[66,28], D. L. Clements[44], S. Colombi[47], F. Couchot[61], A. Coulais[57], B. P. Crill[54,67], F. Cuttaia[39], L. Danese[69], R. J. Davis[55], P. de Bernardis[24], A. de Rosa[39], G. de Zotti[36,69], J. Delabrouille[3], J.-M. Delouis[47], F.-X. Désert[42], C. Dickinson[55], J. M. Diego[52], K. Dolag[63], H. Dole[46], S. Donzelli[40,50], O. Doré[54,8], U. Dörl[63], M. Douspis[46], X. Dupac[31], G. Efstathiou[80], T. A. Enßlin[63], H. K. Eriksen[50], F. Finelli[39], O. Forni[77,7], P. Fosalba[48], M. Frailis[38], E. Franceschi[39], S. Galeotta[38], K. Ganga[3,45], M. Giard[77,7], Y. Giraud-Héraud[3], J. González-Nuevo[69], K. M. Górski[54,83], S. Gratton[56,80], A. Gregorio[26], A. Gruppuso[39], J. Haissinski[61], F. K. Hansen[50], D. Harrison[80,56], G. Helou[8], S. Henrot-Versillé[61], C. Hernández-Monteagudo[63], D. Herranz[52], S. R. Hildebrandt[8,60,51], E. Hivon[47], M. Hobson[79], W. A. Holmes[54], A. Hornstrup[12], W. Hovest[63], R. J. Hoyland[51], K. M. Huffenberger[82], M. Huynh[45], A. H. Jaffe[44], W. C. Jones[17], M. Juvela[16], E. Keihänen[16], R. Keskitalo[54,16], T. S. Kisner[62], R. Kneissl[30,4], L. Knox[20], H. Kurki-Suonio[16,34], G. Lagache[46], A. Lähteenmäki[1,34], J.-M. Lamarre[57], A. Lasenby[79,56], R. J. Laureijs[32], C. R. Lawrence[54], S. Leach[69], J. P. Leahy[55], R. Leonardi[31,32,21], J. León-Tavares[1], C. Leroy[46,77,7], P. B. Lilje[50,9], M. Linden-Vørnle[12], M. López-Caniego[52], P. M. Lubin[21], J. F. Macías-Pérez[60], C. J. MacTavish[56], B. Maffei[55], G. Maggio[38], D. Maino[25,40], N. Mandolesi[39], R. Mann[70], M. Maris[38], F. Marleau[14], D. J. Marshall[77,7], E. Martínez-González[52], S. Masi[24], M. Massardi[36], S. Matarrese[23], F. Matthai[63], P. Mazzotta[27], P. McGehee[45], P. R. Meinhold[21], A. Melchiorri[24], J.-B. Melin[11], L. Mendes[31], A. Mennella[25,38], S. Mitra[54], M.-A. Miville-Deschênes[46,6], A. Moneti[47], L. Montier[77,7], G. Morgante[39], D. Mortlock[44], D. Munshi[71,80], A. Murphy[65], P. Naselsky[66,28], P. Natoli[27,2,39], C. B. Netterfield[14], H. U. Nørgaard-Nielsen[12], F. Noviello[46], D. Novikov[44], I. Novikov[66], I. J. O'Dwyer[54], S. Osborne[75], F. Pajot[46], R. Paladini[74,8], B. Partridge[33], F. Pasian[38], G. Patanchon[3], T. J. Pearson[8,45], O. Perdereau[61], L. Perotto[60], F. Perrotta[69], F. Piacentini[24], M. Piat[3], R. Piffaretti[58,11], S. Plaszczynski[61], P. Platania[53], E. Pointecouteau[77,7], G. Polenta[2,37], N. Ponthieu[46], T. Poutanen[34,16,1], G. W. Pratt[58], G. Prézeau[8,54], S. Prunet[47], J.-L. Puget[46], J. P. Rachen[63], W. T. Reach[78], R. Rebolo[51,29], M. Reinecke[63], C. Renault[60], S. Ricciardi[39], T. Riller[63], I. Ristorcelli[77,7], G. Rocha[54,8], C. Rosset[3], M. Rowan-Robinson[44], J. A. Rubiño-Martín[51,29], B. Rusholme[45], A. Sajina[33], M. Sandri[39], D. Santos[60], G. Savini[68], B. M. Schaefer[76], D. Scott[15], M. D. Seiffert[54,8], P. Shellard[10], G. F. Smoot[19,62,3], J.-L. Starck[58,11], F. Stivoli[41], V. Stolyarov[79], R. Sudiwala[71], R. Sunyaev[63,72], J.-F. Sygnet[47], J. A. Tauber[32], D. Tavagnacco[38], L. Terenzi[39], L. Toffolatti[13], M. Tomasi[25,40], J.-P. Torre[46], M. Tristram[61], J. Tuovinen[64], M. Türler[43], G. Umana[35], L. Valenziano[39], J. Valiviita[50], J. Varis[64], P. Vielva[52], F. Villa[39], N. Vittorio[27], L. A. Wade[54], B. D. Wandelt[47,22], S. D. M. White[63], A. Wilkinson[55], D. Yvon[11], A. Zacchei[38], and A. Zonca[21]